

ABSTRACT

Title of Dissertation: **AN OPERATIONS MANAGEMENT FRAMEWORK
TO IMPROVE GEOGRAPHIC EQUITY
IN LIVER TRANSPLANTATION**

Shubham Akshat
Doctor of Philosophy, 2022

Dissertation Directed by: **Professor S. Raghavan
Department of Decision, Operations, and Information
Technologies**

In the United States (U.S.), on average three people die every day awaiting a liver transplant for a total of 1,133 lives lost in 2021. While 13,439 patients were added to the waiting list in 2021, only 9,236 patients received liver transplantation. To make matters worse, there is significant geographic disparity across the U.S. in transplant candidate access to deceased donor organs. The U.S. Department of Health and Human Services (HHS) is keen to improve transplant policy to mitigate these disparities. The deceased donor liver allocation policy has been through three major implementations in the last nine years, but yet the issue persists. This dissertation seeks to apply operations management models to (i) understand transplant candidate behavior, and (ii) suggest improvements to transplant policy that mitigate geographic disparity.

In the first essay, we focus on reducing disparities in the organ supply to candidate demand (s/d) ratios across transplant centers. We develop a nonlinear integer programming model that allocates organ supply to maximize the minimum s/d ratios across all transplant centers. We

focus on circular donation regions that address legal issues raised with earlier organ distribution frameworks. This enables reformulating our model as a set-partitioning problem and our proposal can be viewed as a heterogeneous donor circle policy. Compared to the current Acuity Circles policy that has fixed radius circles around donation locations, the heterogeneous donor circle policy greatly improves both the worst s/d ratio, and the range of s/d ratios. With the fixed radius policy of 500 nautical miles (NM) the s/d ratio ranges from 0.37 to 0.84 at transplant centers, while with the heterogeneous circle policy capped at a maximum radius of 500NM the s/d ratio ranges from 0.55 to 0.60, closely matching the national s/d ratio of 0.5983.

Broader sharing of organs is believed to mitigate geographic disparity. Recent policies are moving towards broader sharing in principle. In the second essay, we develop a patient's dynamic choice model to analyze her strategic response to a policy change. First, we study the impact of the Share 35 policy, a variant of broader sharing introduced in 2013, on the behavioral change of patients at the transplant centers (i.e., change in their organ acceptance probability), geographic equity, and efficiency (transplant quality, offer refusals, survival benefit from a transplant, and organ travel distance). We find that sicker patients became more selective in accepting organs (acceptance probability decreased) under the Share 35 policy. Second, we study the current Acuity Circles policy and conclude that it would result in lower efficiency (more offer refusals and a lower transplant benefit) than the previous Share 35 policy. Finally, we show that broader sharing in its current form may not be the best strategy to balance geographic equity and efficiency. The intuition is that by indiscriminately enlarging the pool of supply locations from where patients can receive offers, they tend to become more selective, resulting in more offer rejections and less efficiency. We illustrate that the heterogeneous donor circles policy that equalizes the s/d ratios across geographies is better than Acuity Circles in achieving geographic

equity at the lowest trade-off on efficiency metrics.

The previous two essays demonstrate the benefit of equalizing the s/d ratios across geographies. In December 2018 the Organ Procurement and Transplantation Network (OPTN) Board of Directors approved the continuous distribution framework as the desired policy goal for all the organ allocation systems. In this framework, the waiting list candidates will be prioritized based on several factors, each contributing some points towards the total score of a candidate. The factors in consideration are medical severity, expected post-transplant outcome, the efficient management of organ placement, and equity. However, the respective weights for each of these potential factors are not yet decided. In the third essay, we consider two factors, medical severity and the efficient management of organ placement (captured using the distance between the donor hospital and transplant center), and we design an allocation policy that maximizes the geographic equity. We develop a mathematical model to calculate the s/d ratio of deceased-donor organs at a transplant center in a continuous scoring framework of organ allocation policy. We then formulate a set-partitioning optimization problem and test our proposals using simulation. Our experiments suggest that reducing inherent differences in s/d ratios at the transplant centers result in saving lives and reduced geographic disparity.

AN OPERATIONS MANAGEMENT FRAMEWORK TO IMPROVE
GEOGRAPHIC EQUITY IN LIVER TRANSPLANTATION

by

Shubham Akshat

Dissertation submitted to the Faculty of the Graduate School of the
University of Maryland, College Park in partial fulfillment
of the requirements for the degree of
Doctor of Philosophy
2022

Advisory Committee:

Professor S. Raghavan, Chair/Advisor
Professor Sommer Gentry
Professor Liye Ma
Professor Bruce Golden
Professor Xiaojia Guo
Professor David Lovell, Dean's Representative

© Copyright by
Shubham Akshat
2022

Dedication

To my parents, and my sister.

Acknowledgments

I owe my gratitude to all the people who have made this thesis possible and because of whom my graduate experience has been one that I will cherish forever.

The journey couldn't have been complete without the unwavering support and guidance of my advisor, Dr. S. Raghavan. He has been there with me through ups and downs. It is said that completing a Ph.D. needs perseverance. It is not only true for a student but equally for the advisor. He believed in me when I was a novice. He gave me freedom, and I gained confidence with time. I cannot thank him enough for his time, patience, and mentorship. I am grateful to work with Dr. Liye Ma. After every meeting, I came out inspired and motivated. I am amazed by his sharp precision and strong read over the matter. I learned immensely working with him. I remember at the start of the fifth year, I asked him if I should into the job market with the paper we have been working on. He said the market is never bad for good candidates, and our work is solid. When the time, during the middle of the job-market season, was tough and full of uncertainty, both Dr. Raghavan and Dr. Liye Ma advised me to keep doing the work, and things will fall in place eventually. Looking back, there couldn't have been better advice, and I am glad I followed it.

No journey is without obstacles. Not only do they strengthen you, but they also reinforce existing and kindle beautiful bonds with our fellow beings. To my dearest, Rahul and Ayush, who have been there with me, rain or shine! Distance doesn't matter with true friends. Rahul,

you are still alive in my heart. This is a small tribute to our short camaraderie. Justina has been such stalwart support, right from Day 1. I want to especially emphasize the role she has played in making me feel a part of the program, by creating such an inclusive atmosphere. She was so approachable and comforting. I am thankful to Gaurav and Vidit, for all the road trips we made, and weekend parties that instilled joy and learning during my stay in Maryland. I could not have asked for a better colleague than Sahar. The strength of a friendship can be measured by how easy we feel to share our happy and sad moments with each other. And I am happy to develop such a friendship so quickly. It is said that all is well that ends well. In the final year, the outcome would not have been possible without the support of Kashish (my job-market buddy), Vasundhara, Waseem, and Ashish. I thank all the seminar speakers and researchers whose talks and papers motivated me to keep pushing the boundaries.

Looking back, when I was doing my under-graduation at the Indian Institute of Technology, Delhi, never had I thought that I will ever pursue a doctoral degree. But the seed was already planted by Dr. Kiran Seth! His love for Operations Research was infectious. He talked about some ‘common chord’ that doctorate touch, irrespective of their field. The concept still eludes me, but I hope to get it someday, by continuing on the path of scientific research with purity, dedication, and focus. I also want to acknowledge Sarang Deo, who was my inspiration when I was working with him at the Indian School of Business, before starting my doctoral journey.

Finally, I am eternally grateful to my parents for giving me the freedom to pursue my interests, even though it meant facing resistance from their peers for allowing me to move away from my home (country). Words cannot express the gratitude I owe them for their sacrifices in placing me where I am today.

I apologize to those I have inadvertently left out. Thank you all!

Table of Contents

Dedication	ii
Acknowledgements	iii
Table of Contents	v
List of Tables	viii
List of Figures	x
List of Abbreviations	xii
Chapter 1: Introduction	1
1.1 Motivation	1
1.2 Liver Allocation Policy	3
1.2.1 Previous Policies	4
1.2.2 Current Policy: Acuity Circles	5
1.3 Contributions of this Thesis	6
Chapter 2: Heterogeneous Donor Circles for Fair Liver Transplant Allocation	8
2.1 Introduction	8
2.2 Related Research	13
2.3 Model Formulation	16
2.3.1 Supply-Demand Ratio Calculation	19
2.3.2 General Model	20
2.3.3 Circular Contiguity and a Set-Partitioning Model	23
2.4 Data and Results	26
2.4.1 Zip-code Cluster Version	27
2.4.2 DSA Version	31
2.5 Conclusions	39
Chapter 3: Improving Broader Sharing to Address Geographic Inequity in Liver Transplantation	42
3.1 Introduction	42
3.1.1 Contributions	45
3.2 New Liver Allocation Policies	47
3.2.1 Supply-to-demand (s/d) Match Policy	47

3.2.2	National Sharing Policy	48
3.3	Related Research	48
3.4	Data and Evidence	52
3.4.1	Data	52
3.4.2	Model-Free Evidence of Behavioral Change	52
3.5	Patient’s Dynamic Choice Model	55
3.5.1	Utility Function	56
3.5.2	Waiting Cost Function	57
3.5.3	(Simplifying) State Transition Probability	58
3.5.4	Offer Acceptance Probability	59
3.6	Model Estimation	59
3.6.1	Estimation Procedure	59
3.6.2	Parameter Identification	61
3.6.3	Estimates	63
3.6.4	Insights from the Structural Model	64
3.6.5	Benchmarking	67
3.6.6	Comparison of the Pre-Share 35 and Share 35 Policy Eras using the Structural Model	69
3.7	Counterfactual Study	71
3.7.1	Geographic Equity	72
3.7.2	Efficiency	74
3.8	Conclusions	78
Chapter 4: A Continuous Scoring Model for Fair Liver Transplant Allocation		81
4.1	Introduction	81
4.1.1	Contributions and Findings	82
4.2	Model Formulation	83
4.2.1	(Expected) Supply-Demand Ratio Calculation at a Transplant Center	84
4.2.2	Heterogeneous Slopes Model	90
4.3	Data and Results	91
4.3.1	Data	91
4.3.2	Results	92
4.4	Conclusions	95
Chapter 5: Conclusions and Future Research		96
5.1	Conclusions	96
5.2	Future Research	97
Appendix A: Appendix to Chapter 2		98
A.1	Comparing Organ Quality	98
A.2	Linearization of the s/d Ratio and Contiguity Constraints	99
A.3	Set Partitioning Model Computational Details	101
A.4	DSA Neighborhoods	102
Appendix B: Appendix to Chapter 3		106

B.1	Summary Statistics	106
B.2	Comparing the Organ Quality of Declined Offers	110
B.3	Details on Logit Inclusive Value	110
B.4	State Transition Probability	112
B.5	Log-Likelihood Function	115
B.6	Details on Identification of β_{GS}	117
B.7	Relaxing the Assumption of a Fixed Value of CIT	118
B.8	Iterative Method for Estimating the Equilibrium	119
B.9	Numerical Study to Derive Insights from the Structural Model	122
B.10	Models for Benchmarking	126
B.11	Comparison of the Pre-Share 35 and Share 35 Policies on Geographic Equity Using Simulation	128
B.12	Survival Benefit due to a Transplant	129
B.13	s/d Match Policy (Maximum Radius = 600 NM)	130

Bibliography	132
---------------------	------------

List of Tables

1.1	Comparison of deceased-adult donor allocation policies. Local (regional) refers to the donor and candidate belonging to the same DSA (region), and national in the case of different regions.	5
2.1	Model Notation	19
2.2	Comparison of the s/d ratios between fixed and heterogeneous circles (supply and demand locations are zip-code clusters and transplant centers (TCs), respectively).	29
2.3	Comparison of the s/d ratios among different allocation policies in the DSA version (supply and demand locations are 58 DSAs and 52 DSAs, respectively). τ_{max} and $\bar{\tau}$ represent the maximum and average distance, respectively, of the farthest DSA in a neighborhood/region/district in each allocation policy.	32
2.4	Comparison of the s/d ratios among different DSA-based allocation policies (supply and demand locations are 58 DSAs and 52 DSAs, respectively).	35
2.5	Comparison of LSAM simulation results for DSA-based allocation policies under Enhanced Share 15.	37
2.6	Comparison of LSAM simulation results for DSA-based allocation policies under Share 35.	39
3.1	One year Kaplan-Meier graft survival rate based on 2012-2015 transplants. Follow-up done till December 18, 2020.	42
3.2	Model Notation	54
3.3	Summary statistics of probability of acceptance ($P := \#$ of offers accepted/ $\#$ of offers received) for some of the variables in the state space. The variation in P enables the identification of the parameters associated with these variables in the structural model.	62
3.4	Estimation results of the structural model.	63
3.5	Demand and Supply settings used in a numerical study to analyze their effect on a patient’s behavior. *: Set 1 is the baseline setting. 95% confidence intervals of the average probability of organ acceptance are shown in square brackets. #: To model the Acuity Circles policy in this geographic setup of two regions and three DSAs, we assume local \rightarrow Regional \rightarrow National sharing (instead of different circular bands of radii 150, 250, and 500 NM) within each MELD category.	66

3.6	Comparing the goodness-of-fit (out-of-sample) of various models on threshold-independent measures. AUC (ROC) and AUC (PRC) are the area under the receiver operating characteristic and precision-recall curves, respectively. RMSE and MAE stand for the root-mean-square error and mean absolute error, respectively.	68
3.7	Offer acceptance probabilities (in the Share 35 policy era) as a function of the MELD category. Parentheses report the change compared to the Pre-Share 35 policy era. Values are calculated using the structural model (whose parameters are estimated using data from 2010 to 2018).	70
3.8	Comparison of the standard deviation of various geographic equity measures between policies. The s/d Match policy has the lowest values for each of the geographic equity metrics.	73
3.9	Comparison of the travel distance (in NM) between policies.	77
4.1	Model Notation	84
4.2	Comparison of the s/d ratios (across transplant centers) between no proximity score model, heterogeneous slopes model and fixed slopes models.	94
4.3	Comparison of various allocation policies using simulation.	94
A.1	Computational details of the set-partitioning model run on four-digit zip-clusters.	102
A.2	Geographical allocation policy for DSAs when the maximum permitted distance to a neighboring DSA is 500 NM	103
A.3	Geographical allocation policy for DSAs when the maximum permitted distance to a neighboring DSA is 600 NM.	104
A.4	Geographical allocation policy for DSAs when the maximum permitted distance to a neighboring DSA is 700 NM.	105
B.1	Summary statistics of patient, donor, and transplant characteristics.	108
B.2	Offer acceptance probabilities (in the Share 35 policy era) as a function of the MELD category. Parentheses report the change, compared to the Pre-Share 35 policy era. Values are calculated using summary statistics.	111
B.3	MELD transition matrix.	114
B.4	Estimation results of regressing <i>GS</i> .	117
B.5	Comparison of the estimation results of the structural models (when CIT is fixed versus predicted).	119
B.6	Regression estimates of the reduced-form models used for benchmarking.	127
B.7	Survival model estimates.	129
B.8	Comparison of the standard deviation of various geographic equity measures between s/d Match policies.	131
B.9	Comparison of travel distance (in NM) between the two s/d Match policies.	131

List of Figures

1.1	The U.S. divided into 11 regions (left) comprising 58 DSAs (right).	2
1.2	Flowchart of deceased-donor organ allocation process in the U.S.	4
2.1	Lower supply to demand (s/d) ratios at a DSA (left) correspond to a higher MMaT at the DSA (right). The time period of analysis is from July, 2013 to June, 2017. .	11
2.2	Illustration of the difference between Regions/Districts and neighborhoods. (a) Let DSAs A, B, C and D form a region or district. They all share with each other. (b) With the neighborhood displayed, the neighborhood of A consists of DSAs A, B and C. Therefore, A shares only with A, B, and C. Similarly, B shares with B and D; C shares with C and D; and D shares with A, B, C, and D.	15
2.3	Comparing our s/d ratio measure with that of Kilambi and Mehrotra [35]. Their measure artificially inflates the s/d ratio.	17
2.4	Illustration of sharing and receiving contiguity. If $x_{14} = 1$, with sharing contiguity, $x_{12} = x_{13} = 1$; and with receiving contiguity $x_{24} = x_{34} = 1$	21
2.5	Illustration of circular contiguity: If a neighborhood is r units in radius around the supply location, then all demand locations within r units must be in the neighborhood.	24
2.6	Quartiles of radii in the four-digit zip-code cluster models.	31
2.7	(a) Illustration of optimized neighborhoods when $\tau_{max} = 500$. (b) DSAs to which ALOB shares and receives. (c) Sharing and receiving between DSAs identified in (b).	34
3.1	Comparison of MELD at the time of an offer and a transplant between policies using box plots (Status 1A is assigned a MELD score of 41).	55
3.2	Out-of-sample comparison of LSAM with dynamic model prediction.	68
3.3	Comparison of different geographic equity measures between policies.	72
3.4	Comparison of the position at offer acceptance between policies.	74
3.5	Comparison of the fractional change in the utility from the transplant (with respect to the Pre-Share 35 policy) between policies.	75
3.6	Cost of fairness for various policies. It is defined as the fractional decrease in the transplant utility with respect to the Outcome-based policy.	76
3.7	Comparison of the average increase in the survival probability due to transplantation between policies.	77

4.1	Example of continuous scoring framework. Candidate 2 has higher composite score than candidate 1, and thus gets priority.	83
A.1	Comparison of organ quality across the regions using the donor risk index (DRI).	98
B.1	Comparison of positions at which offers were made to patients at different MELD scores between policies (Status 1A is assigned a MELD score of 41).	109
B.2	Supply and demand trends over time.	109
B.3	Comparison of the organ quality of declined offers between the Pre-Share 35 and Share 35 policy eras using the donor risk index (DRI).	110
B.4	Out-of-sample comparison of reduced-form models.	127
B.5	Comparison of the position at offer acceptance, fractional change in utility from the transplant (with respect to Pre-Share 35), and cost of fairness (with respect to Outcome-based) between the two s/d Match policies.	131

List of Abbreviations

CIT	Cold Ischemia Time
CTP	Child-Turcotte-Pugh
DCD	Donation after Circulatory Death
DRI	Donor Risk Index
DSA	Donation Service Area
HHS	Department of Health and Human Services
HR	Hazard Ratio
HRSA	Health Resources and Services Administration
ICU	Intensive Care Unit
LSAM	Liver Simulated Allocation Model
MELD	Model for End-stage Liver Disease
MMaT	Median MELD score at transplant
NM	Nautical Miles
OPO	Organ Procurement Organization
OPTN	Organ Procurement and Transplantation Network
PELD	Pediatric End-Stage Liver Disease
SRTR	Scientific Registry of Transplant Recipients
TC	Transplant Center
UNOS	United Network for Organ Sharing
vMMaT	Variance of Median MELD score at transplant

Chapter 1: Introduction

1.1 Motivation

In the United States (U.S.), an average of three people die every day waiting for a liver transplant, resulting in 1,133 lives lost in 2021. While 13,439 patients were added to the waiting list in 2021, only 9,236 patients received liver transplants. Liver transplantation is the only treatment option for patients with end-stage liver disease when other medical therapies have failed. Deceased donations have contributed to greater than 95% of liver donations in the last 15 years in the U.S. Unlike living donations, which can be arranged privately by a patient-donor pair, deceased-donor organs are considered *national* resources by law (whose allocation is determined by government policy). The U.S. is divided into 11 geographic regions (Figure 1.1), consisting of 58 Donation Service Areas (DSAs). A DSA-based allocation policy had been in place for thirty years (from 1989 to Feb. 4, 2020) but was recently replaced by the Acuity Circles policy (Section 1.2.2). Medical urgency, used to rank patients for an organ offer, is quantitatively measured by the Model for End-Stage Liver Disease (MELD) score. The Pediatric End-Stage Liver Disease (PELD) severity score, a measure calculated slightly differently, is used for patients ≤ 12 years old. The MELD score reflects the probability of death within three months and ranges from 6 to 40, with a higher score indicating a greater mortality risk [20]. More serious patients are assigned Status 1A (for adults) and 1B (for non-adults); their number is fewer than 50 nationwide at any

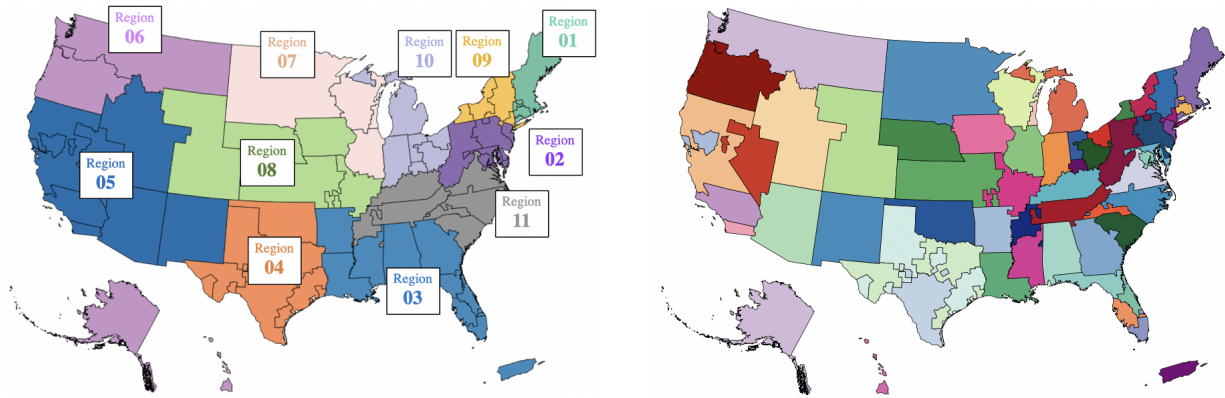


Figure 1.1: The U.S. divided into 11 regions (left) comprising 58 DSAs (right).

time.

The U.S. government created the Organ Procurement and Transplantation Network (OPTN) in 1984 to coordinate a nationwide transplant system and optimize the use of limited donor organs for transplants. Since 1986, the United Network for Organ Sharing (UNOS), a nonprofit private organization, has overseen the operations of OPTN. A key regulatory framework guiding organ transplantation is the ‘Final Rule’, which was adopted in 1998 by the Department of Health and Human Services (HHS) to establish a more detailed framework for the structure and operations of OPTN [33]. The Final Rule states that policies shall not be based on the candidate’s place of residence or place of listing (a patient lists herself at the transplant center and joins the waiting list), except to the extent mandated by the other requirements of the Rule.

However, disparities in organ access have been a serious issue for more than two decades. Geographic inequity in accessing liver transplantation across DSAs is well documented in the literature [56]. In 2012, the OPTN board adopted a strategic plan that included reducing geographic disparities in accessing transplantation. Hughes [34] provides an excellent summary of the laws enacted to improve liver allocation policies in the U.S.

In November 2017, New York City resident Miriam Holman (a patient with a rare form of pulmonary hypertension for which there is no medical therapy, and which is rapidly fatal without lung transplantation) filed a lawsuit (hereafter, ‘lung lawsuit’) against HHS.¹ Due to the particular lung allocation policy in place at that time, a donor lung could become available across the river in New Jersey (less than four miles away). However, because the location of the donor lung was in a different geographical DSA, it had to be offered to every candidate waiting for lungs in that New Jersey DSA (even to candidates who were much farther away and far less medically critical) before it could be offered to Holman [25]. In July 2018, six liver transplant waiting list patients in New York, California, and Massachusetts filed a lawsuit (hereafter, ‘liver lawsuit’) against HHS.² The liver lawsuit pointed out the wide geographical variability in the median MELD scores in recipients for deceased donor transplants, arguing that the place of residence largely determines the chances of one’s survival in the existing policy.

1.2 Liver Allocation Policy

UNOS supervises the transplantation network in the U.S. Its primary responsibilities include managing the national transplant waiting list, matching organs from deceased donors to candidates, establishing the medical criteria for allocating organs, facilitating organ distribution, framing equitable policies, and so forth. Some of the main UNOS members are the 142 liver transplant centers (TCs) and Organ Procurement Organizations (OPOs) in the 58 DSAs. The OPO coordinates the local procurement of deceased-donor organs and allocation within a DSA.

Figure 1.2 shows the flowchart of deceased-donor liver allocation for transplantation. A TC

¹Miriam Holman v. HHS, (S.D.N.Y 17-CV-09041).

²Cruz et al. v. HHS, (S.D.N.Y 18-CV-06371).

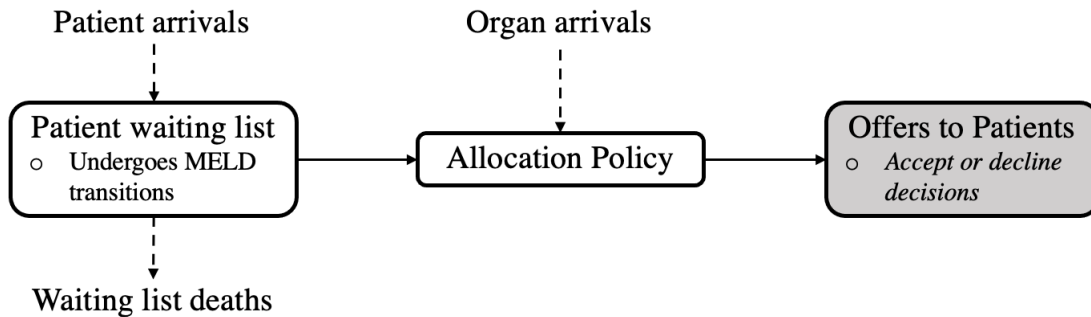


Figure 1.2: Flowchart of deceased-donor organ allocation process in the U.S.

evaluates a candidate and decides whether or not to add her to the waiting list. The medical data of the candidates are shared with UNOS. These pooled data of candidates across all transplant hospitals are constantly updated when new candidates are added, and existing candidates are either removed or their medical conditions (e.g., MELD scores) are updated. When a deceased-donor organ becomes available, the OPO sends the organ donor’s medical data to UNOS. Subsequently, the UNOS matching system compares the donor information with the candidate pool to rank candidates for organ offers according to the allocation policy. Upon receiving an offer, the transplant surgeon or physician, in consultation with the candidate, decides whether to accept the offer. The only clinically approved preservation method in the case of a liver is simple cold storage [39]. Because organs lose viability due to a lack of oxygen, a liver often gets discarded after around 10-12 hours after its recovery.

1.2.1 Previous Policies

The first objective scoring system adopted by OPTN/UNOS was the Child-Turcotte-Pugh (CTP) score in 1998. However, this score was not effective in discriminating the illness severity [47]. Since February 2002, MELD has been used in allocation policies to quantify the urgency

Sequence #	Pre-Share 35	Share 35
1	Status 1 (local)	Status 1 (local)
2	Status 1 (regional)	Status 1 (regional)
3	MELD ≥ 15 (local)	MELD ≥ 35 (local and regional, with preference to local candidates at each MELD)
4	MELD ≥ 15 (regional)	MELD ≥ 15 (local)
5	MELD < 15 (local)	MELD ≥ 15 (regional)
6	MELD < 15 (regional)	Status 1 (national)
7	Status 1 (national)	MELD ≥ 15 (national)
8	MELD ≤ 40 (national)	MELD < 15 (local)
9	-	MELD < 15 (regional)
10	-	MELD < 15 (national)

Table 1.1: Comparison of deceased-adult donor allocation policies. Local (regional) refers to the donor and candidate belonging to the same DSA (region), and national in the case of different regions.

level. Table 1.1 compares the policy in place before and after June 2013 (until February 4, 2020) for adult donors. We refer to the policy before June 2013 as the Pre-Share 35 policy. The Share 35 policy brought about the following two changes: it increased the priority of regional patients with a MELD ≥ 35 and prioritized high-MELD national patients over low-MELD (< 15) local/regional patients. Because the Share 35 policy led to prioritizing sick patients registered outside the DSA and region, it can be seen as a broader sharing policy. In the above policies, the offer-priority hierarchy is based on the MELD and sharing type (local/regional/national).

1.2.2 Current Policy: Acuity Circles

This policy progressively shares organs in circle radii of 150 NM, 250 NM, and 500 NM around the donor hospital, with the following hierarchy: (1) Status 1 candidates at TCs within 500 NM; (2) candidates with a MELD ≥ 37 within 150 NM, then 250 NM, and then 500 NM; (3) candidates with a MELD ≥ 33 within 150 NM, then 250 NM, and then 500 NM; (4) candidates with a MELD ≥ 29 within 150 NM, then 250 NM, and then 500 NM; (5) candidates with a

MELD ≥ 15 within 150 NM, then 250 NM, and then 500 NM, then nationally; (6) candidates with a MELD < 15 within 150 NM, then 250 NM, then 500 NM, and then nationally. This is a ‘one-size-fits-all’ policy, as it does not account for the organ arrival rate, candidate waiting list, or distances of the TCs from a donor hospital.

1.3 Contributions of this Thesis

In Chapter 2, we focus on equalizing supply (deceased donors)-to-demand (waiting list patients) ratios across transplant centers (and DSAs). We develop a novel metric to calculate the supply-to-demand (s/d) at a geographical unit when a supply location can share its organ with multiple demand locations. We provide a general nonlinear integer programming formulation to the problem. We focus on circular donation regions that address legal issues raised with earlier organ distribution frameworks. This enables reformulating our model as a set-partitioning problem and our proposal can be viewed as a heterogeneous donor circle policy. Compared to the current Acuity Circles policy that has fixed radius circles around donation locations, the heterogeneous donor circle policy greatly improves both the worst s/d ratio, and the range of s/d ratios. With the fixed radius policy of 500 nautical miles (NM) the s/d ratio ranges from 0.37 to 0.84 at transplant centers, while with the heterogeneous circle policy capped at a maximum radius of 500NM the s/d ratio ranges from 0.55 to 0.60, closely matching the national s/d ratio of 0.5983.

In Chapter 3, we develop a patient’s dynamic choice model to analyze her strategic response to a policy change. We use nine-year liver transplant dataset to estimate the behavioral primitives of the model. We compare the Pre-Share 35 and Share 35 policies to accurately capture the

change in a patient's behavior. We study counterfactual policies, including the current Acuity Circles and heterogeneous donor circles policy (that we develop in Chapter 2) on geographic equity (inter-regional variation in the transplant rates, patient survival rates, waiting time, and organ offers), and efficiency (transplant quality, offer refusals, survival benefit from a transplant, and organ travel distance) metrics. We find that the Acuity Circles policy is worse than the previous Share 35 policy, especially in efficiency metrics. We show that equalizing s/d ratios across geographies (as done by the heterogeneous donor circles policy) has the highest efficiency among the policies studied while improving upon geographic equity measures.

Eventually, the transplant community is moving towards a continuous distribution framework as the desired policy goal for all the organ allocation systems. However, there is still a debate over how to decide the policy parameters in the new framework. In Chapter 4, we contribute to the literature by developing a novel expression to calculate the s/d ratio at a transplant center in the continuous distribution framework. We then develop a set-partitioning optimization model to design an equitable allocation policy with an objective to equalize the s/d ratios across transplant centers.

Chapter 2: Heterogeneous Donor Circles for Fair Liver Transplant Allocation

2.1 Introduction

Geographic inequity in access to liver transplantation across DSAs is well documented in the literature [56]. Indeed, as early as 2008, an HHS Advisory Committee on Transplantation recommended that organ allocation be evidence-based and not on the arbitrary boundaries of the DSAs. In 2012, the OPTN board adopted a strategic plan that included reducing geographic disparities in access to transplantation. Despite implementation in 2013 of broader organ sharing in a region for candidates with MELD scores ≥ 35 , geographic inequities remained in the system. The U.S. Scientific Registry of Transplant Recipients' (SRTR's) Liver Transplant Waiting List Outcomes Tool¹ (built on historical data from 2017 to 2019) shows that for waitlisted candidates in Los Angeles with MELD scores in the range of 25-29, only 15% received a transplant within 90 days, while for candidates in Indianapolis (with MELD scores in the range of 25-29), 72% received a transplant within 90 days. The DSA/Region allocation policy resulted in significant disparities even for candidates on transplant lists in close proximity. For example, SRTR's Liver Transplant Waiting List Outcomes Tool shows that for waitlisted candidates in New York City with MELD scores in the range of 25-29, only 15% received a transplant within 90 days, while for

¹<https://www.srtr.org/reports-tools/waiting-list-calculator/>, accessed June 26, 2020.

similar candidates in Newark, New Jersey, just 15 miles away, 41% received a transplant within 90 days. Because MELD scores directly correlate with the probability of death in the absence of an organ transplant in the next 90 days, different transplant wait times for candidates with the same MELD score across DSAs imply (i) significantly different mortality rates for candidates with the same MELD score in different DSAs, and (ii) significant variation in the median MELD score at transplant (MMaT).² Indeed, MMaT variance has typically been used by UNOS as a key metric in evaluating a proposal's effectiveness in mitigating geographic disparity (i.e., a lower value of MMaT variance indicates less disparity).

The accumulating dissent against the organ allocation policy in place prompted urgent actions in the U.S. The UNOS board (based on the recommendations of a Geography Committee formed in December 2017) adopted the following set of principles in June 2018 to guide future organ transplant policy relating to geographic aspects of organ distribution (that were also identified to be consistent with the Final Rule).

1. Reduce inherent differences in the ratio of the donor supply and demand across the country.
2. Reduce travel time expected to have a clinically significant effect on ischemic time and organ quality.
3. Increase organ utilization and prevent organ wastage.
4. Increase efficiencies of donation and transplant system resources.

The Geography Committee identified three potential distribution frameworks that fit with these four principles: (1) fixed distance from the donor hospital, (2) mathematically optimized boundaries,

²This is seen for example in 2016 data [37] where the highest MMaT is 39 and the lowest MMaT is 20.

and (3) continuous scoring (candidates to be ranked on the offer list on a combination of their clinical characteristics and proximity to a donor).³

Following public comment, on December 3, 2018, the UNOS board adopted an Acuity Circle policy (an implementation of the fixed distance from the donor hospital framework). Although there were legal challenges and political pressures from several quarters to maintain the existing system, the new Acuity Circle policy was implemented on May 14, 2019. However, within a day, on May 15, 2019, a federal court issued an injunction, and UNOS was required to revert to the prior system while legal challenges to the policy were pending. On January 16, 2020, the federal court reversed itself and decided not to keep the injunction in place while the case was pending. Subsequently, the Acuity Circle policy was once again implemented again on February 4, 2020.

Due to differences in demographics, disease incidence, and mortality leading to organ donations among the DSAs, there was a huge disparity in the *s/d* ratios across the DSAs. Figure 2.1 shows the wide variability in the *s/d* ratio (left) and an inverse relationship of this variability with observed MMaT scores (right). The *s/d* ratios (at DSAs) varied from 0.31 in NYRT (a DSA in New York) to 1.98 in FLWC (a DSA in Florida). This disparity primarily drove the differences in MMaT among the DSAs. In a study by Wey et al. [55], the *s/d* ratios in a DSA were found to be associated with MMaT in DSAs ($r = -0.56$; $P < 0.001$).

In this chapter, we use UNOS's stated principle of reducing inherent differences in the ratio of the supply to demand (*s/d*) as our objective explicitly within a mathematical optimization framework to design heterogeneous sized areas around the donation locations. One approach to

³https://optn.transplant.hrsa.gov/media/2506/geography_recommendations_report_201806.pdf, accessed April 30, 2022.

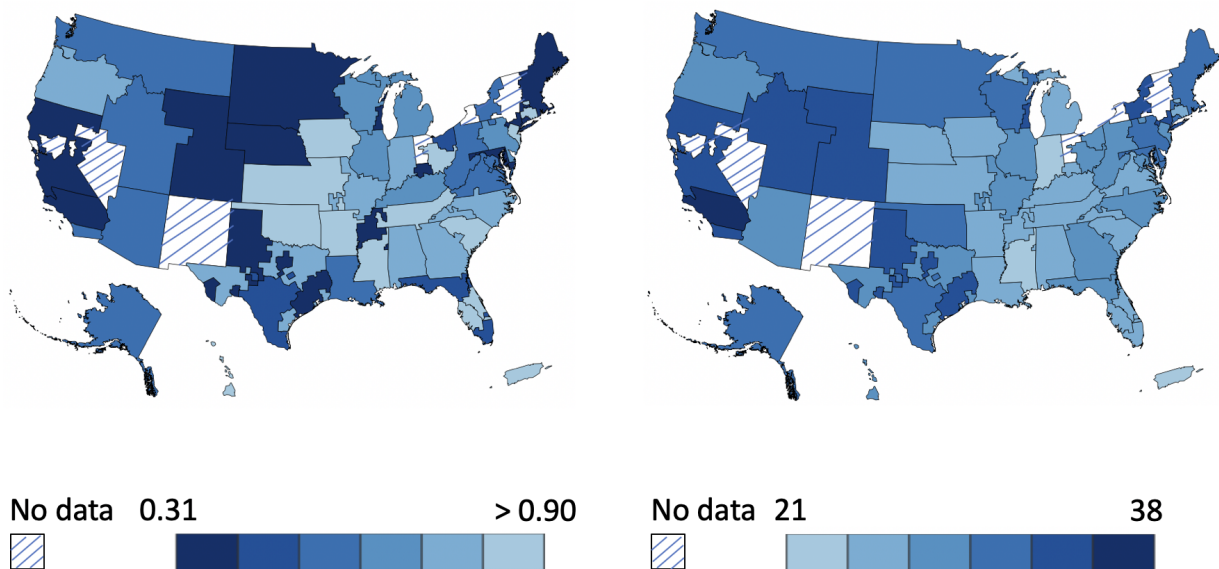


Figure 2.1: Lower supply to demand (s/d) ratios at a DSA (left) correspond to a higher MMaT at the DSA (right). The time period of analysis is from July, 2013 to June, 2017.

reduce inequity is through the central distributive principle, proposed by Rawls [42]: the least well-off group in the society should be made as well off as possible. We use this *maximin* principle to design heterogeneous sized areas that maximize the minimum value of the s/d ratio across all transplant centers (or DSAs). We then apply a secondary optimization to minimize the disparity between the transplant centers (or DSAs) with the highest and lowest s/d ratios.

Our mathematical optimization model can be applied using zip codes or DSAs as the geographical units. When using zip codes as the geographical units, the model may be viewed as a heterogeneous radii circle policy (as compared to a fixed radius circle policy⁴). When using DSAs as the geographical units, the model may be viewed as a type of neighborhood model [35], where the neighborhood around a DSA is somewhat circular in shape.

Without organ sharing among DSAs, we found that the s/d ratio ranges from 0.31 to 1.98.

⁴In a fixed radius circle policy, the radii of the circles around the donor hospitals are identical, whereas in a heterogeneous radii circle policy, the radii of circles around the donor hospital can take different values. We drop radius/radii and refer to them as a fixed circle and a heterogeneous circle policy.

With 500 nautical-mile (NM) fixed circles, the s/d ratio improves and ranges from 0.37 to 0.84. We show that when heterogeneous circles are used around the donation zip codes, the s/d ratio ranges from 0.55 to 0.60, meaning that there is a much lower disparity in organ access among the transplant centers. Further, when we examine the s/d ratio disparity for transplant centers that are close to one another (specifically, within 150 NM of each other) the heterogeneous circle policy reduces the s/d ratio disparity to one-fourth compared to the fixed 500 NM circle policy.

We ran simulations with SRTR's Liver Simulated Allocation Model (LSAM, version 2014) using historical patient and organ donor data. The version of the tool available to us was based on DSAs. Hence, we compared our optimized geographical neighborhoods using DSAs. The results show that in comparison to the prior OPTN 11 region policy (in place until February 4, 2020), an allocation policy based on our optimized heterogeneous circular neighborhoods (around DSAs), with a maximum radius of 500 NM and full regional sharing of all organs with MELD scores ≥ 15 , drastically reduces the variance of MMaT across DSAs (from 13.66 to 2.00) and average annual deaths (from 3,745 to 3,568), for a modest increase in average travel distance (from 199 NM to 258 NM).

A key policy insight is that the one-size-fits-all framework (i.e., the currently proposed Acuity Circle policy) approach taken by UNOS does not adequately address the problem of reducing differences in the ratio of the donor supply to demand across the country. Rather, a customized approach that accounts for where the organ supply and demand occur and adjusts radii of the circles more effectively addresses UNOS' stated goal of equalizing s/d ratios. The remainder of the chapter is organized as follows. In the next section, we give a brief overview of the liver allocation system in the U.S., and review proposals and related research. Section 2.3 presents our optimization methodology. Section 2.4 describes our findings and projected outcomes.

Section 2.5 summarizes and provides concluding remarks.

2.2 Related Research

Redistricting is a problem that occurs frequently in multiple domains (e.g., political redistricting, school redistricting, and sales territory assignments) where a finite, denumerable set of non-overlapping geographical units are aggregated into regions/districts subject to some criteria. Hess et al. [32] and [21] introduced the use of optimization techniques for political redistricting. Zoltners and Sinha [59] discuss an application of redistricting in sales territory assignments, and Caro et al. [15] discuss school redistricting using integer programming. Much of the redistricting literature focuses on political redistricting [28, 36, 43, 53]. Two important considerations in redistricting problems are the contiguity and compactness of the districts. In this regard, Shirabe [46] proposed a flow-based model for contiguity constraints, which has been typically used in subsequent integer programming approaches. However, contiguity constraints make redistricting problems notoriously hard to solve exactly [36, 43].

Focusing on transplants, and disregarding geographical equity for the moment, Kong et al. [38] studied the problem of maximizing efficiency by maximizing total intraregional transplants by redesigning of the liver allocation regions. They formulate the problem as a set-partitioning problem and use a branch-and-price algorithm to approximate solutions. Stahl et al. [49] consider geographic equity (measured by minimum OPO intraregional transplant rate), along with efficiency (measured by total intraregional transplants), but they restrict their regions to contain up to eight DSAs due to computational challenges.. Extending their work, Demirci et al. [17] developed a branch-and-price algorithm to incorporate a larger set of potential regions and explored the

efficient frontier in a trade-off between efficiency and geographical equity. Their metric of geographical equity maximizes the minimum in-district viability-adjusted transplant rates per waiting list candidate, which is sensitive to the number of waiting list patients added by the transplant centers. This is problematic because for low-MELD patients, the survival benefit of transplantation is minimal [40], and the chances of receiving an organ vary across geographies. Consequently, the transplant centers differ in their practices of adding low-MELD patients to the waiting list.

Gentry et al. [23] used optimization to reorganize DSAs into regions/districts to reduce geographical disparity. Their objective was to minimize the sum of the absolute differences between the number of deceased-donor livers recovered in each district and the ideal number of livers that would be offered in each district if each liver was given to the medically most urgent candidate in the country. Working closely with the liver committee of UNOS, they proposed eight-district and four-district (reorganized DSA) maps. The proposed maps were under active consideration by UNOS from 2015 to 2017. However, ultimately after significant debate and public comment, they were not adopted.

Kilambi and Mehrotra [35] introduced the neighborhood framework in organ allocation as a way to provide for broader sharing and improve geographic equity. Each DSA has its own neighborhood, which consists of a unique set of other DSAs (or neighbors) with which it shares its organs. A DSA can be part of multiple neighborhoods; therefore, the neighborhoods can be overlapping, which makes it difficult to represent all neighborhoods on a single map. Interconnectivity and overlap among neighborhoods provide resilience to supply and demand uncertainty. The neighborhood framework reduces to redistricting when all the DSAs in a neighborhood have the identical neighborhood. Thus, the redistricting framework can be viewed

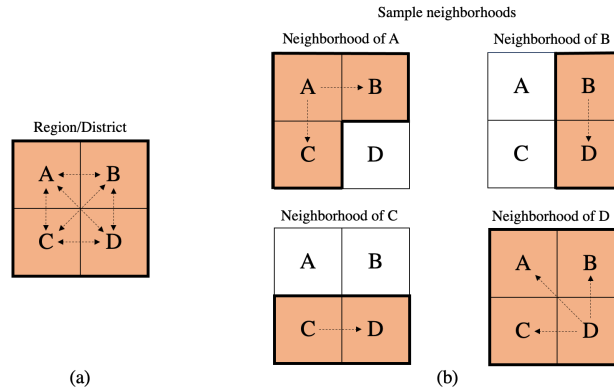


Figure 2.2: Illustration of the difference between Regions/Districts and neighborhoods. (a) Let DSAs A, B, C and D form a region or district. They all share with each other. (b) With the neighborhood displayed, the neighborhood of A consists of DSAs A, B and C. Therefore, A shares only with A, B, and C. Similarly, B shares with B and D; C shares with C and D; and D shares with A, B, C, and D.

as a special case of a neighborhood framework. Figure 2.2 illustrates the difference between regions/districts and the neighborhood framework. Using the neighborhood framework, Kilambi and Mehrotra [35] developed an optimization model to design DSA neighborhoods to minimize the absolute deviation of the s/d ratios across neighborhoods from the national average.

Ata et al. [10] used fluid approximation and game theory to show that multiple listings (a patient is listed at more than one transplant center, potentially in another DSA or region so that he/she can get organ offers from multiple places) can reduce geographical disparity in kidney allocation. However, fewer than 2% of patients waiting for a liver transplant multiple list (on April 14, 2021, the OPTN website shows that only 181 out of 11868 candidates are multiple listed). Bertsimas et al. [14] suggest the use of tradeoff curves to assess the three organ distribution frameworks identified by the Geography Committee. Running a large number of simulations for the three distribution frameworks, they plot tradeoff curves of efficiency (measured as average travel distance) versus fairness (measured as deaths or variance of MMaT). For a given value of the efficiency metric, the tradeoff curve then identifies the policy with the greatest

fairness. However, they did not consider the neighborhood or heterogeneous circle distribution frameworks in their study. In a recent study, Ata et al. [8] analyze a broad class of ranking policies in kidney allocation using an analytical framework. They find that allowing different patients' ranking rules, depending on the quality of the kidney, can reduce organ wastage.

There are two methods of organ donation: (1) living donation and (2) deceased donation. Alagoz et al. [3] study the optimal timing of living-donor liver transplantation when the patient is either ineligible or has decided not to receive organs from deceased donors. They ignore the risk to living donors in their model. Ergin et al. [18] model liver exchange as a market-design problem, where they account for risk to donors and compatibility issues. Using data from South Korea, they show that their proposed mechanism can increase the number of living-donor transplants by 30%. However, deceased donation has been contributing to greater than 95% of liver donations in the last 15 years in the U.S. Unlike living donation, which can be arranged privately between a patient-donor pair, deceased donor organs are considered national resources (whose allocation is determined by government policy). We focus on deceased donation in this study; the parameters used in our model and their policy implications are likely to remain unaffected with recent promising developments in living donation.

2.3 Model Formulation

Consistent with UNOS' stated principles, our approach is to design an organ distribution policy that equalizes s/d ratios across transplant centers, and thus, mitigates geographical disparities. We start by aggregating the historical supply and demand of organs by geographical location for the period of study. We assume that the distribution of organ quality (Appendix A.1 compares

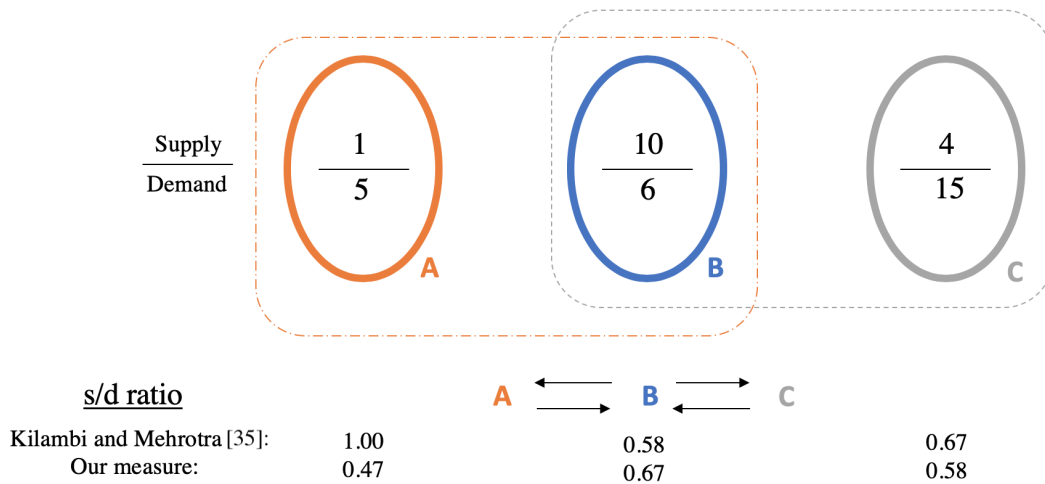


Figure 2.3: Comparing our s/d ratio measure with that of Kilambi and Mehrotra [35]. Their measure artificially inflates the s/d ratio.

transplant organ quality on a four-year dataset used in our study; we find that there are no significant differences in the distribution of organ quality at recovery across the different regions) and the patient’s health characteristics are similar across donor hospitals and transplant centers. While there are certainly differences currently in the patient health characteristics from state to state (e.g., at present, California has a higher proportion of high-MELD candidates than Tennessee), this is largely a function of accumulated disparity over the years; in steady state with no disparity in the s/d ratios, the distribution of MELD scores should be similar.

We formulate an Integer Programming model (IP) that uses a neighborhood framework. Each supply location (e.g., a DSA, zip code, or donor hospital, depending on the context) is assigned a unique set of demand locations (a DSA or transplant center), which is referred to as its neighborhood. In a setting where the geographical units of supply and demand are DSAs, a neighborhood of a DSA consists of other DSAs (including itself) with which it shares its organs.

Kilambi and Mehrotra [35] pioneered the idea of defining neighborhoods for DSAs. However, their definition of a supply-to-demand ratio at a DSA is somewhat problematic. They model the

s/d ratio of a DSA as the ratio of the total supply to the total demand in the DSA's neighborhood. In other words, they treat all DSAs in that neighborhood as a single unit. However, a DSA can also be part of another neighborhood, which results in the artificial inflation of the s/d ratio. To illustrate, consider three DSAs A (Supply: 1, Demand: 5), B (Supply: 10, Demand: 6), and C (Supply: 4, Demand: 15), as shown in Figure 2.3. A shares with B and receives from B; B shares with and receives from both A and C; and C shares with B and receives from B. The neighborhood of A consists of A and B; the neighborhood of B consists of A, B, and C; and the neighborhood of C consists of B and C. Kilambi and Mehrotra [35] compute the s/d ratios of A, B, and C as 1.00 (11/11), 0.58 (15/26), and 0.67 (14/21), respectively. However, in aggregate, the s/d ratio for this three-region system is only 0.58! Further, their objective function is to minimize the absolute deviation of the s/d ratios from a target value (the national average), which effectively treats deviations below the average identically to deviations above the average. Unfortunately, locations with deviations below the average (i.e., lower s/d ratios and higher MMaT scores) have poorer outcomes (greater chances of dying while waiting for a transplant) than locations with deviations above the average. Thus, in a setting where the desire is to minimize disparities, it does not seem appropriate to treat these two deviations identically. By maximizing the worst s/d ratio, our primary focus is on minimizing the deviation below the national average. Finally, we note that our model does not require symmetric organ sharing (which they enforce), giving more flexibility in optimization.

Notation	Description
$i \in \mathcal{I} = \{1, \dots, N_{sup}\}$	Supply location (e.g., a DSA, zip code, or donor hospital)
$j \in \mathcal{J} = \{1, \dots, N_{dem}\}$	Demand location (e.g., a DSA or transplant center)
Parameters:	
s_i	Number of livers from deceased donors recovered (or supply) at i
d_j	Number of incident waiting list additions (or demand) at j
τ_{ij}	Distance between locations i and j
τ_{max}	Maximum permissible distance from a supply location to a demand location
c_j	Number of transplant centers in demand location j
$c_i^{(r)}$	Number of transplant centers that are $\leq r$ distance units away from supply location i
c_{min}	Minimum number of transplant centers with which a supply location must share its organs
$\lambda_{[S-1]}^*$	Minimum s/d ratio value to be used in Stage 2 optimization
$s_{ij}^{(r)}$	Apportioned share of organs from i to j when the farthest demand location in i 's neighborhood is r units away
Decision variables:	
x_{ij} (General model)	1 if i shares its organs with j , and 0 otherwise
x_{ir} (Set-partitioning model)	1 if the farthest member in the neighborhood of i is r units away from i , and 0 otherwise
λ	Minimum s/d ratio for an allocation
β	Maximum s/d ratio for an allocation

Table 2.1: Model Notation

2.3.1 Supply-Demand Ratio Calculation

First, we define our s/d ratio measure. Recall that we assumed the MELD scores of candidates across geographies are independent and identically distributed (i.i.d.); and when an organ is recovered, all locations in the neighborhood are treated alike. For a given demand location j in the neighborhood of supply location i , we model the expected supply received (by j) from i to be proportional to j 's demand over the total demand competing for i 's supply. Using this expected allocation of the supply in the example in Figure 2.3, we find that 5/11 units of the supply from A are allotted to A, and 6/11 units of the supply from A are allotted to B. Similarly,

$(5/26) \times 10$, $(6/26) \times 10$, and $(15/26) \times 10$ units of the supply from B are allotted to A, B, and C, respectively. Finally, $(6/21) \times 4$ units of the supply from C are allotted to B, and $(15/21) \times 4$ units of the supply from C are allotted to C. Dividing the expected supply provided to each location by its demand, we find the s/d ratios of 0.47, 0.67, and 0.58 for A, B, and C, respectively, with our measure. Using the notation described in Table 2.1, we formally calculate,

$$\text{Expected supply from } i \text{ to } j = \frac{d_j}{\sum_{k=1}^{N_{dem}} d_k x_{ik}} s_i x_{ij}$$

To determine the overall supply-to-demand ratio, we first sum the expected supply over all supply locations and then divide by j 's demand, d_j giving:

$$\text{s/d ratio at } j = \sum_{i=1}^{N_{sup}} \frac{1}{\sum_{k=1}^{N_{dem}} d_k x_{ik}} s_i x_{ij}$$

We note that the way we calculate the expected s/d ratio does not account for organs that a DSA may receive only due to national sharing. However, these organs are generally a very small fraction (less than 4% in a four-year dataset used in our study) and should not significantly impact the s/d ratios realized in practice.

2.3.2 General Model

We now describe our model, which solves the problem in two stages. In Stage 1, we apply the *maximin* equity principle to maximize the performance of the worst demand location (i.e., we maximize the value of the lowest s/d ratio across all demand locations). In Stage 2, we reduce the disparity among the different demand locations. To do this, we minimize the disparity

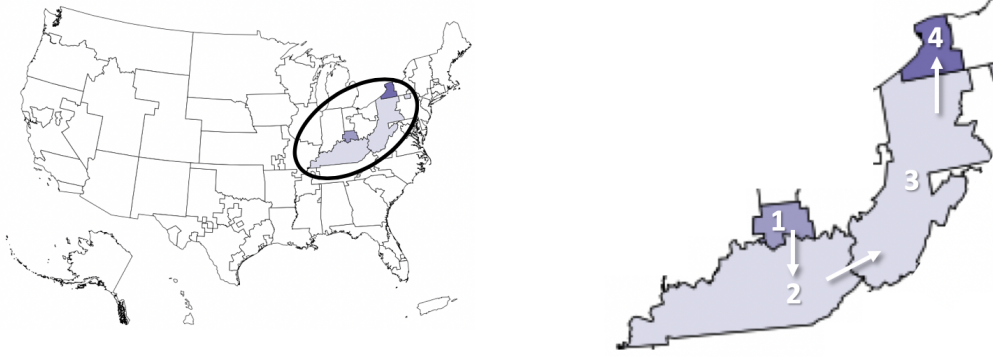


Figure 2.4: Illustration of sharing and receiving contiguity. If $x_{14} = 1$, with sharing contiguity, $x_{12} = x_{13} = 1$; and with receiving contiguity $x_{24} = x_{34} = 1$.

between the best and worst demand locations, while ensuring the s/d ratio of the worst demand location remains at the optimum value obtained from the Stage 1 optimization. We now present the Mixed-Integer Linear Programs (MIPs) for the different stages.

2.3.2.1 Stage 1 Formulation

In Stage 1, we seek to maximize the s/d ratio of the worst demand location.

$$\text{[S-1] Maximize } \lambda \tag{2.1}$$

$$\text{subject to: } \lambda \leq \sum_{i=1}^{N_{sup}} \frac{1}{\sum_{k=1}^{N_{dem}} d_k x_{ik}} s_i x_{ij} \quad \forall j \in \mathcal{J} \tag{2.2}$$

$$x_{ij} \tau_{ij} \leq \tau_{max} \quad \forall i \in \mathcal{I}, j \in \mathcal{J} \tag{2.3}$$

$$x_{ij} = 1 \quad \forall i = j, i \in \mathcal{I}, j \in \mathcal{J} \tag{2.4}$$

$$\sum_{j=1}^{N_{dem}} c_j x_{ij} \geq c_{min} \quad \forall i \in \mathcal{I} \tag{2.5}$$

$$\text{Contiguity constraints} \tag{2.6}$$

$$x_{ij} \in \{0, 1\} \quad \forall i \in \mathcal{I}, j \in \mathcal{J} \tag{2.7}$$

Constraint (2.2) models λ as the lower bound of the s/d ratios across all the demand locations, and the objective is to maximize this lower bound. Constraint (2.3) limits the size of the neighborhood (by limiting how far an organ can be transported for transplantation); constraint (2.4) implies that if a supply-and-demand location coincide (e.g., a DSA or zip code that has both a donor hospital and a transplant center), it must share with itself; and constraint (2.5) ensures that there are at least c_{min} transplant centers in a neighborhood.⁵ We also include contiguity constraints to ensure that the designed neighborhoods are contiguous and somewhat compact in shape. This is enforced by an adjacency matrix, which describes locations that are geographically adjacent to each other, and two types of contiguity constraints. Sharing contiguity ensures that if location r supplies organs to location t (which is not adjacent to it), then all locations between r and t also receive organs from location r . Receiving contiguity ensures that if location r supplies organs to location t (which is not adjacent to it), then all locations between r and t also supply organs to location t . Figure 2.4 illustrates receiving and sharing contiguity, ensuring that if location 1 shares its organs with location 4, locations 2 and 3 also share their organs with location 4, and locations 2 and 3 also receive organs from location 1. Appendix A.2 describes flow-based mathematical constraints, applying Shirabe’s [46] approach, which can be used to enforce sharing and receiving contiguity with any geographical shapes, as well as a linearization of constraint (2.2) in the nonlinear integer programming model [S-1].

⁵Deceased-donor livers vary in quality, and marginal livers are more likely to be used and less likely to be discarded when more competition exists among transplant centers [22, 30]. Thus UNOS requires that a minimum number of transplant centers be in contention for organs from a supply location.

2.3.2.2 Stage 2 Formulation

In Stage 2, we minimize the maximum absolute difference of the s/d ratios among demand locations. This is achieved by constraining the lowest s/d ratio value to be greater than or equal to the Stage 1 objective $\lambda_{[S-1]}^*$, and by minimizing the maximum s/d ratio value across all demand locations.

[S-2] Minimize β

$$\text{subject to: } \beta \geq \sum_{i=1}^{N_{sup}} \frac{1}{\sum_{k=1}^{N_{dem}} d_k x_{ik}} s_i x_{ij} \quad \forall j \in \mathcal{J} \quad (2.8)$$

$$\lambda \geq \lambda_{[S-1]}^* \quad (2.9)$$

$$\text{All constraints from [S-1]} \quad (2.10)$$

The optimal values of x_{ij} obtained by optimizing [S-1], followed by [S-2], are used to construct the new optimized geographical scheme.

2.3.3 Circular Contiguity and a Set-Partitioning Model

One of the chief complaints in the liver and lung lawsuits was that a candidate receiving the transplant organ may be geographically farther away from the donated organ than another sicker candidate. In other words, neighborhood boundaries that allow an organ to be transported farther away to a less sick candidate than a closer sicker candidate (because the sicker candidate is outside the neighborhood) goes against generally accepted perceptions of fairness. This notion suggests that we consider (roughly) *circular contiguity* for neighborhoods. If the radius of a

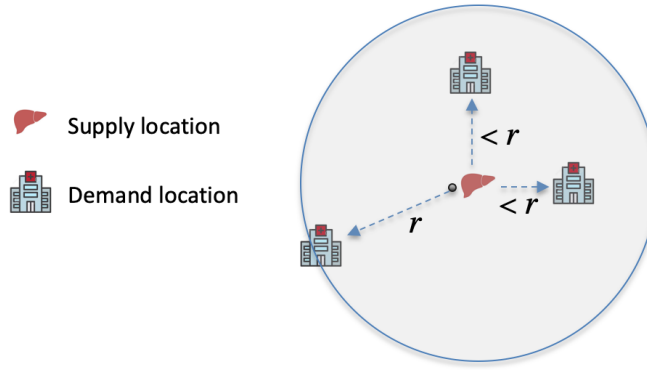


Figure 2.5: Illustration of circular contiguity: If a neighborhood is r units in radius around the supply location, then all demand locations within r units must be in the neighborhood.

neighborhood is r units around the supply location, then all demand locations within r units away are in the neighborhood (Figure 2.5).

Circular contiguity allows for a more computationally tractable reformulation of the previous model. For a neighborhood of a given radius r , one can easily calculate (a priori) the amount of supply allocated to each demand location in the neighborhood. This enables us to reformulate [S-1] and [S-2] linearly as *Set-Partitioning Problems*, which also makes them scalable. In the set-partitioning formulation, x_{ir} is a binary decision variable that takes a value 1 if the radius of the neighborhood of i is r units (all demand locations $\leq r$ units from i are part of the neighborhood), and 0 otherwise.

2.3.3.1 Stage 1 Formulation

$$\text{[SP-1] Maximize } \lambda \tag{2.11}$$

$$\text{subject to: } \lambda \leq \sum_{i=1}^{N_{sup}} \sum_{r \in \mathcal{R}_i} \frac{x_{ir} s_{ij}^{(r)}}{d_j} \quad \forall j \in \mathcal{J} \tag{2.12}$$

$$\sum_{r \in \mathcal{R}_i} x_{ir} = 1 \quad \forall i \in \mathcal{I} \tag{2.13}$$

$$\sum_{r \in \mathcal{R}_i} c_i^{(r)} x_{ir} \geq c_{min} \quad \forall i \in \mathcal{I} \tag{2.14}$$

$$x_{ir} \in \{0, 1\} \quad \forall i \in \mathcal{I}, \forall r \in \mathcal{R}_i \tag{2.15}$$

For a given radius r , $s_{ij}^{(r)}$ denotes the apportioned share of i 's organs that are expected to be offered to location j . In other words, $s_{ij}^{(r)} = \frac{d_j}{\sum_{k: \tau_{ik} \leq r} d_k} s_i$, which can be precomputed for a given radius r . Note that for a given supply location i , we do not need to consider a continuum of possible neighborhood radii. Rather (because this apportionment of organs will only change when a new demand location is added to the neighborhood), we only need to consider a finite set of values of r that correspond to the distance from i to each of the other demand locations that are within τ_{max} . In [SP-1], the set \mathcal{R}_i contains the possible values of r created accordingly for supply location i . Constraint (2.12) models λ as the lower bound of the s/d ratios across all demand locations; and the objective is to maximize this lower bound. Constraint (2.13) allows one assignment of r to each supply location; and constraint (2.14) ensures a minimum number of transplant centers in the neighborhood.

2.3.3.2 Stage 2 Formulation

Once the optimal solution $\lambda_{[SP-1]}^*$ to [SP-1] is obtained, we can solve [SP-2] to minimize the maximum s/d ratio while ensuring that the minimum s/d ratio remains at least $\lambda_{[SP-1]}^*$.

$$\begin{aligned} \text{[SP-2] Minimize } & \beta \\ \text{subject to: } & \beta \geq \sum_{i=1}^{N_{sup}} \sum_{r \in \mathcal{R}_i} \frac{x_{ir} s_{ij}^{(r)}}{d_j} \quad \forall j \in \mathcal{J} \end{aligned} \quad (2.16)$$

$$\lambda \geq \lambda_{[SP-1]}^* \quad (2.17)$$

$$\text{All constraints from [SP-1]} \quad (2.18)$$

2.4 Data and Results

This study used data from SRTR. The SRTR data system includes data on all donors, waitlisted candidates, and transplant recipients in the U.S., submitted by members of the OPTN. The Health Resources and Services Administration (HRSA), U.S. Department of Health and Human Services, provides oversight to the activities of OPTN and SRTR contractors.

In the data, encompassing the four years starting from July 2013 and ending in June 2017, the supply or the total number of livers (from deceased donors) donated from all donor hospitals in the U.S. is 26,899. The patient pool is dynamic: new patients enlist, waiting candidates die or become too sick for transplant and are removed, and the MELD scores get updated periodically. We measure demand (44,959) as the total incident⁶ adult patients whose MELD scores became at least 15 during the four years, which gives a national s/d ratio of 0.5983. There are two reasons

⁶We consider incident patients so that the model parameters are not biased due to accumulated disparity, and thus are exogenous to the geographical scheme.

for excluding low-MELD patients from the demand: (1) patients with MELD scores <15 have no survival benefit from transplantation [40]; therefore, our demand measure is less sensitive to the number of low-MELD patients added to the waiting list and (2) transplant centers differ in their practices of listing low-MELD patients, across the country (which would create an artificial increase in demand for a transplant center listing low-MELD patients compared to a transplant center that does not). In practice, the fraction of transplants to low-MELD patients is relatively very low—about 1.08% (in the four years encompassing our study), supporting the decision to exclude them.

We apply the set-partitioning optimization model to two versions of the data: a zip-code cluster version where the supply locations are zip-code clusters (clustered by the first three digits and first four digits) and the demand locations are the 142 transplant centers, and a DSA version where the supply and demand locations are the DSAs. We restrict r (radius around the supply locations) within the range 150 NM to τ_{max} for every \mathcal{R}_i , constraining the minimum and maximum size of the neighborhoods. We set $c_{min} = 3$, ensuring that at least three transplant centers are present in a neighborhood.⁷ We used R 3.5.1 and the commercial solver Gurobi 8.1.1 to solve the set-partitioning optimization models on a 3.2 GHz 6-Core Intel Core i7 iMac with 32 GB RAM.

2.4.1 Zip-code Cluster Version

The locations of the zip codes and transplant centers are indicated by their latitude and longitude values. To calculate the distance between a three-digit (four-digit) zip-code cluster and a transplant center, we first find the centroid of the zip-codes in the cluster having the same

⁷For every DSA with demand, there are close to three ($142/52=2.73$) transplant centers.

first three digits (four digits) and then use the “geosphere” package in R to calculate the shortest distance between two points (centroid of the zip cluster and transplant center) according to the “Vincenty (ellipsoid)” method.

There are a total of 641 three-digit and 1,380 four-digit zip-code clusters with the supply in our data.⁸ We vary τ_{max} from 350 NM to 700 NM in steps of 50 NM. We do not include the zip codes in Hawaii and Puerto Rico in our analysis, given that they are more than 1,000 miles from the transplant centers in the mainland U.S. Consistent with the current policy zip codes in Alaska are considered to be situated at the Seattle Tacoma Airport in Washington State. We require that the minimum radius of a neighborhood be 150 NM (to try and keep parity with the radius of the innermost concentric circle in the Acuity Circle policy). Because a transplant hospital may not necessarily be exactly 150 NM from a zip-code cluster, this is enforced by ensuring that the closest transplant center greater than or equal to 150 NM away is included in the neighborhood, unless it is greater than τ_{max} miles away. Appendix A.3 provides computational details—the problem size, running times, cutting planes, simplex iterations, etc.—for the set-partitioning model on the four-digit zip-clusters.

Table 2.2 provides a comparison of the s/d ratios. To compare against the fixed radius type of policy currently in place (i.e., Acuity Circle), we also computed the s/d ratio for homogeneous radii circles by fixing the radius of each zip-code cluster to τ_{max} . Compared to the heterogeneous radius circle policy, the ‘one-size-fits-all’ fixed radius policy does a poor job at equalizing the s/d ratios across transplant centers. The heterogeneous circle policy at $\tau_{max} = 500$ NM is able to keep the ratio at transplant centers between 0.55 and 0.60 (compared to the national s/d ratio of

⁸Recall that the optimization variable is x_{ir} . In the zip-code cluster version, i is the three-digit (four-digit) zip-code cluster, and r is the radius selected (from the discrete set of possible radii choices).

Allocation Policy	s/d ratio		Maximum (Median) s/d ratio
	Range	Std. deviation	difference within 150 NM from TC
$\tau_{max} = 350$ NM			
Fixed radius circles (Three-digit zip)	0.39-1.09	0.123	0.59920 (0.04611)
Fixed radius circles (Four-digit zip)	0.38-1.09	0.123	0.60235 (0.04559)
Three-digit zip-code cluster model	0.51-0.88	0.098	0.33043 (0.05047)
Four-digit zip-code cluster model	0.51-0.88	0.103	0.33813 (0.07085)
$\tau_{max} = 400$ NM			
Fixed radius circles (Three-digit zip)	0.37-0.85	0.112	0.23255 (0.03690)
Fixed radius circles (Four-digit zip)	0.37-0.84	0.112	0.22818 (0.03633)
Three-digit zip-code cluster model	0.53-0.62	0.033	0.08571 (0.00042)
Four-digit zip-code cluster model	0.53-0.61	0.030	0.07763 (0.00028)
$\tau_{max} = 450$ NM			
Fixed radius circles (Three-digit zip)	0.38-0.88	0.124	0.20629 (0.02900)
Fixed radius circles (Four-digit zip)	0.38-0.87	0.124	0.19770 (0.02048)
Three-digit zip-code cluster model	0.54-0.61	0.023	0.05277 (0.00108)
Four-digit zip-code cluster model	0.54-0.61	0.024	0.06125 (0.00043)
$\tau_{max} = 500$ NM			
Fixed radius circles (Three-digit zip)	0.37-0.84	0.137	0.20941 (0.03632)
Fixed radius circles (Four-digit zip)	0.37-0.84	0.137	0.20851 (0.04489)
Three-digit zip-code cluster model	0.55-0.60	0.022	0.04621 (0.00009)
Four-digit zip-code cluster model	0.55-0.60	0.021	0.04922 (0.00025)
$\tau_{max} = 550$ NM			
Fixed radius circles (Three-digit zip)	0.37-0.91	0.145	0.17331 (0.03808)
Fixed radius circles (Four-digit zip)	0.36-0.91	0.146	0.17213 (0.03882)
Three-digit zip-code cluster model	0.55-0.60	0.020	0.05070 (0.00029)
Four-digit zip-code cluster model	0.55-0.60	0.019	0.04387 (0.00025)
$\tau_{max} = 600$ NM			
Fixed radius circles (Three-digit zip)	0.34-0.97	0.152	0.17767 (0.04866)
Fixed radius circles (Four-digit zip)	0.34-0.96	0.152	0.17819 (0.04473)
Three-digit zip-code cluster model	0.55-0.60	0.018	0.05407 (0.00113)
Four-digit zip-code cluster model	0.55-0.60	0.018	0.03613 (0.00015)
$\tau_{max} = 650$ NM			
Fixed radius circles (Three-digit zip)	0.33-0.94	0.152	0.16743 (0.02449)
Fixed radius circles (Four-digit zip)	0.33-0.93	0.152	0.17091 (0.02457)
Three-digit zip-code cluster model	0.55-0.60	0.017	0.05049 (0.00016)
Four-digit zip-code cluster model	0.55-0.60	0.018	0.03336 (0.00012)
$\tau_{max} = 700$ NM			
Fixed radius circles (Three-digit zip)	0.32-0.94	0.145	0.17881 (0.04773)
Fixed radius circles (Four-digit zip)	0.32-0.94	0.145	0.18275 (0.04654)
Three-digit zip-code cluster model	0.55-0.60	0.016	0.05100 (0.00010)
Four-digit zip-code cluster model	0.55-0.60	0.017	0.03402 (0.00007)

Table 2.2: Comparison of the s/d ratios between fixed and heterogeneous circles (supply and demand locations are zip-code clusters and transplant centers (TCs), respectively).

0.5983), while the fixed 500 NM radius circle policy has an s/d ratio variation between 0.37 and 0.84.

We also examine the difference in the s/d ratio of nearby transplant centers (defined as being within 150 NM). Table 2.2 provides both the maximum and median values of this difference. As is evident, in the heterogeneous circles policy, the value of the s/d ratio at nearby transplant centers is very similar—which can hopefully lead to more equitable transplant outcomes in nearby transplant centers. For most of the transplant centers, the difference in the s/d ratio is

at the scale of 10^{-4} , as indicated by the median values.

As we increase τ_{max} from 350 NM to 700 NM, the minimum s/d ratio increases, and the range of the s/d ratio decreases. When $\tau_{max} = 400$ NM, the s/d ratio range is already quite narrow at 0.53-0.61, and once $\tau_{max} = 500$ NM, the s/d ratio range stays steady at 0.55-0.60. Figure 2.6 shows the quartiles of the radii when using four-digit zip-code clusters. When τ_{max} is 500 NM, the first, second, and third quartiles of the radii are 211, 305, and 415 NM, respectively. Compared to the fixed radius circle policy, the heterogeneous radii circle policy achieves an equalization in the s/d ratio (near the national average) while keeping transport distances lower. This has an added benefit. Because the radii of the circles are smaller, each donor zip-code cluster on average has 24 (median of 20) transplant centers, as compared to the fixed radii circles that have on average 39 transplant centers (median of 43). The logistics of a donor hospital (zip-code cluster) coordinating with a smaller number of transplant centers can be much simpler. One may wonder whether fixed population circles (i.e., the radius of the circle around each transplant center is set so that they all cover the same number of people) would reduce disparity. Using the s/d metric defined and introduced in this chapter, Haugen et al. [31] analyze the disparity in the s/d ratios across transplant centers with fixed population circles. They find that circles covering a population of 12 million individuals provides s/d values ranging from 0.27 to 2.14. Increasing the size of the circles to cover 50 million individuals decreases the s/d variation to 0.43–1.01.

To check whether our solution is robust to variations in the supply and demand across time, using the optimal radii obtained with the four years of data, we recalculate the s/d ratio range, skipping one year of (supply and demand) data at a time. We find that, on average, the minimum (absolute) s/d ratio changes by 0.016 points, and the maximum (absolute) changes by 0.018 points (based on $\tau_{max} = 500, 550, 600, 650, \text{ and } 700$ NM), which indicates that the results

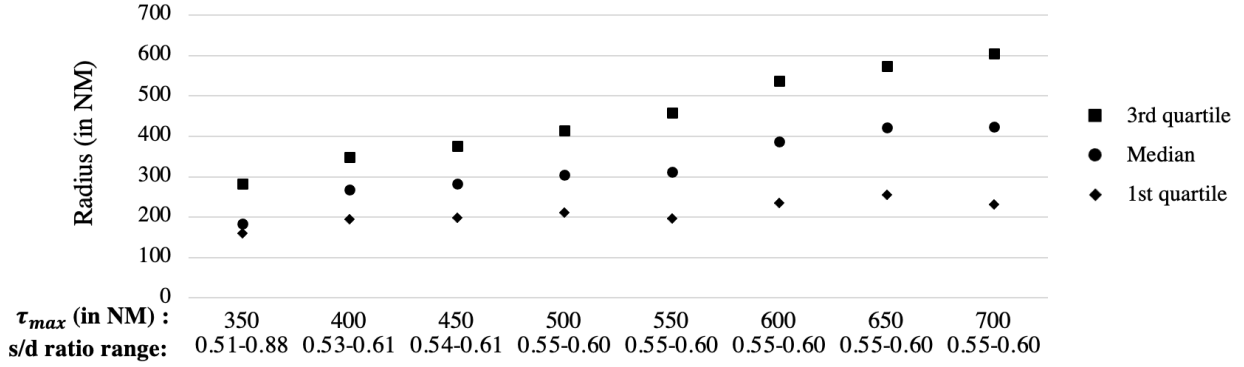


Figure 2.6: Quartiles of radii in the four-digit zip-code cluster models.

are fairly robust to variations in the data.

Given that the current implementation of LSAM does not support schemes based on zip-code clusters, we could not evaluate our zip-code based allocation policy via the LSAM simulation model. Instead, we use the results of the DSA version described in the next section and run the LSAM simulation on the neighborhoods it generates to evaluate the effectiveness of our allocation policy in reducing geographical disparity.

2.4.2 DSA Version

Using DSAs as the geographical unit preserves the existing important relationships between donor hospitals and the OPO in each DSA. If indeed, the court rules in a manner that reinstates DSAs as a geographical unit, then our method shows how they could share organs to achieve equitable outcomes with regard to the s/d ratio.

The distance between any two DSAs i and j , τ_{ij} , is calculated as the mean of the transplant-volume-weighted distance between donor hospitals in DSA i and the transplant centers in DSA j , and the reverse. Because six DSAs do not have a transplant hospital, there are 58 DSAs with supply and 52 DSAs with demand. Consistent with Gentry et al. [23] and Kilambi and Mehrotra

Allocation Policy	s/d ratio		$\tau_{max}, \bar{\tau}$ (in NM)	Max. (Median) s/d ratio difference among adjacent DSAs
	Range	Std. deviation		
OPTN 11 regions	0.42-0.76	0.109	843, 401	0.228 (0.117)
Gentry et al. [23]	0.52-0.69	0.054	975, 569	0.120 (0.036)
Kilambi and Mehrotra [35]	0.35-0.99	0.157	1380, 666	0.615 (0.246)
[SP-2], $\tau_{max} = 500$ NM	0.50-0.65	0.054	500, 349	0.151 (0.086)
[SP-2], $\tau_{max} = 600$ NM	0.52-0.65	0.051	600, 409	0.132 (0.077)
[SP-2], $\tau_{max} = 700$ NM	0.53-0.63	0.033	700, 422	0.096 (0.036)

Table 2.3: Comparison of the s/d ratios among different allocation policies in the DSA version (supply and demand locations are 58 DSAs and 52 DSAs, respectively). τ_{max} and $\bar{\tau}$ represent the maximum and average distance, respectively, of the farthest DSA in a neighborhood/region/district in each allocation policy.

[35], we allow (as exceptions to τ_{max}) the DSAs located in Hawaii and Puerto Rico to share and receive organs from other DSAs located in California and Oregon, and Florida, respectively.

Table 2.3 summarizes the results for τ_{max} set to 500 NM, 600 NM, and 700 NM, and compares it with the prior 11-region system and other proposed geographical allocation policies. As is evident, our model produces a neighborhood that results in the narrowest range of s/d ratios across DSAs: 0.15 when $\tau_{max} = 500$ NM, 0.13 when $\tau_{max} = 600$ NM, and 0.10 when $\tau_{max} = 700$ NM, as compared to 0.34 (OPTN 11 regions), 0.17 [23, 8 districts], and 0.64 [35]. Our model also produces relatively more uniform and smaller-sized neighborhoods. It does not contain any unusually large neighborhoods (as evidenced by the value of τ_{max}). Our solutions have a fair degree of reciprocity (that is, if DSA i shares its organs with DSA j , then DSA j shares its organs with DSA i). About 56.0% of DSA pairs had reciprocity when $\tau_{max} = 500$ NM, 62.1% when $\tau_{max} = 600$ NM, and 52.7% when $\tau_{max} = 700$ NM. Further, the average distance of the farthest DSAs in the neighborhoods ($\bar{\tau}$) is much smaller than that of Gentry et al. [23] and Kilambi and Mehrotra [35], and is comparable with OPTN 11 regions. The maximum s/d ratio difference among adjacent DSAs is also reduced significantly. For example, with $\tau_{max} = 700$ NM, the

maximum difference of the s/d ratio among adjacent DSAs is 0.096, much smaller compared to OPTN 11 regions (0.228).

Table 2.4 presents the s/d ratios for each DSA in the different proposals. This allows a deeper examination of how each DSA is affected by the proposed reallocations. The maximum and minimum s/d ratio values in every proposal are highlighted in bold. Appendix A.4 describes the DSA neighborhoods obtained by our models for $\tau_{max} = 500, 600,$ and 700 NM, respectively. Figure 2.7(a) depicts the neighborhoods (when $\tau_{max} = 500$) using a directed graph.⁹ An arc from a node (i.e., DSA) i to a node j means that DSA i is sharing its organs with DSA j . In the event of reciprocity between DSA's i and j , the link between the two nodes is bidirectional. It is interesting to observe that in the mainland U.S., the DSA CORS (which comprises Colorado and Wyoming) forms a cut node (i.e., its removal separates the graph representing the neighborhood into two components). Although there are additional arcs (and sharing between DSAs) with $\tau_{max} = 600$ and 700 NM, CORS remains a cut node separating the DSAs to the east and west. This suggests that sharing between DSAs largely occurs exclusively between DSAs to the east of CORS, and exclusively between DSAs to the west of CORS (i.e., DSAs to the east of CORS do not share with DSAs to the west of CORS and vice versa). Given that there is a lot of information packed into Figure 2.7(a), Figure 2.7(b) focuses on the neighborhood of DSA ALOB. It shows the DSAs with which ALOB shares its organs and also shows which DSAs share their organs with ALOB. Figure 2.7(c) provides a few additional details and adds in sharing and receiving between the DSAs identified in Figure 2.7(b) (it excludes information about sharing and receiving between the 14 DSAs in the figure and the remaining DSAs).

⁹To represent a DSA on the map, we averaged the latitude and longitude values of the transplant centers in that DSA.

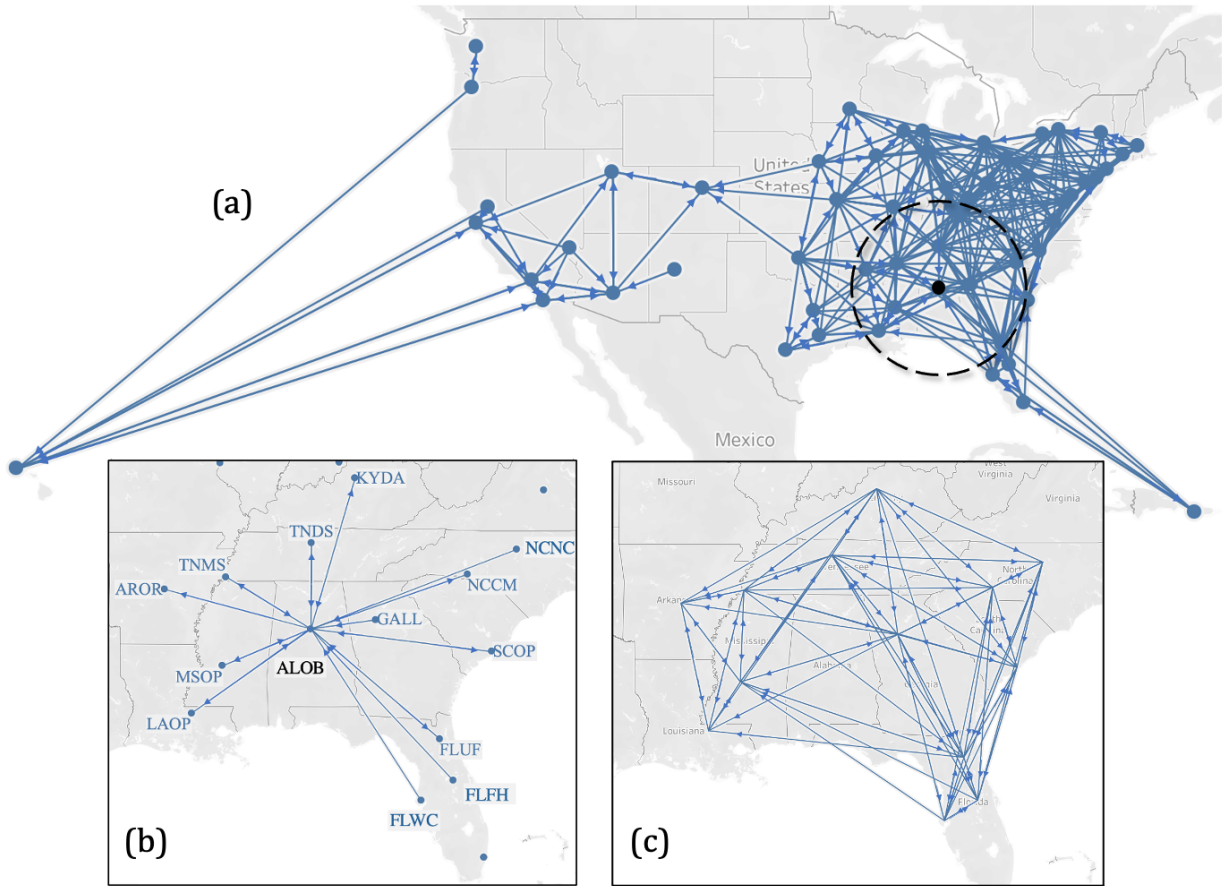


Figure 2.7: (a) Illustration of optimized neighborhoods when $\tau_{max} = 500$. (b) DSAs to which ALOB shares and receives. (c) Sharing and receiving between DSAs identified in (b).

The computational benefit of [SP-1] over [S-1] is easily seen in the DSA version. For example, when $\tau_{max} = 500$ NM, the size of [S-1] using only sharing contiguity was 16,286 rows and 18,883 columns, and the MIP gap ($\text{MIP gap} = \frac{|\text{Objective bound} - \text{Objective value}|}{|\text{Objective value}|}$) was 1.19% after two hours of running time. Meanwhile, the size of [SP-1] was 110 rows and 742 columns, and took only 0.66 seconds to reach optimality.

DSA	s/d ratio							
	Local, or	OPTN 11 regions	Gentry et al. [23]	Kilambi and Mehrotra [35]	[SP-2]			
	no sharing	$\tau_{max} = 843$ NM	$\tau_{max} = 975$ NM	$\tau_{max} = 1380$ NM	τ_{max} :	500 NM	600 NM	700 NM
ALOB	0.72	0.76	0.61	0.56		0.62	0.65	0.63
AROR	0.97	0.76	0.61	0.96		0.65	0.52	0.58
AZOB	0.55	0.52	0.54	0.88		0.53	0.53	0.59
CADN	0.38	0.52	0.52	0.45		0.51	0.52	0.53
CAOP	0.39	0.52	0.52	0.5		0.54	0.53	0.53
CASD	0.55	0.52	0.52	0.35		0.5	0.53	0.59
CORS	0.37	0.64	0.54	0.77		0.51	0.54	0.53
CTOP	0.95	0.42	0.57	0.4		0.56	0.62	0.59
DCTC	0.58	0.57	0.57	0.46		0.64	0.64	0.63
FLFH	1.3	0.76	0.61	0.65		0.54	0.52	0.62
FLMP	0.5	0.76	0.61	0.65		0.61	0.65	0.61
FLUF	0.47	0.76	0.61	0.81		0.65	0.58	0.61
FLWC	1.98	0.76	0.61	0.65		0.64	0.52	0.62
GALL	0.72	0.76	0.57	0.99		0.65	0.65	0.62
HIOP	0.97	0.66	0.52	0.37		0.63	0.64	0.54
LAOP	1.23	0.64	0.64	0.58		0.62	0.64	0.61
ILIP	0.69	0.55	0.69	0.62		0.65	0.62	0.62
INOP	0.78	0.66	0.69	0.67		0.62	0.63	0.59
KYDA	0.66	0.76	0.69	0.69		0.65	0.64	0.6
LAOP	0.55	0.76	0.61	0.64		0.63	0.65	0.63
MAOB	0.39	0.42	0.57	0.4		0.54	0.61	0.56
MDPC	0.34	0.57	0.57	0.67		0.64	0.65	0.63
MIOP	0.68	0.66	0.69	0.49		0.54	0.64	0.63
MNOP	0.4	0.55	0.64	0.53		0.51	0.56	0.56
MOMA	0.71	0.64	0.61	0.73		0.65	0.63	0.63
MSOP	1.49	0.76	0.61	0.56		0.58	0.55	0.63
MWOB	1.04	0.64	0.64	0.7		0.5	0.52	0.56
NCCM	0.73	0.76	0.57	0.44		0.65	0.64	0.62
NCNC	0.77	0.76	0.57	0.63		0.65	0.6	0.62
NEOR	0.41	0.64	0.64	0.44		0.51	0.54	0.63
NJTO	1.19	0.57	0.57	0.47		0.65	0.65	0.63
NYFL	0.56	0.42	0.69	0.59		0.53	0.53	0.62
NYRT	0.31	0.42	0.57	0.47		0.65	0.65	0.63
OHLB	0.47	0.66	0.69	0.67		0.65	0.65	0.62
OHLP	0.9	0.66	0.69	0.83		0.65	0.61	0.62
OHOV	0.33	0.66	0.69	0.51		0.65	0.65	0.61
OKOP	0.91	0.53	0.64	0.81		0.58	0.52	0.63
ORUO	0.71	0.66	0.52	0.62		0.62	0.65	0.58
PADV	0.62	0.57	0.57	0.6		0.62	0.65	0.63
PATF	0.58	0.57	0.69	0.83		0.64	0.59	0.63
PRLL	1.69	0.76	0.57	0.56		0.54	0.6	0.53
SCOP	1.02	0.76	0.57	0.38		0.65	0.62	0.62
TNDS	1.17	0.76	0.69	0.77		0.65	0.64	0.63
TNMS	0.36	0.76	0.61	0.85		0.65	0.64	0.62
TXGC	0.36	0.53	0.61	0.52		0.64	0.58	0.63
TXSA	0.5	0.53	0.61	0.44		0.53	0.52	0.53
TXSB	0.77	0.53	0.61	0.5		0.64	0.55	0.62
UTOP	0.53	0.52	0.54	0.47		0.54	0.55	0.56
VATB	0.6	0.76	0.57	0.85		0.63	0.65	0.62
WALC	0.6	0.66	0.52	0.6		0.62	0.62	0.55
WIDN	0.4	0.55	0.69	0.5		0.5	0.54	0.62
WIUW	0.61	0.55	0.69	0.72		0.62	0.63	0.63

Table 2.4: Comparison of the s/d ratios among different DSA-based allocation policies (supply and demand locations are 58 DSAs and 52 DSAs, respectively).

2.4.2.1 Liver Simulated Allocation Model (LSAM) Results

Next, we wanted to see how the proposed (DSA-based) allocation policies perform on metrics that policymakers have traditionally examined to evaluate policies, such as the variance of MMaT across geographies, distance traveled, and number of deaths. To this end, we use LSAM to simulate our neighborhoods [SP-2], OPTN 11 regions, Gentry et al. [23, 8 districts], and Kilambi and Mehrotra's [35] neighborhoods. There are two main inputs to LSAM: (1) patient and organ arrival processes, and (2) the allocation policy that includes geographical schemes and offer prioritization rules.

LSAM uses the historical data of donors and patients to simulate the waitlisted patient's health state transitions, organ acceptance behavior, and post-transplant survival outcomes. When an organ becomes available, candidates on the waiting list are prioritized for the organ offer as per the allocation policy. When a candidate receives a transplant, the simulation determines the survival time of the transplanted organ and uses this information to determine when in the future the candidate may die or relist. Using LSAM in its current form does have some limitations. It uses a probability acceptance function built on past data, where distance is more strongly correlated with acceptance of an organ due to the lack of broader sharing. It also does not account for organ availability in determining organ acceptance. These limitations may underestimate the effects of broader sharing and the equalization of the s/d ratios. Despite these limitations, it is instructive to use LSAM as a first step in evaluating the potential benefit of the heterogeneous radii circle policy.

In the simulation study (to model broader sharing within a circle), we allow for full sharing of organs to Status 1A/1B and MELD ≥ 15 candidates in the neighborhood or region/district in

Allocation Policy	Avg. (Quartiles)	Waitlist	Total	Across DSAs	
	travel distance (in NM)	deaths (annual)	deaths (annual)	Var/Avg of MMaT	Std. deviation of avg travel distance (NM)
OPTN 11 regions	258 (75, 194, 347)	1411.6	3658.8	7.26/30.0	109
Gentry et al. [23]	309 (101, 226, 429)	1376.1	3600.0	5.22/31.1	124
Kilambi and Mehrotra [35]	305 (124, 240, 395)	1348.2	3555.4	2.68/31.6	142
[SP-2], $\tau_{max} = 500$ NM	258 (112, 220, 341)	1356.4	3567.7	2.00/31.3	56
[SP-2], $\tau_{max} = 600$ NM	283 (125, 251, 384)	1343.6	3551.4	1.98/31.7	55
[SP-2], $\tau_{max} = 700$ NM	293 (125, 250, 399)	1343.4	3544.6	1.61/31.7	64

Table 2.5: Comparison of LSAM simulation results for DSA-based allocation policies under Enhanced Share 15.

which the organ is recovered in the first level of allocation. In the next allocation level, the organ is offered nationally to Status 1A/1B, then nationally to candidates with MELD ≥ 15 . Next, it is offered to candidates with MELD < 15 locally (the DSA in which the organ is recovered), then in the neighborhood or region/district, and then nationally before being discarded after 100 offers. The above policy (which we refer to as ‘Enhanced Share 15’) skips sequences # 3 and 4 of the Share 35 policy described in Table 1.1. For benchmarking, we also compared using the prior Share 35 policy. We simulated the different DSA-based geographical allocation policies using the organ and patient arrival data, consisting of three years (July 2013 to June 2016). We ran the simulation 10 times (the maximum allowed by LSAM) by resampling the input files.

Table 2.5 compares the simulation results under Enhanced Share 15. The average number of annual waitlist deaths and total deaths is smallest for [SP-2], $\tau_{max} = 700$ NM, with a projected savings of 114 lives annually, compared to OPTN 11 regions. The average travel distance, although slightly higher in our allocation policy compared to OPTN 11 regions, is smaller than that of the other policies. To measure the differences between DSAs, we consider the variance of MMaT and the standard deviation of the average organ travel distance across DSAs. The

variance of MMaT across the DSAs is smallest in our allocation policies (2.00 when $\tau_{max} = 500$ NM, 1.98 when $\tau_{max} = 600$ NM, and 1.61 when $\tau_{max} = 700$ NM), compared to 7.26, 5.22, and 2.68 in OPTN 11 regions, Gentry et al. [23], and Kilambi and Mehrotra [35], respectively. Because the different proposals vary in their efficiency (travel distance) and fairness (MMaT) metrics, it is instructive to compare the fairness of the proposals with similar efficiency levels. To this end, comparing [SP-2], $\tau_{max} = 500$ NM against OPTN 11 regions shows a significant reduction in both total deaths and variance of MMaT. Similarly, comparing [SP-2], $\tau_{max} = 700$ NM against Gentry et al. [23] and Kilambi and Mehrotra [35] shows a significant reduction in the variance of MMaT. Overall, we see that greater fairness can be achieved by DSA-based geographical allocation policies that equalize s/d ratios. The standard deviation of the average travel distance across the DSAs (Hawaii and Puerto Rico are excluded from our distance analysis) in our allocation policies is less than half that of the others. This finding indicates that there is less disparity in the travel distance between DSAs because our neighborhoods have relatively similar sizes.

Table 2.6 compares the LSAM simulation results under Share 35. We note that our neighborhoods are optimized under the assumption of full sharing, which is closer to Enhanced Share 15 than Share 35; and thus, the full benefits of the improved MMaT are less likely to be seen. Given that there is less sharing under Share 35 (organ offers are restricted to within-DSA patients ($15 \leq \text{MELD} < 35$) before being offered broadly (neighborhood or region/district and nationally)), the average travel distance significantly decreased, and the number of waitlist and total deaths increased for all policies. Even so, comparing [SP-2], $\tau_{max} = 500$ NM against OPTN 11 regions shows a significant reduction in both total deaths and variance of MMaT. Similarly, comparing [SP-2], $\tau_{max} = 600$ NM against Gentry et al. [23] and Kilambi and Mehrotra [35] shows a

Allocation Policy	Avg. (Quartiles)	Waitlist	Total	Across DSAs	
	travel distance (in NM)	deaths (annual)	deaths (annual)	Var/Avg of MMaT	Std. deviation of avg. travel distance (NM)
OPTN 11 regions	199 (20, 105, 258)	1455.5	3744.9	13.66/28.5	88
Gentry et al. [23]	231 (25, 130, 314)	1419.5	3696.4	10.49/29.5	102
Kilambi and Mehrotra [35]	230 (32, 150, 309)	1389.0	3656.3	11.87/30.2	104
[SP-2], $\tau_{max} = 500$ NM	203 (29, 142, 291)	1399.9	3664.8	10.30/29.7	57
[SP-2], $\tau_{max} = 600$ NM	221 (32, 157, 326)	1384.8	3645.2	8.80/30.3	57
[SP-2], $\tau_{max} = 700$ NM	233 (36, 162, 344)	1397.3	3636.4	10.04/30.3	64

Table 2.6: Comparison of LSAM simulation results for DSA-based allocation policies under Share 35.

significant reduction in the variance of MMaT. Similar to Enhanced Share 15, we observe again that the standard deviation of the average travel distance (across DSAs) is much lower for our allocation policies.

Ultimately, comparing our allocation policy $\tau_{max} = 500$ NM under Enhanced Share 15 against the OPTN 11 regions under Share 35 shows that a drastic reduction in the variance of MMaT across DSAs (from 13.66 to 2.00) and deaths (from 3,745 to 3,568) can be achieved with a modest increase in the average travel distance (from 199 NM to 258 NM).

2.5 Conclusions

We use the Rawlsian *maximin* principle to minimize the variability in deceased donor liver access across geographies. In contrast to the current fixed radius policy, we propose heterogeneous radii circles. The benefit of heterogeneous radii circles is that they account for where the organ supply and demand occur, and adjust the radii of the circles so that each transplant center's s/d ratio can be close to the national average. Moreover, equalizing the s/d ratios at the transplant centers is achieved without a significant increase in anticipated travel distance. In fact, the median

radius is approximately 305 NM. In other words, the optimization model only increases the radii of donor circles when necessary.

By using a DSA as the geographical unit, we demonstrate that low geographical variation in the s/d ratio can be achieved while maintaining DSA boundaries by judiciously creating neighborhoods for each DSA. An LSAM evaluation of our DSA neighborhoods predicts a significant reduction in the number of deaths, overall variation in MMaT, and average travel distance across DSAs.

As noted earlier, there are limitations of our analysis, as LSAM's organ acceptance function may not accurately reflect the change in the candidate/transplant center behaviors when organ accessibility and availability changes. For instance, candidates at organ-rich locations might behave more selectively in accepting organs than at locations with low s/d ratios. In the next chapter, we develop a patient's dynamic choice model to analyze his/her strategic response to a policy change. We show that the policy framework developed in this chapter (i.e., equalizing s/d ratios across the geography) indeed promotes the greatest geographic equity and transplant efficiency in comparison to the current Acuity Circle policy and the prior Share 35 policy.

In terms of logistical implementation of the heterogeneous circle policy, we have a few suggestions. First, we believe the circles should be defined around the donor location rather than the transplant location (note that in a fixed radius policy, there is no difference between the circles defined around donor and transplant locations, but with heterogeneous circles, there is a difference), or else the issues raised in the lawsuits (i.e., organs being offered to a less sicker candidate who is farther away) would not be addressed. Second, we expect small variations in the supply and demand over time. Hence, we suggest that the optimization model be run occasionally to account for demographic changes.

Our approach can be viewed as a combination of the fixed distance from a donor hospital and a mathematical optimized boundaries framework identified by the Geography Committee. There is considerable debate in the transplant community about using continuous scoring (the third distribution framework identified by the Geography Committee). The following two papers [41, 48] provide an overview of the continuous scoring concept. Rather than a one-size-fits-all framework for continuous scoring, which we do not believe will adequately address geographical inequities, we would recommend a mathematically optimized continuous scoring function that accounts for regional differences in the supply and demand. In Chapter 4, we develop an optimization model (to equalize supply-to-demand ratios across transplant centers) that uses a continuous function to assign points to patients based on their distance to the donor hospital.

Clearly, the optimization concepts applied to mitigate geographical disparities in the liver transplantation setting could also be applied to other organs. We hope this research will spur similar work in other organ transplantation settings, and thus reduce/mitigate the geographical disparities that are inherent to all of these systems!

Chapter 3: Improving Broader Sharing to Address Geographic Inequity in Liver Transplantation

3.1 Introduction

This chapter develops an endogenous patient choice model to study the change in allocation policy. The goal is to understand how a patient’s behavior would change with policy and to develop a framework to conduct counterfactual analyses of various policies. This address the shortcomings of the prior studies that assumed no change in a patient’s behavior in response to a policy change.

In June 2013, the Share 35 policy was introduced, with the intent of reducing waiting list mortality and addressing geographic disparities across DSAs. It allowed broader organ sharing for high-MELD patients beyond the local DSA (where the organ was recovered). The

Candidate UNOS status at transplant	Number functioning (Alive)	Survival rate
MELD/PELD 6-14	760	89.8
MELD/PELD 15-29	12549	90.2
MELD/PELD 30-34	3495	89.3
MELD/PELD ≥ 35	5286	87.0
Status 1A	934	83.8
Status 1B	377	89.0

Table 3.1: One year Kaplan-Meier graft survival rate based on 2012-2015 transplants. Follow-up done till December 18, 2020.

summary statistics show that while the waiting list mortality rate (number of patients who died on the waiting list divided by the number of new patients joining the waiting list) decreased from 12.0% in the Pre-Share 35 era to 9.4% in the Share 35 era, the median waiting time for a transplant increased by 5% (and its standard deviation across regions increased by 28%), and a greater fraction of transplants were offered to higher-MELD (transplants for MELD ≥ 29 patients increased from 44% to 52%) patients. However, the survival rates of patients with transplants in Table 3.1 from 2012 to 2015 indicate that higher MELD candidates have poorer survival outcomes. To sum up, determining the impact of the Share 35 policy is not straightforward. Our first *research objective* is to study the impact of the Share 35 policy on patient organ acceptance behavior (which is in response to the expected future value in the new policy). No previous work (to the best of our knowledge) has used an endogenous patient choice model to study this policy change. Moreover, building an endogenous patient choice model is useful in its own right in evaluating other (counterfactual) allocation policies, which is a key objective of this chapter.

Despite implementing broader organ sharing in a region for candidates with MELD scores ≥ 35 in 2013, geographic inequities have remained in the system. The highest reported median MELD score was 39 in Los Angeles, California (DSA: CAOP), and the lowest was 20 in Indianapolis, Indiana (DSA: INOP) [37]. In July 2018, six waiting list patients in New York, California, and Massachusetts filed a lawsuit (Cruz et al. v. U.S. Dept. of Health and Human Services, S.D.N.Y 18-CV-06371) against the Health Resources and Services Administration (HRSA), an agency of the HHS. The lawsuit pointed out two main issues: 1. Significant geographic variability existed in the median MELD scores of candidates for deceased-donor transplants such that one's place of residence largely determined her chances of survival in the Share 35 policy; and 2. In the previous DSA-based Share 35 allocation policy (due to rigid boundaries), it was possible for

an organ to be offered to a less sick candidate in a more distant transplant center over a sicker candidate in a closer transplant center. HRSA has already been under pressure over the last two decades to address geographic disparities [34]. The lawsuit precipitated a change from the Share 35 allocation policy to the Acuity Circles policy in February 2020. The new policy addressed the second issue of the lawsuit. Nevertheless, it is unclear whether the first issue (i.e., geographic inequity) will be addressed by the new policy.¹ Our second *research objective* is to study whether the current Acuity Circles policy is better than the Share 35 policy in terms of geographic equity and efficiency metrics.

Managing the trade-off between equity and efficiency has been a very active area for researchers (see Section 3.3) and policymakers. Recent policies are moving toward broader sharing in principle. To provide some perspective, the Pre-Share 35 policy historically allowed organ sharing mainly within the DSA (the average distance between the donor hospital and the transplant center (TC) pairs within the same DSA is 66 nautical miles (NM)). After that, the Share 35 policy allowed organ sharing at the regional level for sicker patients (the average distance between the donor hospital and the TC pairs within the same region is 262 NM). The current Acuity Circles policy allows organ sharing up to 500 NM for sicker patients. The future policy framework aims to further increase this distance. Our third and final *research objective* is to investigate whether there is a better alternative (in making an equity-efficiency trade-off) than broader organ sharing as currently implemented. Overall, our unique study fills a knowledge gap by evaluating an earlier policy's impact and using the insights gleaned to propose a new policy.

To assess a new proposal and predict its impact, the transplant community uses the Liver

¹Due to the pandemic, data on the current Acuity Circles policy would not be useful because hospital resources were shifted to COVID treatment. Moreover, the priorities of the waiting list transplant patients also changed in light of the new situation.

Simulated Allocation Model (LSAM).² One of its main shortcomings is that it cannot model forward-looking behavior in a patient due to a new policy (more in Section 3.6.5). This model assumes the same organ acceptance probability function, irrespective of policy, geography, or organ access. Goel et al. [26] compared the LSAM predictions due to the Share 35 policy with the actual results observed. They found that LSAM overestimated the increase in the transplant rates for MELD/PELD ≥ 35 candidates (46% predicted versus 36% observed), and underestimated the decrease in the transplant rates for MELD/PELD 30-34 candidates (1% predicted versus 33% observed). Prior research [50] has also shown that ignoring a patient's choice leads to overestimating the efficiencies.

3.1.1 Contributions

This chapter makes the following key contributions to the literature. First, we build a structural model and provide a framework to analyze a patient's strategic response to a policy change in the context of liver transplantation. Our model is based on approximately 40 medical characteristics of patients and donors. We use the *logit inclusive value* technique to make the analysis computationally tractable (see Section 3.5.3). Our model's predictions are much better than the existing model (LSAM) and other reduced-form models (see Section 3.6.5). Secondly, we use our model to give accurate policy evaluations to inform decision makers.

The findings are as follows: 1. We perform a comparative study of the Pre-Share 35 and Share 35 policies and demonstrate the heterogeneity in the behavioral (i.e., organ acceptance probability) change of patients as a function of their region and MELD scores. We find that

²<https://www.srtr.org/requesting-srtr-data/simulated-allocation-models/> accessed on July 12, 2020.

sicker patients benefited and became more selective in their behavior (i.e., their organ acceptance probability decreased for the same organ in consideration). However, there was heterogeneity in the behavioral change across geographies in less sick patients. Overall, the Share 35 policy reduced geographic disparity compared to its predecessor policy; 2. The Acuity Circles policy was implemented in February 2020 to ‘improve’ upon the ‘Share 35’ policy. We observe that, compared to the Share 35 policy, the Acuity Circles policy performs very similarly in geographic equity metrics but results in more offer refusals and a lower transplant benefit; and 3. We illustrate that broader sharing in its current form may not be the best strategy for balancing geographic equity and efficiency. The intuition is that by indiscriminately enlarging the pool of supply locations from where patients can receive offers, these patients tend to become more selective, resulting in more offer rejections and less efficiency. We suggest an alternative approach, one that equalizes the supply (deceased donors)-to-demand (waiting list patients) ratios across geographies by selectively increasing the sharing radius around donor hospitals. We show that this approach has the highest efficiency among the policies studied while improving upon geographic equity measures.

The structure of the rest of this chapter is as follows. In the next section, we provide a brief overview of the new liver allocation policies that we study in this chapter. Section 3.3 reviews the relevant literature. Section 3.4 describes the data and a few model-free pieces of evidence regarding behavioral change. Section 3.5 presents our optimization model. Section 3.6 describes our estimation procedure and results. Section 3.7 performs a counterfactual study comparing various allocation policies, including our proposed alternative ‘s/d Match’. Finally, we summarize and conclude in Section 3.8.

3.2 New Liver Allocation Policies

In addition to the Pre-Share 35, Share 35 and Acuity Circles policies, we study the following (hypothetical) policies in this study.

3.2.1 Supply-to-demand (s/d) Match Policy

We use the optimization framework proposed in Chapter 2 and apply the *maximin* principle to design heterogeneous radii circles that maximize the minimum value of the supply-to-demand (s/d) ratio across all TCs. The s/d Match policy adheres to the Final Rule and the principles adopted by the UNOS board in 2018 for all future organ policies.³ We set the minimum and maximum circle radii around the donor hospitals to be 150 NM and 500 NM (in line with the innermost and outermost radii used in the Acuity Circles policy) as an illustration. Based on the setup considered in Section 3.7, the optimized set of circles results in a minimum (maximum) s/d ratio (at the TC level) of 0.58 (0.83). In contrast, if we consider 500 NM circles around every donor hospital, the s/d ratio range is 0.45-1.14. (We note that a tighter s/d range can be obtained by changing the maximum radius value. See Appendix B.13 for details on the s/d range and performance measures when we allow the maximum radius around the donor hospital to be 600 NM.)

³https://optn.transplant.hrsa.gov/media/2506/geography_recommendations_report_201806.pdf, accessed April 30, 2022.

3.2.2 National Sharing Policy

As the name suggests, candidates are first ranked based on their MELD scores, irrespective of their location in the U.S. In the case of a tie (i.e., conditional on the MELD), local candidates are preferred over regional candidates, and regional candidates are preferred over candidates outside the region (we set this preference order because Feng et al. [19] document the increased risk of graft failure from local to regional, and from regional to national sharing). Therefore, we try to mitigate (although not eliminate entirely) the role of one's location through this policy. We note that this policy might involve long-distance travel and may not be an appealing or practical idea, given that it may increase the chance of the organ being discarded.⁴

3.3 Related Research

There are three main streams of literature relevant to our study: 1. Proposals to address geographic disparities, 2. Efficiency-equity trade-offs, and 3. Dynamic optimization modeling in organ transplantation.

Redistricting has been proposed by many researchers in the operations community to address the issue of geographic inequity. Redistricting is a problem that occurs frequently in multiple domains (e.g., political redistricting, school redistricting, and sales territory assignment) where a finite, denumerable set of non-overlapping geographic units are aggregated into regions/districts subject to some criteria. Hess et al. [32] and Garfinkel and Nemhauser [21] introduced the use of optimization techniques for political redistricting. Stahl et al. [49] considered geographic equity

⁴Implementing a National Sharing policy is likely to increase CIT substantially. Although Gentry et al. [24] concluded that the estimated transport time for livers comprised only 21% of the CIT, we note that their model was based on historical data.

(measured by minimum OPO intraregional transplant rate), along with efficiency (measured by total intraregional transplants), but they restrict their regions to contain up to eight DSAs due to computational challenges. Extending their work, Demirci et al. [17] developed a branch-and-price algorithm to incorporate a larger set of potential regions and explored the efficient frontier in a trade-off between efficiency and geographic equity. Gentry et al. [23] used optimization to reorganize DSAs into regions/districts to reduce geographic disparities. Working closely with the liver committee of UNOS, they proposed eight-district and four-district (reorganized DSA) maps. The proposed maps were under active consideration by UNOS from 2015 to 2017, but ultimately after significant debate and public comment, they were not adopted. Kilambi and Mehrotra [35] introduced the neighborhood framework in organ allocation as a way to provide for broader sharing and improve geographic equity. Each DSA has its own neighborhood consisting of a unique set of other DSAs (or neighbors) with which it shares its organs. Rectifying the shortcomings in the supply-to-demand ratio measure used by Kilambi and Mehrotra [35], Akshat et al. [2] proposed heterogeneous circles around donor hospitals to create an equitable geographic distribution by developing a scalable set-partitioning optimization model. Ata et al. [10] used fluid approximation and game theory to show that multi-listing (a patient is listed at more than one TC, potentially in other DSAs or regions, so that she can get organ offers from multiple places) can reduce geographic disparity in kidney allocation. However, fewer than 2% of patients (on April 14, 2021, the OPTN website showed that fewer than 181 out of 11,868 candidates were multiple listed) waiting for a liver transplant were multi-listed. Moreover, multi-listing would not make the system fair; indeed, it would instead create disparity based on a candidate's economic means. Bertsimas et al. [14] suggest using trade-off curves to assess three organ distribution frameworks identified by UNOS. Running a massive number of simulations for

the three distribution frameworks,⁵ they plotted trade-off curves of efficiency (measured as the average travel distance) versus fairness (measured as deaths or variance in the median MELD at the time of the transplant). For a given value of the efficiency metric, the trade-off curve then identifies the policy with the greatest fairness. Most of the above studies rely on LSAM to assess the performance of their proposals, owing to policymakers' reliance on it. LSAM is a sophisticated patient-level simulation that handles MELD scores and models whether a candidate accepts or declines an offer [52]. However, it ignores the heterogeneity in patients' organ acceptance behavior and its dependence on the policy.

Zenios et al. [57] study the trade-off between clinical efficiency (measured as Quality Adjusted Life Years (QALY)) and equity (types of patients defined based on their demographics) in the kidney allocation problem using a fluid model and ignoring patients' choices. They propose a heuristic dynamic index policy to maximize the multi-criteria objective function. Su and Zenios [50] use a sequential assignment model (of n transplant patients and n kidneys) to investigate the impact of a patient's choice in the kidney allocation system. They focus on a social planner's objective of maximizing the overall social welfare and conclude that ignoring the patient's choice leads to overestimating the efficiencies in the policies they studied. Bertsimas et al. [12] study the α -fairness scheme (see [11]) to trade off efficiency and fairness. Their measure of efficiency is the sum total of utilities, and they do not focus on geographic disparity. Su and Zenios [51] find that introducing information asymmetry (the transplantation system does not know the post-transplant outcome, which is known to the patient) in the allocation policy achieves an overall outcome in the middle of the efficiency-equity spectrum. Bertsimas et al. [13]

⁵https://optn.transplant.hrsa.gov/media/2565/geography_publiccomment_201808.pdf accessed on July 1, 2022.

proposed a method to design a point-based kidney allocation system, where policymakers can select the fairness constraints. This method maximizes the medical efficiency (captured using life-years gained from the transplant); however, Bertsimas et al. [13] test policies assuming an exogenous organ acceptance model for patients. Arikian et al. [7] use a probit model to elicit differences in the intent for organ (kidney) procurement at the level of DSAs between marginal-quality organs and the rest. They conclude that geographically broader sharing of the bottom 15% quality kidneys can help enhance the kidney supply.

Other papers [27,54] have studied the effect of the Share 35 policy using logistic regression model, which is not appropriate for studying the dynamic optimization problem setting. Zhang [58] is the closest paper to ours in terms of the methodology. Their focus is on studying the presence of observational learning in patient behavior regarding the deceased-donor kidney allocation process. Agarwal et al. [1] and Ata et al. [9] study deceased-donor kidney allocation policies using structural models. Besides the difference in the context (liver versus kidney), there are three key differences between these two papers and our study. First, in addition to transplantation, dialysis is also a treatment option for kidney failure. Second, these two papers assume patient health transitions to be deterministic, whereas we model the stochastic transition of MELD scores. Third, the liver allocation policy evolution presents a unique opportunity to study the impact of broader sharing on patient outcomes. Furthermore, Agarwal et al. [1] do not study geographic disparity. Alagoz et al. [6] use a discrete-time, infinite-horizon discounted Markov decision process model to study the patient's decision to accept an offer or wait. They find that the optimal policy is typically of the control-limit type. However, they also assume a fixed cost of waiting, whereas our model uses a richer set of variables to model the utility and waiting cost. In addition, their model assumes the same reward (or utility) from local, regional

or national offers whereas our model allows for different utilities from these offers.

3.4 Data and Evidence

3.4.1 Data

This study used data from the Scientific Registry of Transplant Recipients (SRTR). The SRTR data system includes data on all donors, wait-listed candidates, and transplant recipients in the U.S., submitted by the members of the Organ Procurement and Transplantation Network (OPTN). The Health Resources and Services Administration (HRSA), U.S. Department of Health and Human Services provides oversight to the activities of the OPTN and SRTR contractors.

The dataset used in the study contains candidates' information at the time of registration, the transition of their MELD scores while waiting, donor information, and the candidates' decisions regarding organ offers. We use nine years (2010 to 2018) of candidate and donor information in our structural model analysis. This covers both the Pre-Share 35 and Share 35 policy eras. We restrict our analysis to deceased-donor organs from adult donors and to adult candidates (allocation policies are different for donors <18 years). Because we are interested in analyzing geographic disparity across policies, we use data from all 11 regions. For the purpose of estimating MELD transitions, we use a larger dataset of 16 years (January 2003 to February 2019). Appendix [B.1](#) provides the summary statistics of a few key variables in the data.

3.4.2 Model-Free Evidence of Behavioral Change

Figure [3.1](#) compares the MELD at the time of an offer and at the time of a transplant (of candidates who accepted the offer) between the Pre-Share 35 and Share 35 policies using

box plots. Consistent with the Share 35 policy that prioritizes sicker patients, the MELD at the time of an offer increased. The MELD at the time of a transplant also increased slightly, suggesting that a greater number of sicker patients received transplants, and therefore, avoided death. However, the relative increase in the MELD at the time of a transplant is smaller than the MELD at the time of an offer, suggesting more offer refusals. One may wonder whether these refusals are due to lower-quality organs being offered, or whether the candidates became more selective in their behavior. We find no significant differences in the organ quality of the declined offers between the two policy eras (see Appendix B.2). Thus, it is likely that the refusals are due to behavioral change. Offer refusals tend to increase the waiting time for an organ transplant, thereby deteriorating the organ quality (and its utility from transplantation). On the one hand, the Share 35 policy seems to save more lives, while it may lead to a decrease in transplant quality (in terms of the graft survival probability) due to more offer rejections on the other hand. Further, we also see interaction effects. Conditional on offers to candidates with a MELD <35 (MELD ≥ 35), the average MELD at an offer acceptance increased (decreased) by 0.68 (0.43). Next, we use a straightforward metric to calculate the acceptance probability (ratio of the number of offers accepted and the number of offers received). Table B.2 reports the change in acceptance probabilities as a function of MELD in different regions. We see cases of both an increase and decrease in acceptance probabilities.

Notation	Description
i	Patient
$t = 1, \dots, \infty$	Organ arrival time (in days)
δ	Daily discount factor
Payoff-relevant variables	
Candidate specific variables:	
$MELD_{it}$	MELD score of patient i at time t
Rec_age_{it}	Candidate i 's age group at time t
$Rec_life_support_{it}$	Candidate i 's life support status ('Yes' or 'No') at time t
$Rec_med_cond_{it}$	Candidate i 's medical condition ('ICU': Intensive Care Unit, 'H': Hospitalized, or 'NH': Not Hospitalized) at time t
Organ specific variables:	
Don_age_{it}	Age of the donor whose organ is offered to candidate i at time t
Don_race_{it}	Race of the donor whose organ is offered to candidate i at time t
Don_cod_{it}	Cause of death of the donor whose organ is offered to candidate i at time t
Don_dcd_{it}	Indicates donation after circulatory death ('Yes' or 'No') of the donor whose organ is offered to candidate i at time t
Joint candidate-donor variables:	
Z_{it}	Candidate's and donor's medical attributes used in the SRTR Risk Adjustment Model (uses 41 attributes)
GS_{it}	One-year graft survival probability modeled as a function of ($MELD_{it}$, Rec_age_{it} , $Rec_life_support_{it}$, $Rec_med_cond_{it}$, Q_{it})
$Sharing_type_{it}$	Denotes whether the organ offer (with respect to patient i 's DSA) at time t is classified as <i>local</i> , <i>regional</i> , or <i>national</i> sharing
Q_{it}	(Don_age_{it} , Don_race_{it} , Don_cod_{it} , Don_dcd_{it})
S_{it}	($MELD_{it}$, Rec_age_{it} , $Rec_life_support_{it}$, $Rec_med_cond_{it}$, Q_{it} , Z_{it} , $Sharing_type_{it}$)
$\mathcal{P}(S_{i,t+1} S_{it})$	Transition probability of candidate i 's state from t to $t + 1$
Payoff functions	
$U_{it}(S_{it})$	Utility to candidate i upon accepting an offer at time t
$W_{it}(S_{it})$	One period of candidate i 's waiting cost at time t
$V(S_{it})$	Patient's maximum expected present discounted value associated with state S_{it}
Decision variable	
d_{it}	1 if candidate i accepts the offer at time t , and 0 otherwise

Table 3.2: Model Notation

3.5 Patient’s Dynamic Choice Model

We now describe the choice model of a patient. When the patient is offered an organ, she evaluates the utility (in terms of her survival chances) derived from that organ and decides to either accept it and undergo transplantation or decline it and wait for the next offer (anticipating a better one). A patient, in consultation with a transplant surgeon, evaluates an offer (for confidentiality reasons, the SRTR data does not contain surgeon-level information). While waiting, her health state will evolve stochastically, affecting her priority for future offers. In accordance with the allocation policy in the U.S., there is no implication of a patient’s offer refusal on her future offers. Now, we formally introduce our model. Table 3.2 describes the notation used in the formulation.

We model the patient’s problem as a discrete-time infinite-horizon dynamic optimization problem, where she faces the trade-off between accepting the current offer and waiting for future offers. We consider the Markov perfect equilibrium, and patients account for only payoff-relevant variables, compositely represented by S_{it} , in their decision-making.

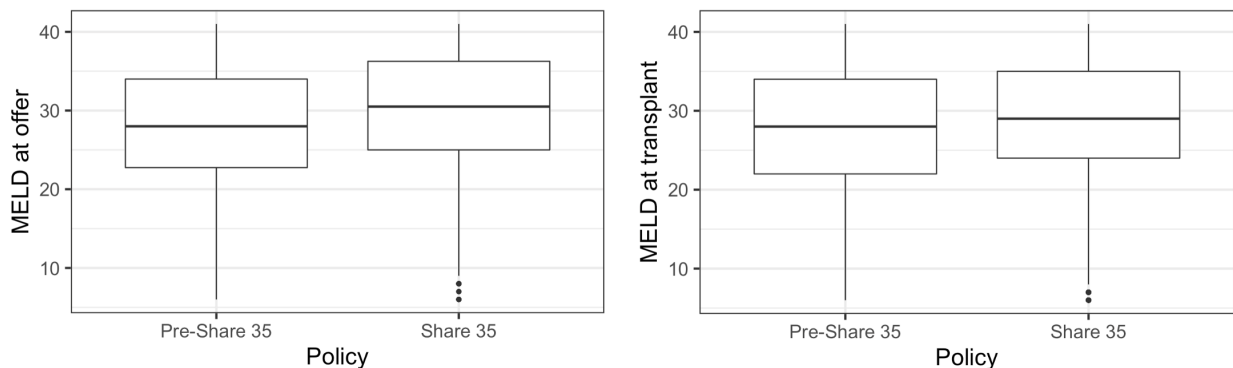


Figure 3.1: Comparison of MELD at the time of an offer and a transplant between policies using box plots (Status 1A is assigned a MELD score of 41).

Upon accepting an offer, a patient receives an expected utility of $EU(S_{it})$ and is removed from the waiting list (and we assume that she never joins again). $EU(S_{it})$ captures the expected present discounted payoff from accepting an offer (in state S_{it}). If a patient declines the offer, then she incurs an immediate waiting cost (as modeled in Section 3.5.2) and expects to receive some utility in the future (as modeled in Section 3.6.1.1). Formally, the Bellman equation for patient i 's dynamic optimization problem at time t is

$$V(S_{it}) = \max \left\{ EU(S_{it}), -EW(S_{it}) + \delta \sum_{S_{i,t+1}} \mathcal{P}(S_{i,t+1}|S_{it}, d_{it} = 0) \times V(S_{i,t+1}) \right\} \quad (3.1)$$

3.5.1 Utility Function

We consider a linear functional form for modeling the utility associated with a candidate-donor pair. For a pair, we estimate the graft survival probability using the SRTR Risk Adjustment Model,⁶ which is based on a total of 41 predictors (Z_{it}) that include the candidate's and donor's medical attributes, and CIT. Using the post-transplant outcome in the utility is in line with the extant literature [51]. Moreover, we believe that a patient would be interested in maximizing her eventual survival outcome (post-transplantation) without incorporating her survival chance without a transplant. The CIT is realized and observed only for transplants that took place. Predicting CIT for an offer is very difficult primarily due to the nonavailability of data on the mode of organ transport (driving, helicopter, or fixed-wing), and non-transport factors (such as back-table preparation) at the SRTR [24]. We set CIT equal to its median value (=6.9 hours) both in Z_{it} and the graft survival probability function (SRTR Risk Adjustment Model), and include the *Sharing_type* variable to capture the effect of the elapsed time between organ recovery and

⁶<https://www.srtr.org/reports-tools/posttransplant-outcomes/> accessed on July 12, 2020.

transplantation on the (prospective) transplant quality. We model the utility of the transplantation to be derived from the one-year graft survival probability (GS_{it} to be precise; see Section 3.5.3 for details) and the $Sharing_type_{it}$, which captures the effect of CIT. The utility to patient i at time t is given by:

$$U_{it}(S_{it}) = \begin{cases} \beta_0 + \beta_{GS} GS_{it} + \beta_{Sharing} Sharing_type_{it} + \epsilon_{it}, & \text{if candidate } i \text{ accepts organ at time } t, \\ \epsilon_{it}. & \text{otherwise.} \end{cases} \quad (3.2)$$

GS_{it} and $Sharing_type_{it}$ are observable to both patient i . β_{GS} and $\beta_{Sharing}$ are the associated utility parameters; β_0 is the intercept. ϵ_{it} denotes the idiosyncratic utility shock experienced by patient i while evaluating the offer at time t . It represents the random factors (playing a role in the decision-making) that are unobserved to the econometrician such as weather conditions, momentary inconvenience to the patient, surgery-related factors, randomness involved in the survival probability assessment, etc. ϵ_{it} is assumed to follow an independent and identically distributed (i.i.d.) Gumbel distribution across patients and offers. We subtract $E(\epsilon_{it})$, a constant, from the utility so that the expected utility upon accepting an offer is given by:

$$EU(S_{it}) = \beta_0 + \beta_{GS} GS_{it} + \beta_{Sharing} Sharing_type_{it} \quad (3.3)$$

3.5.2 Waiting Cost Function

A candidate incurs a waiting cost if she declines the offer or does not receive one at time t . To model her waiting cost, we use variables such as age, life support status, and medical condition. ω_{Age} , ω_{LS} , and ω_{MC} are the associated waiting cost parameters. Given that $Death$ is an

undesirable and terminal state, we add the term $\mathbb{1}_{\{MELD_{it}=Death\}}$ to the waiting cost function such that a patient incurs a one-time expected cost of $\frac{1}{1-\delta} \times \omega_d$ upon *Death*. Formally,

$$W_{it}(S_{it}) = \begin{cases} \omega_d + \epsilon_{i0t}, & \text{if candidate dies at time } t, \\ \omega_{Age} Rec_age_{it} + \omega_{LS} Rec_life_support_{it} + \omega_{MC} Rec_med_cond_{it} + \epsilon_{i0t}. & \text{otherwise.} \end{cases} \quad (3.4)$$

where ϵ_{i0t} is an independent and identically distributed (i.i.d.) Gumbel distribution across patients and times. We subtract $E(\epsilon_{i0t})$, a constant, from the function so that the expected waiting cost is given by:

$$EW(S_{it}) = \mathbb{1}_{\{MELD_{it}=Death\}}\omega_d + \mathbb{1}_{\{MELD_{it}\neq Death\}}[\omega_{Age} Rec_age_{it} + \omega_{LS} Rec_life_support_{it} + \omega_{MC} Rec_med_cond_{it}] \quad (3.5)$$

3.5.3 (Simplifying) State Transition Probability

In our dynamic model, patients have perceptions over future states. They need to know the evolution of every element in the state space, including Z_{it} . Following the extant literature on the *logit inclusive value* [29], we make a simplifying assumption: the evolution of Z_{it} is approximated using a one-dimensional GS_{it} . In doing so, we consider a patient to be boundedly rational, and they use fewer elements to form predictions about the future.

We model GS_{it} as a function of $(MELD_{it}, Rec_age_{it}, Rec_life_support_{it}, Rec_med_cond_{it}, Q_{it})$. We group the offers by $(MELD_{it}, Rec_age_{it}, Rec_life_support_{it}, Rec_med_cond_{it}, Q_{it})$, and GS_{it} is the average of the graft survival probabilities (calculated using the respective Z_{it} 's) for these offers. Thus, we only need the evolution of GS_{it} , which is relatively easier to estimate than the

evolution of Z_{it} . Appendix B.3 provides details.

If a patient declines an offer or does not receive one, she transitions to a new state on the next day. Appendix B.4 gives the detailed expression for $\mathcal{P}(S_{i,t+1}|S_{it}, d_{it} = 0)$.

3.5.4 Offer Acceptance Probability

It follows from the i.i.d. Gumbel assumption of the idiosyncratic shocks in the payoff functions, and the fact that the difference of two Gumbel-distributed random variables follows a logistic distribution, that the logit choice probability of accepting an offer is:

$$P(\text{accepting an offer}|S_{it}) = \frac{e^{EU(S_{it})}}{e^{EU(S_{it})} + e^{-EW(S_{it}) + \delta \sum_{S_{i,t+1}} \mathcal{P}(S_{i,t+1}|S_{it}, d_{it}=0) \times V(S_{i,t+1})}}, \quad (3.6)$$

where $EU(\cdot)$ and $EW(\cdot)$ represent the expected utility and waiting cost, respectively.

3.6 Model Estimation

In this section, we describe the estimation procedure, parameter identification, and results. Our estimation framework closely follows Zhang [58], in combination with the *logit inclusive value* technique of Gowrisankaran and Rysman [29] to make our model tractable.

3.6.1 Estimation Procedure

We estimate the model using the nested fixed point algorithm [44]. First, given a set of parameter values, an ‘inner’ algorithm computes the value function, $EV(S_{it})$. Then, the log-likelihood function is calculated using the parameter values and the value function vector. An ‘outer’ algorithm chooses the next set of parameters to maximize the log-likelihood function.

3.6.1.1 Value Function.

The value function, denoted by $EV(S_{it})$, is defined as the total future value that candidate i expects to receive when she waits (declines or does not receive an offer) at time t . The future value depends on her state transition, and the expected payoff in the new state.

$$EV(S_{it}) = \sum_{S_{i,t+1}} \mathcal{P}(S_{i,t+1}|S_{it}, d_{it} = 0) \times V(S_{i,t+1}) \quad (3.7)$$

Substituting equation (3.7) into equation (3.1), we get:

$$V(S_{it}) = \max \{EU(S_{it}), -EW(S_{it}) + \delta EV(S_{it})\} \quad (3.8)$$

Using the aggregation properties of the Gumbel distribution,

$$V(S_{it}) = \ln [e^{EU(S_{it})} + e^{-EW(S_{it}) + \delta EV(S_{it})}] \quad (3.9)$$

We can rewrite the value function as follows:

$$EV(S_{it}) = \sum_{S_{i,t+1}} \mathcal{P}(S_{i,t+1}|S_{it}, d_{it} = 0) \times \ln [e^{EU(S_{i,t+1})} + e^{-EW(S_{i,t+1}) + \delta EV(S_{i,t+1})}] , \quad (3.10)$$

where the second term under summation corresponds to the expected payoff when in state $S_{i,t+1}$.

The state space (described in Section 3.6.2) in our setting is discrete. Let K be the dimension of the state space, and let Π be a $K \times K$ Markov transition matrix of the state elements (calculated using equation B.5). The value function can be concisely represented as:

$$EV(.) = \Pi \times \ln [e^{EU(.)} + e^{-EW(.) + \delta EV(.)}] , \quad (3.11)$$

where $EV(\cdot)$, $EU(\cdot)$, and $EW(\cdot)$ are all $K \times 1$ vectors. This nonlinear system of equations can be solved iteratively using a fixed-point algorithm.

3.6.1.2 Log-Likelihood Function.

We use the maximum likelihood estimation approach to estimate the structural model parameters. Appendix B.5 describes the derivation and final expression of the log-likelihood function. We maximize the overall log-likelihood function, equation B.11, to estimate the parameters (β_0 , β_{GS} , $\beta_{Sharing}$, ω_d , ω_{Age} , ω_{LS} , and ω_{MC}).

3.6.2 Parameter Identification

Before we present the parameter estimates, we expand on some of the state variables. We discretize *Rec_age* into three groups: R1: < 45 years, R2: $(45 - 65)$ years, and R3: ≥ 65 years; *Don_age* into four groups: $(18 - 39)$ years, $(40 - 49)$ years, $(50 - 59)$ years, and ≥ 60 years; *Don_race* into ‘White’ and ‘Others’ categories; *Don_cod* into ‘Anoxia’, ‘Cerebrovascular accident (CVA)’, and ‘Others’ categories; *Rec_life_support* into ‘Yes’ and ‘No’; *Rec_med_cond* into ‘ICU’ (Intensive Care Unit), ‘H’ (Hospitalized), and ‘NH’ (Not Hospitalized) categories; and *Don_dcd* into ‘Yes’ and ‘No’.

The variable selection and discretization are primarily motivated by the medical literature [19,45]. We categorize the MELD scores into six classes: MELD 6-14, MELD 15-28, MELD 29-32, MELD 33-34, MELD 35-36, and MELD >36 , and add the terminal *Death* state. This creates a 7×7 MELD transition matrix (see Table B.3). The above classification of MELD scores provides sufficient granularity to evaluate the Pre-Share 35, Share 35, and Acuity Circles policies. Overall,

Sharing type	$P(\%)$	Candidate age group	$P(\%)$	Candidate life support	$P(\%)$	Candidate medical condition	$P(\%)$
Local	9.0	R1	6.7	No	5.8	NH	5.5
Regional	4.4	R2	6.1	Yes	20.9	H	13.3
National	1.2	R3	5.2			ICU	24.5

Table 3.3: Summary statistics of probability of acceptance ($P := \#$ of offers accepted/ $\#$ of offers received) for some of the variables in the state space. The variation in P enables the identification of the parameters associated with these variables in the structural model.

there are 18 patient types, 49 organ types, and 15,678 elements in the state space; consequently, every geographic unit (DSA or TC, depending on the allocation policy) has its own $K \times K$ Markov transition matrix, where $K = 15,678$.

Now we discuss the identification of the structural model parameters. GS_{it} is a function of the MELD category, age group, life support status, medical condition, and organ type (see Appendix B.3 for details). A variation in the accept/decline decisions of patients with their MELD score, and organ type is sufficient to identify β_{GS} . For example, patients might have a different probability of offer acceptance at a lower MELD score, keeping everything else (age group, life support status, medical condition, sharing type, and organ type) the same. This difference in the probability of offer acceptance can be attributed to the difference in GS_{it} . Appendix B.6 provides more details on the identification of the parameter associated with GS_{it} .

We summarize the probability of acceptance (calculated as the ratio of the number of offers accepted and the number of offers received) for some of the variables that are part of the state space in Table 3.3. The variation in the acceptance probability enables the identification of the parameters associated with these variables in the structural model. After controlling for the candidate and donor-specific state variables, there exists variation in the sharing type (local/regional/national) of the offers. The differences in the candidates' acceptance behavior

Variable	Parameter	Estimate	Standard Error
<u>Utility Function:</u>			
Intercept	β_0	-21.7803	0.3145
Sharing type: Regional	$\beta_{Sharing}$	-1.0348	0.0113
Sharing type: National		-2.3328	0.0243
Graft survival probability (GS)	β_{GS}	19.5200	0.3353
<u>Waiting Cost Function:</u>			
Death	ω_d	0.1160	0.0007
Candidate age group: R2 (45-65 years)	ω_{Age}	0.0057	0.0002
Candidate age group: R3 (≥ 65 years)		0.0061	0.0003
Candidate life support: Yes	ω_{LS}	0.0134	0.0008
Candidate medical condition: H	ω_{MC}	0.0114	0.0004
Candidate medical condition: ICU		0.0229	0.0008
No. of observations = 890,402			
Log-likelihood = -173,630.9			

Table 3.4: Estimation results of the structural model.

help identify $\beta_{Sharing}$. A candidate might die if she keeps declining offers and continues to wait. The MELD transition matrix, $\mathcal{P}(MELD_{i,t+1} | MELD_{it}, d_{it} = 0)$, enables us to identify ω_d . In the data, we have candidates of various age groups, life support statuses, and medical conditions. The variations in their offer acceptance behaviors facilitate the identification of the parameters (ω_{Age} , ω_{LS} , and ω_{MC}). We assume the daily discount factor, $\delta = 0.99$, in our estimation. Our value of δ is in line with that of Zhang [58], who uses a discount factor of 0.99 for every six days (equivalent to a daily discount factor of 0.991).

3.6.3 Estimates

Table 3.4 reports the estimates of the structural model.⁷ The estimates of the parameters associated with *Sharing_type: Regional* and *Sharing_type: National* (with respect to *Sharing_type:*

⁷We used Julia 1.5.3 and the KNITRO solver to estimate our model on a 3.2 GHz 6-Core Intel Core i7 MAC with 32 GB RAM. Due to the size of the problem, it took approximately two weeks to solve the model.

Local) are negative, and national sharing is associated with the least utility. This is reasonable, given that local organs are generally associated with fewer prior refusals, and the organs outside the region are associated with a higher number of prior refusals; thus, are usually of lower quality and less desirable. In fact, Feng et al. [19] found similar estimates (0.105 for regional sharing and 0.244 for national sharing, with respect to local sharing) in their estimation of the donor risk index (DRI), a measure of the riskiness of graft failure associated with a donor organ. The estimate of β_{GS} is positive, which is consistent with the fact that organs that provide better survival are more desirable. *Death* is associated with a positive estimate and translates to a candidate incurring a one-time expected cost of $\frac{1}{1-\delta} \times \omega_d (=11.6)$ upon death. We observe that the waiting cost increases with age (most likely due to a decrease in well-being and the chances of comorbidities). Thus, older patients are more likely to accept an offer. Patients on life support incur a higher waiting cost than their counterparts. Compared to patients who are not hospitalized, hospitalized patients incur more costs, and ICU patients incur double the cost, compared to hospitalized patients. A higher waiting cost indicates greater urgency in accepting an offer. As a test for robustness, we relax the assumption of a fixed value of CIT in the utility function, and report the parameter estimates in Appendix B.7.

3.6.4 Insights from the Structural Model

Now we study how patients would react to the possibility of a transplant, both based on their health status and future prospects of being offered an organ. We use a stylized setup of two regions and three DSAs (Region A: DSA 1 and DSA 2; Region B: DSA 3), each with a single TC, in our numerical study to draw key insights. We compare five settings of demand and

supply across the DSAs (Set 1,..., Set 5; see Table 3.5). Note that the future prospect (captured by $EV(S_{it})$) depends on the organ offer probability, which depends on the supply and demand in various geographies (e.g., DSAs) and on the allocation policy in place (we consider both Share 35 and Acuity Circles). For this reason, we study the effect of a change in supply and demand on a patient's organ acceptance behavior (the steady state equilibrium organ acceptance probabilities are estimated using Algorithm 1 in Appendix B.8). By comparing the patient's organ acceptance behavior between these sets, we draw inferences of the effect of the supply and demand volume, and the s/d ratio.

We consider a single patient type (Rec_age : (45 – 65) years, $Rec_life_support$ ='No', Rec_med_cond ='NH'), and a single organ type (Don_age : (18 – 39) years, Don_race = 'White', Don_cod = 'Others', Don_dcd = 'No'). They represent the most frequent patient and organ types. We simulate the organ and candidate arrivals for a two-year time period ($t = 1, \dots, 730$).

The main insights are as follows: (1) When the s/d ratio differs between two DSAs, the difference (in terms of probability of offer acceptance) is greater for lower-MELD patients. The difference is attenuated at higher MELD scores due to the prioritization of higher-MELD patients through broader sharing (Share 35 and the Acuity Circles policy). If the s/d ratio decreases at a DSA, a patient reacts by becoming aggressive in organ acceptance behavior (i.e., the organ acceptance probability increases for the same organ). (2) Increasing the supply and demand volume (keeping the s/d ratio the same) in a DSA leads to an enlarged supply from where patients can receive an offer, which induces more selective behavior. This behavioral change is not merely limited to the DSA at which a change is made; indeed, it also has a spillover effect on other DSAs. Appendix B.9 provides a detailed comparison.

		Set 1*		Set 2		Set 3		Set 4		Set 5	
		d	s/d								
Region A:											
	DSA 1	250	0.7	250	0.7	250	0.7	250	0.7	250	0.7
	DSA 2	250	0.7	250	0.5	250	0.7	350	0.7	250	0.7
Region B:											
	DSA 3	500	0.7	500	0.7	500	0.5	500	0.7	700	0.7
<hr/>											
<u>Share 35:</u>											
MELD 6-14	DSA 1	[0.073, 0.073]		[0.074, 0.074]		[0.074, 0.074]		[0.073, 0.073]		[0.073, 0.073]	
	DSA 2	[0.073, 0.073]		[0.076, 0.076]		[0.074, 0.074]		[0.073, 0.073]		[0.073, 0.073]	
	DSA 3	[0.072, 0.073]		[0.073, 0.073]		[0.077, 0.077]		[0.072, 0.073]		[0.072, 0.073]	
MELD 15-28	DSA 1	[0.076, 0.077]		[0.079, 0.079]		[0.077, 0.078]		[0.076, 0.077]		[0.077, 0.077]	
	DSA 2	[0.076, 0.077]		[0.084, 0.085]		[0.078, 0.078]		[0.074, 0.075]		[0.076, 0.077]	
	DSA 3	[0.074, 0.075]		[0.074, 0.075]		[0.086, 0.087]		[0.074, 0.074]		[0.072, 0.073]	
MELD 29-32	DSA 1	[0.141, 0.144]		[0.143, 0.146]		[0.143, 0.147]		[0.136, 0.141]		[0.137, 0.141]	
	DSA 2	[0.139, 0.143]		[0.149, 0.153]		[0.145, 0.149]		[0.129, 0.134]		[0.135, 0.139]	
	DSA 3	[0.124, 0.128]		[0.126, 0.13]		[0.137, 0.14]		[0.12, 0.124]		[0.112, 0.117]	
MELD 33-34	DSA 1	[0.271, 0.28]		[0.273, 0.282]		[0.275, 0.289]		[0.256, 0.27]		[0.254, 0.266]	
	DSA 2	[0.266, 0.277]		[0.276, 0.287]		[0.278, 0.291]		[0.246, 0.263]		[0.252, 0.264]	
	DSA 3	[0.241, 0.256]		[0.247, 0.261]		[0.258, 0.269]		[0.231, 0.24]		[0.222, 0.234]	
MELD 35-36	DSA 1	[0.467, 0.486]		[0.469, 0.486]		[0.473, 0.492]		[0.441, 0.467]		[0.438, 0.46]	
	DSA 2	[0.464, 0.48]		[0.471, 0.487]		[0.483, 0.501]		[0.432, 0.462]		[0.431, 0.459]	
	DSA 3	[0.437, 0.46]		[0.447, 0.467]		[0.456, 0.472]		[0.426, 0.444]		[0.416, 0.435]	
MELD >36	DSA 1	[0.694, 0.718]		[0.697, 0.717]		[0.702, 0.724]		[0.667, 0.697]		[0.663, 0.686]	
	DSA 2	[0.687, 0.704]		[0.694, 0.71]		[0.705, 0.724]		[0.661, 0.691]		[0.657, 0.688]	
	DSA 3	[0.666, 0.687]		[0.681, 0.697]		[0.682, 0.701]		[0.661, 0.679]		[0.648, 0.669]	
<u>Acuity Circles#:</u>											
MELD 6-14	DSA 1	[0.073, 0.073]		[0.074, 0.074]		[0.074, 0.074]		[0.073, 0.073]		[0.073, 0.073]	
	DSA 2	[0.072, 0.073]		[0.076, 0.076]		[0.074, 0.074]		[0.072, 0.073]		[0.073, 0.073]	
	DSA 3	[0.073, 0.073]		[0.073, 0.074]		[0.077, 0.077]		[0.073, 0.073]		[0.073, 0.073]	
MELD 15-28	DSA 1	[0.076, 0.077]		[0.079, 0.079]		[0.078, 0.079]		[0.076, 0.077]		[0.076, 0.077]	
	DSA 2	[0.076, 0.077]		[0.083, 0.084]		[0.079, 0.079]		[0.074, 0.075]		[0.076, 0.077]	
	DSA 3	[0.074, 0.075]		[0.075, 0.076]		[0.085, 0.086]		[0.074, 0.074]		[0.072, 0.073]	
MELD 29-32	DSA 1	[0.133, 0.136]		[0.135, 0.138]		[0.137, 0.141]		[0.126, 0.131]		[0.126, 0.132]	
	DSA 2	[0.131, 0.136]		[0.137, 0.141]		[0.138, 0.143]		[0.123, 0.128]		[0.125, 0.129]	
	DSA 3	[0.122, 0.127]		[0.125, 0.129]		[0.134, 0.137]		[0.118, 0.122]		[0.111, 0.115]	
MELD 33-34	DSA 1	[0.26, 0.27]		[0.261, 0.271]		[0.266, 0.281]		[0.24, 0.256]		[0.237, 0.252]	
	DSA 2	[0.253, 0.266]		[0.259, 0.272]		[0.268, 0.282]		[0.237, 0.255]		[0.236, 0.249]	
	DSA 3	[0.239, 0.255]		[0.245, 0.259]		[0.254, 0.266]		[0.229, 0.238]		[0.22, 0.233]	
MELD 35-36	DSA 1	[0.468, 0.488]		[0.466, 0.485]		[0.473, 0.493]		[0.441, 0.468]		[0.433, 0.457]	
	DSA 2	[0.462, 0.48]		[0.471, 0.487]		[0.484, 0.502]		[0.43, 0.461]		[0.424, 0.455]	
	DSA 3	[0.436, 0.46]		[0.446, 0.466]		[0.453, 0.471]		[0.423, 0.443]		[0.414, 0.434]	
MELD >36	DSA 1	[0.696, 0.721]		[0.697, 0.72]		[0.702, 0.726]		[0.667, 0.698]		[0.66, 0.685]	
	DSA 2	[0.687, 0.706]		[0.696, 0.713]		[0.706, 0.727]		[0.66, 0.692]		[0.652, 0.688]	
	DSA 3	[0.667, 0.689]		[0.682, 0.698]		[0.684, 0.704]		[0.661, 0.681]		[0.649, 0.67]	

Table 3.5: Demand and Supply settings used in a numerical study to analyze their effect on a patient's behavior.

*: Set 1 is the baseline setting. 95% confidence intervals of the average probability of organ acceptance are shown in square brackets. #: To model the Acuity Circles policy in this geographic setup of two regions and three DSAs, we assume local → Regional → National sharing (instead of different circular bands of radii 150, 250, and 500 NM) within each MELD category.

3.6.5 Benchmarking

Our data cover two policy regimes (Pre-Share and Share 35). The observations (accept/decline decisions) provide ground truth, which provides an opportunity to conduct an out-of-sample comparison, i.e., training a model using the Pre-Share 35 policy era observations, and testing it on the Share 35 policy era. This lays the foundations of a strongly validated structural model, which we use to study counterfactual policies in the next section.

We compare various models (different versions of the dynamic and reduced-form models) on several important goodness-of-fit metrics in Table 3.6. In the category of dynamic models, we consider three structural models: our model (referred to as the Full Model), one without *Sharing_type* (DM1; as done in [5, 6]),⁸ and one without the richness in the waiting cost function (DM2; [4–6] assume a fixed reward upon waiting, and not as a function of the patient’s characteristics). In the category of reduced-form models, we consider three logistic regression models (RM1, RM2, and RM3), with the accept/decline decision as the dependent variable. To make it comparable with the dynamic models, we consider the following independent variables (Appendix B.10 describes the regression estimates). We find that the structural model (Full Model) outperforms all other models in every metric (except MAE, where RM1 and RM2 are better).

⁸Although the studies [5, 6] consider regional and national offers (in terms of their arrival rate), they assume that the rewards (or utilities) from these offers are the same.

Measure	Dynamic Models			Reduced-form Models		
	Full Model	DM1	DM2	RM1	RM2	RM3
AUC (ROC)	0.772	0.694	0.772	0.756	0.728	0.762
AUC (PRC)	0.202	0.166	0.197	0.194	0.141	0.182
Log-likelihood	-118,076.2	-125,045.4	-118,792.5	-119,525.8	-124,941.3	-121,758
RMSE	0.224	0.227	0.225	0.225	0.229	0.227
MAE	0.103	0.110	0.106	0.101	0.102	0.116

Table 3.6: Comparing the goodness-of-fit (out-of-sample) of various models on threshold-independent measures. AUC (ROC) and AUC (PRC) are the area under the receiver operating characteristic and precision-recall curves, respectively. RMSE and MAE stand for the root-mean-square error and mean absolute error, respectively.

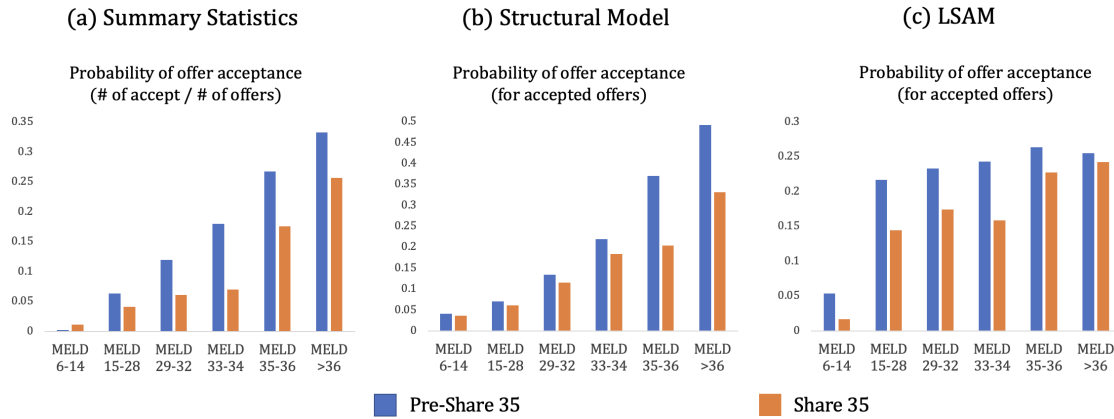


Figure 3.2: Out-of-sample comparison of LSAM with dynamic model prediction.

$$\mathbf{RM1: } d_{it} = a + bGS_{it} + cP(\text{death}|MELD_{it}) + \mathbf{dSharing_type}_{it} + \mathbf{eRec_age}_{it} + fRec_life_support_{it} + \mathbf{gRec_med_cond}_{it}$$

$$\mathbf{RM2: } d_{it} = a + bGS_{it} + cWait_time\ (in\ years) + \mathbf{dSharing_type}_{it} + \mathbf{eRec_age}_{it} + fRec_life_support_{it} + \mathbf{gRec_med_cond}_{it}$$

$$\mathbf{RM3: } d_{it} = a + \mathbf{bMELD}_{it} + \mathbf{dSharing_type}_{it} + \mathbf{eRec_age}_{it} + fRec_life_support_{it} + \mathbf{gRec_med_cond}_{it}$$

Next, we compare our structural model (Full Model) with LSAM (which is based on

59 parameters). Many studies [26, 27] have already pointed out the limitations of LSAM in predicting a patient’s offer acceptance behavior in a counterfactual policy. Nevertheless, to illustrate, we consider the Pre-Share 35 and Share 35 policies. The LSAM’s probability of acceptance model uses the SRTR’s parameter estimates. Our structural model uses the Pre-Share 35 policy era observations to estimate the parameters; and we then use them to predict the probability of offer acceptance in the Share 35 policy era. In Figure 3.2(a), we plot the average probability of offer acceptance (calculated as a fraction of the offers that were accepted) by the MELD category and use this as a reference. In Figures 3.2(b) and (c), we plot our structural model’s and the LSAM’s predicted probabilities of offer acceptance, respectively. Our structural model (in comparison to LSAM) more accurately captures: (i) the trend of offer acceptance probability (with the MELD category), and (ii) the regime shift (from the Pre-Share 35 to Share 35 policy). Appendix B.10 provides a few more out-of-sample comparisons.

3.6.6 Comparison of the Pre-Share 35 and Share 35 Policy Eras using the Structural Model

We compare the candidates as a function of their MELD class, region-wise. Given that the probability of an offer acceptance depends on the candidate’s state (S_{it}), we weigh the states to come up with a single number for each MELD class and region. For each MELD class (in a region), the weights assigned to the corresponding states (associated with that MELD class) reflect the empirical probabilities (estimated using the data) of being in those states. In Table 3.7, we report the candidate’s offer acceptance probabilities in the Share 35 policy era. Parentheses report the change compared to the Pre-Share 35 policy era.

	MELD 6-14	MELD 15-28	MELD 29-32	MELD 33-34	MELD 35-36	MELD >36
Region 1	4% (0%)	4.4% (-0.2%)	7.5% (-0.3%)	13.6% (-0.3%)	22.1% (-1.1%)	33.7% (-1.5%)
Region 2	3.8% (0.1%)	4.1% (-0.1%)	7% (-0.5%)	11% (-1.3%)	14.9% (-4.9%)	23.5% (-7.7%)
Region 3	3.1% (0.2%)	4.5% (0.1%)	6.6% (0.3%)	10.2% (-0.2%)	12.7% (-4.3%)	21.5% (-6.4%)
Region 4	4.6% (-0.2%)	4.7% (-0.6%)	7.7% (-1.3%)	12.9% (-2.6%)	16.9% (-7.1%)	27.2% (-10.2%)
Region 5	3.9% (-0.1%)	4.1% (-0.4%)	6.3% (-0.9%)	10.2% (-1.3%)	15.7% (-3.4%)	25.7% (-7%)
Region 6	4.2% (0.1%)	4.8% (-0.1%)	7.7% (-0.5%)	13.6% (-2.1%)	19.8% (-4.8%)	31.8% (-7.5%)
Region 7	3.6% (-0.1%)	4.1% (-0.5%)	6.8% (-1.1%)	11.9% (-2.3%)	16.5% (-6%)	27.1% (-8.8%)
Region 8	3.7% (0.1%)	4.5% (0%)	7.3% (0.4%)	11.4% (0.5%)	16.7% (-1.4%)	27.1% (-3%)
Region 9	4.6% (0.2%)	4% (0.1%)	6.3% (0.3%)	11% (0.3%)	19.9% (0.8%)	31.5% (1.7%)
Region 10	3.6% (0%)	4.5% (-0.2%)	6.8% (-1%)	9.3% (-2%)	14.5% (-5.7%)	24% (-9.3%)
Region 11	2.9% (0.1%)	4.2% (0%)	6.6% (-0.2%)	10.5% (-0.9%)	14.4% (-5.5%)	23.5% (-8.6%)

Table 3.7: Offer acceptance probabilities (in the Share 35 policy era) as a function of the MELD category. Parentheses report the change compared to the Pre-Share 35 policy era. Values are calculated using the structural model (whose parameters are estimated using data from 2010 to 2018).

We see that high-MELD candidates (MELD ≥ 35) in all regions (except region 9) became more selective in the Share 35 policy era, as their acceptance probabilities decreased.⁹ Given that the Share 35 policy prioritized sicker candidates in a geographically broader sense, allowing access outside their DSAs, they can afford to be more selective. For lower-MELD classes, we observe heterogeneity (across regions) in their behavioral change. For example, MELD 6-14 candidates experienced a negative effect and became aggressive in more than half of the regions (Regions: 2, 3, 6, 8, 9, 11). It turns out that these regions were associated with a relatively higher organ supply. The average supply (number of deceased donors)-to-demand (number of new patients joining the waiting list) ratio (based on the 2010 to 2018 time period) in these regions was 0.82, compared to 0.67 in the rest of the regions. Because the Share 35 policy increased

⁹Region 9 had the lowest ratio (0.51) of the number of deceased donors to the number of new patients joining the waiting list among all regions (2010 to 2018). It is likely that the Share 35 policy increased competition among the already organ-deficient DSAs (in Region 9), which led to an increase in aggressive behavior in even higher-MELD categories in Region 9 in the Share 35 policy era.

the priority of national patients over low-MELD (<15) local/regional patients, the low-MELD patients in the regions with a higher organ supply became aggressive in response to potentially losing access to organs that were now offered to candidates outside their respective regions.

3.7 Counterfactual Study

We now discuss the various performance metrics to measure geographic equity and efficiency, as emphasized by HHS [33], and compare the following policies of interest: (1) Pre-Share 35, (2) Share 35, (3) Acuity Circles, (4) s/d Match, and (5) National Sharing. To delineate the effect of the allocation policy from other factors such as changes in the patient and organ arrival processes, we simulate various policies using common data on patient and organ arrivals. In our simulation setup, we have 5,000 patients and 3,600 donors arriving at different points in time.

Recent studies [1, 9] have widely used the iterative simulation approach to estimate the new equilibrium organ offer probabilities in a counterfactual study. Instead of a simulation-based iterative approach, we derive analytical expressions to calculate quantities such as the number of offers, transplants, deaths, and so forth. We use these in an iterative framework (see Appendix B.8 for details, including the simulation setup) to compute the equilibrium organ offer probabilities in an allocation policy. The benefit of using analytical expressions is that it avoids randomness due to the candidates' accept/decline decisions and their MELD transitions, which helps achieve faster convergence with tighter tolerance limits. For performance metrics whose analytical computations are cumbersome, we simulate the organ allocation policy 50 times (using its equilibrium organ offer probabilities) and report the *average*. Performance metrics based on analytical computations are reported as an *expected* quantity.

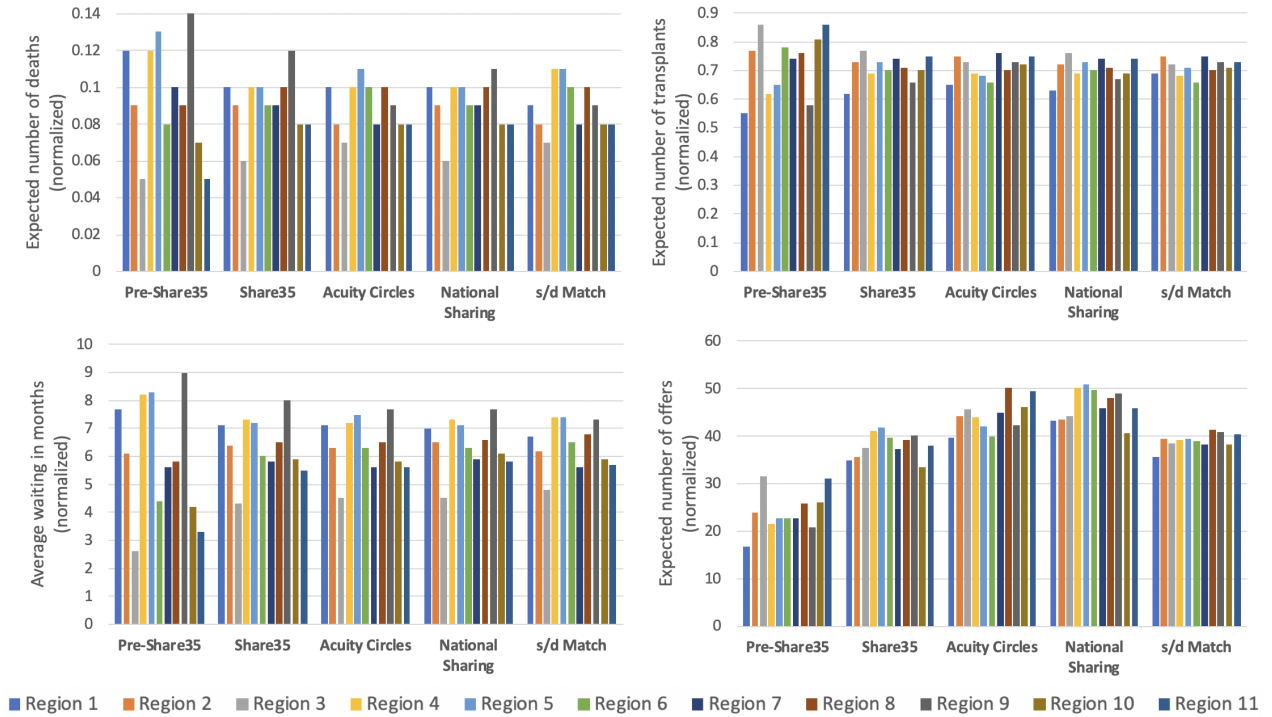


Figure 3.3: Comparison of different geographic equity measures between policies.

3.7.1 Geographic Equity

Figure 3.3 compares the expected number of deaths, expected number of transplants, average waiting time in months (that a patient spends on the waiting list until transplantation, death or the end of a simulation), and expected number of offers across regions and between various allocation policies. We report the values after normalizing them with the waiting list volumes in their respective regions. Comparing the Pre-Share 35 and Share 35 policies, we find that the benefit due to the Share 35 policy is higher for regions with lower supply-to-demand ratios in the simulation setup (see Appendix B.11 for details). In Table 3.8, we report the standard deviations, calculated across regions, for different geographic equity metrics and allocation policies. Compared to the Pre-Share 35 policy, other policies (Share 35, Acuity Circles, National Sharing, and s/d Match)

Geographic equity	Standard deviation across regions				
	metrics (normalized)	Pre-Share 35	Share 35	Acuity Circles	National Sharing
Deaths	0.031	0.015	0.013	0.014	0.013
Transplants	0.109	0.043	0.038	0.037	0.028
Waiting (in months)	2.164	1.024	0.964	0.878	0.801
Offers	4.350	2.626	3.413	3.364	1.553

Table 3.8: Comparison of the standard deviation of various geographic equity measures between policies. The s/d Match policy has the lowest values for each of the geographic equity metrics.

increase geographic equity (as indicated by the decrease in the variability of the performance metrics across regions). The s/d Match (Pre-Share 35) policy has the lowest (highest) variability across all performance measures. Even if we exclude the Pre-Share 35 policy from the comparison, the s/d Match policy has a (0-13)% lower standard deviation (compared to the rest) in the expected number of deaths, (24-35)% less variability in the expected number of transplants, (9-22)% less variability in the average waiting time, and (41-54)% less variability in the expected number of offers.

On an aggregate basis, we find that, out of a total of 5,000 patients in our study, the Pre-Share 35 policy resulted in 499.0 expected deaths; the Share 35 policy resulted in 463.2 deaths; the Acuity Circles policy resulted in 462.2 deaths; the s/d Match policy resulted in 459.9 deaths; and the National Sharing policy resulted in the least number of deaths, 454.1. Out of a total of 3,600 organs, the Pre-Share 35 policy resulted in 3,575.4 expected transplants; the Share 35 policy resulted in 3,570.4 transplants; the Acuity Circles policy resulted in 3,564.3 (lowest) transplants; the s/d Match policy resulted in 3,570.8 transplants; and the National Sharing policy resulted in 3,564.6 transplants.

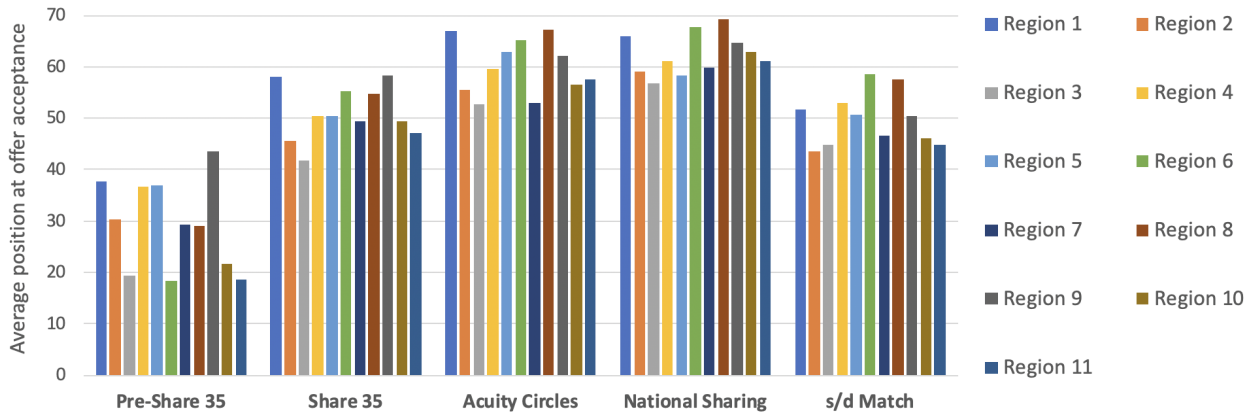


Figure 3.4: Comparison of the position at offer acceptance between policies.

3.7.2 Efficiency

We capture efficiency using four performance metrics: position in the queue at offer acceptance, utility derived from transplantation, increase in the patient’s survival probability (calculated at the end of one year) due to the transplant, and distance traveled by the organ.

In Figure 3.4, we compare the average position at which a candidate accepts an offer across regions and between various allocation policies. The three policies (Pre-Share 35, Share 35, and National Sharing) are in increasing order of broader sharing. The Pre-Share 35 policy prioritizes local patients; the Share 35 policy allows more regional and national sharing than its predecessor policy, while the National Sharing policy does not consider geography conditional on the patient’s MELD. The Acuity Circles policy can be seen as a broader sharing analogue of the s/d Match policy (given that the latter allows the radius around a donor hospital to be less than 500 NM). We observe that as sharing becomes broader, the position at acceptance and offer refusals increase as a consequence. This is consistent with the takeaway we had drawn (i.e., the Share 35 policy resulted in higher offer refusals) while discussing Figure 3.1.

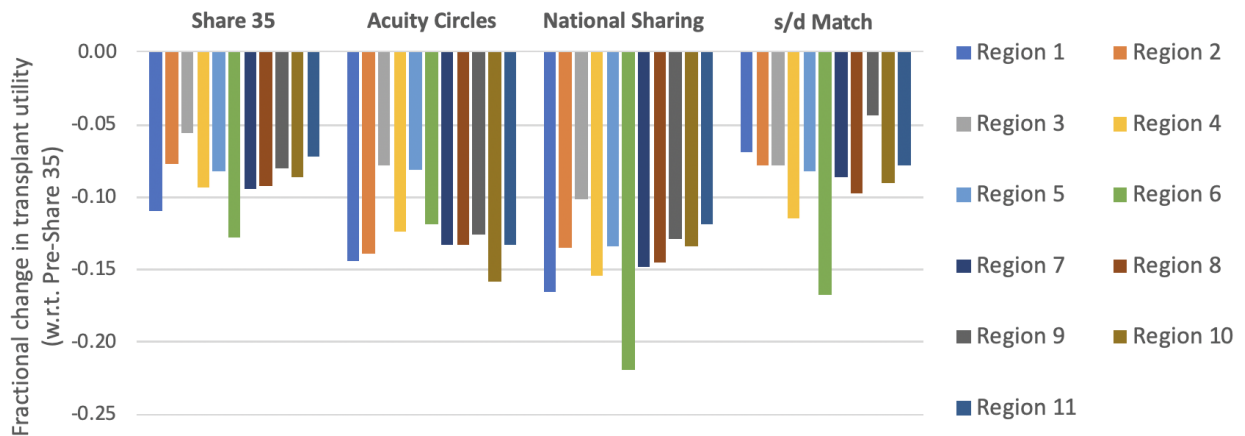


Figure 3.5: Comparison of the fractional change in the utility from the transplant (with respect to the Pre-Share 35 policy) between policies.

Given that utility on its own has no physical interpretation, we report the fractional change in the average utility from transplantation with respect to the Pre-Share 35 policy in Figure 3.5. We see that all policies are associated with lower transplant utility (as compared to the Pre-Share 35 policy). We also observe that, as the position at the offer acceptance increases, the transplant utility decreases. This is reasonable because offer refusals tend to deteriorate the quality of the organ, and thus, the transplant utility.

Further, we simulate a new policy, Outcome based, where the candidates are sequenced (for organ offers) in decreasing order of the prospective expected utility derived from transplantation. It sets a benchmark for the best outcomes that can be expected for an allocation policy (we note that the Outcome-based policy does not follow the federal guidelines because it does not offer the organ to the sickest patient first). We then estimate the cost of fairness (fractional decrease in the transplant utility with respect to the Outcome-based policy) in Figure 3.6. The Share 35 and s/d Match policies have the least cost (a 13% decrease in the transplant utility with respect to the Outcome-based policy), while the Acuity Circles and National Sharing policies result in 17%

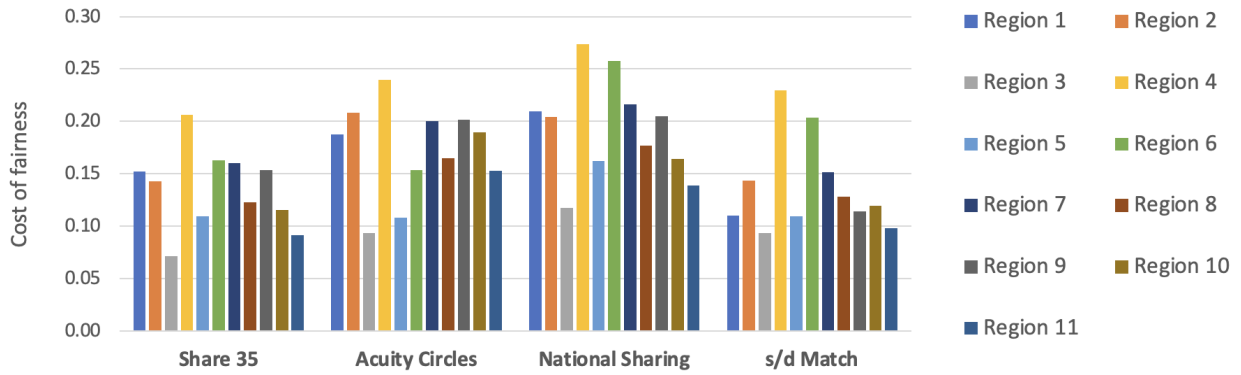


Figure 3.6: Cost of fairness for various policies. It is defined as the fractional decrease in the transplant utility with respect to the Outcome-based policy.

and 19% decrements, respectively.

Next, we calculate the increase in a patient’s survival probability due to a transplant as the difference between the probability of graft survival and the probability of a patient’s survival without a transplant, both measured at the end of one year. Appendix B.12 provides methodological details. We simulate a new policy, Survival Benefit, where the candidates are sequenced (for organ offers) in decreasing order of the increment in the patient’s survival probability due to the transplant. It sets a benchmark for the greatest benefits (in terms of survival probability) that can be expected for an allocation policy (again this policy does not follow the federal guidelines). In Figure 3.7, we report the average increase in the survival probability due to a transplant in different policy scenarios. We see that the Survival Benefit and National Sharing policies result in the highest benefits (survival probability increases by 0.186 on average), followed by the s/d Match (0.183), Acuity Circles (0.181), Share 35 (0.180), and Pre-Share 35 (0.169) policies. The s/d Match policy is comparable with the benchmark, if not the best.

In Table 3.9, we compare the travel distance between the policies (we exclude the observations associated with the donor hospitals and transplant centers situated at HIOP (DSA in Hawaii) and

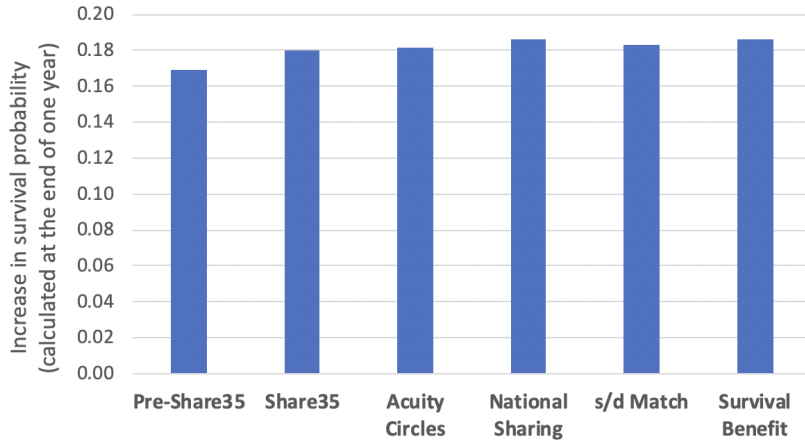


Figure 3.7: Comparison of the average increase in the survival probability due to transplantation between policies.

	Pre-Share 35	Share 35	Acuity Circles	National Sharing	s/d Match
Mean	240	390	357	503	360
1st quartile	46	59	56	71	52
Median	114	176	197	279	180
3rd quartile	282	528	435	760	417

Table 3.9: Comparison of the travel distance (in NM) between policies.

PRL (DSA in Puerto Rico) from the analysis). The distance between any two DSAs' i and j is calculated as the mean of the transplant-volume-weighted distance between the donor hospitals in DSA i and the transplant centers in DSA j , and the reverse. We see that the National Sharing policy results in the largest travel distance, while the Pre-Share 35 policy results in the smallest travel distance. This is reasonable, given that they are at the two extremes of the broader sharing level. The s/d Match policy is marginally better than the Acuity Circles policy and outperforms the Share 35 policy (in all but the median travel distance).

Overall, the s/d Match policy, which is based on equalizing the s/d ratios by selectively increasing the sharing of donor organs, has the lowest trade-off on the efficiency metrics (compared to the Pre-Share 35 policy) in addressing the issue of geographic inequity. In fact, when a larger

radius is allowed around a donor hospital, the s/d ratios are much closer at the transplant centers (i.e., equalized better), and the efficiency metrics are further improved. See Appendix [B.13](#) for details. Thus, the s/d Match policy offers a significantly better alternative to the Acuity Circles policy while following the guiding allocation principles laid out by UNOS.

3.8 Conclusions

We develop a structural model that endogenizes the forward-looking behavior of patients with the allocation policy. We formulate the problem as a discrete-time infinite-horizon dynamic optimization model and use a rich set of patient and donor medical attributes without losing the model's tractability. We compare our dynamic model with LSAM and other reduced-form models to establish the credibility of our structural model, which we use to study counterfactual policies.

First, we study the impact of the Share 35 liver allocation policy (introduced in June 2013) on patients' organ acceptance behavior. We find that the Share 35 policy induced more selective behavior and benefited high-MELD (sicker) patients, with mixed results in low-MELD patients across regions. We also find that the Share 35 policy reduced geographic disparity in metrics such as the number of deaths, access to transplants, waiting time, and organ offers. We observe that the regions with lower supply (deceased donors)-to-demand (new patients) ratios reaped greater benefits. However, the Share 35 policy resulted in more offer refusals and lower average utility from the transplantations.

Recent policies are moving toward broader sharing in principle. The current 'one-size-fits-all' Acuity Circles policy performs very similarly to the Share 35 policy under geographic equity metrics. However, it leads to even lower efficiency (more offer refusals and less utility

from transplantation). We illustrate that broader sharing in its current form *is not the best strategy to balance geographic equity and efficiency*. The intuition is that by indiscriminately enlarging the pool of supply locations from where patients can receive offers, the patients tend to become more selective, resulting in more offer rejections and less efficiency. Instead, a customized approach (equalizing the supply-to-demand ratios across geographies) through the s/d Match policy performs best in addressing the issue of geographic inequity while sacrificing the least efficiency (compared to the Pre-Share 35 policy). This policy selectively enhances the radii around donor hospitals, increasing broader sharing as necessary to equalize the supply and demand. *We strongly recommend that policymakers move away from a ‘one-size-fits-all’ approach to broader sharing and instead develop broader sharing in a framework that matches the supply and demand*. Such a policy has the greatest potential to score well both in terms of efficiency and geographic equity.

Previous policy proposals have been assessed using LSAM, which uses the same probability acceptance function for candidates and does not consider whether a candidate is residing in an organ-rich/-deficient location. Our study provides a framework for researchers and policymakers to incorporate patients’ potential behavioral change into assessing a new policy proposal, which influences their acceptance probability. There is a considerable push in the transplant community to eventually move to a continuous scoring framework. (This framework conceptually gets rid of boundaries. For each organ offer it computes a composite score (used to determine offer sequence) for candidates on the waitlist, which is a combination of factors related to medical priority, the efficiency of organ placement, expected post-transplant outcome, and equity.¹⁰ At

¹⁰<https://optn.transplant.hrsa.gov/governance/public-comment/continuous-distribution-of-lungs-concept-paper/>

this point, the policy parameters (i.e., weights on the different components of the score) are yet to be determined.) An interesting and potentially impactful future study would be to determine the policy parameters in this continuous scoring framework to equalize the s/d ratios across transplant centers.

We limit our study to focus only on geographic inequity (as motivated by prior lawsuits) and do not consider other kinds of disparities such as race, gender, socio-economic factors, organ size, and blood type. Developing a model to incorporate and mitigate these additional disparities is an interesting direction for future research.

Disclaimer: The data reported here have been supplied by the Hennepin Healthcare Research Institute (HHRI) as the contractor for the Scientific Registry of Transplant Recipients (SRTR). The interpretation and reporting of these data are the responsibility of the author(s) and in no way should be seen as an official policy of or interpretation by the SRTR or the U.S. government.

Chapter 4: A Continuous Scoring Model for Fair Liver Transplant Allocation

4.1 Introduction

The Health Resources and Services Administration (an agency of the HHS) has been under pressure over the last two decades to address geographic disparities [34]. The liver lawsuit precipitated a change to the Acuity Circles policy, as an interim policy in February 2020. Going forward, it is a goal that all the organ allocation systems (including liver) will be based on the *Continuous Distribution Framework*.¹ In this framework, the waiting list candidates will be prioritized based on a *composite score*, which will depend on several factors, each contributing towards the total score of a candidate. The factors in consideration are medical severity, expected post-transplant outcome, the efficient management of organ placement, equity, and so on. However, the respective weights for each of these potential factors are not yet decided.

In this chapter, we consider two factors, medical severity and the efficient management of organ placement (captured using the *proximity score*, which is a function of the distance between donor hospital and transplant center) to design an allocation policy in a continuous scoring framework. We use UNOS's stated principle of reducing inherent differences in the ratio of the supply to demand (s/d) across transplant centers as our objective explicitly within a

¹<https://optn.transplant.hrsa.gov/governance/public-comment/continuous-distribution-of-lungs-concept-paper/>

mathematical optimization framework. One approach to reduce inequity is through the central distributive principle, proposed by Rawls [42]: the least well-off group in the society should be made as well off as possible. We use this *maximin* principle to maximize the minimum value of the s/d ratio across all transplant centers. We then apply a secondary optimization to minimize the disparity between the transplant centers with the highest and lowest s/d ratios.

4.1.1 Contributions and Findings

We make the following contributions to the literature: (1) We develop a novel analytical method to model s/d ratio (at a transplant center) in the contribution distribution framework; and (2) Our optimization framework can be applied to other organ settings to design policy parameters. With 500 nautical-mile (NM) fixed circles (representative of the current Acuity Circles), the s/d ratio ranges from 0.36 to 0.87. We show that when heterogeneous slopes (for proximity score functions) are used at the donor hospitals, the s/d ratio ranges from 0.56 to 0.61, meaning that there is a much lower disparity in organ access among the transplant centers. Note that the radii around the donor hospitals are the same (unlike Chapter 2), but instead we use the proximity score function to achieve parity in the s/d ratio.

We use a simulation model that replicates the SRTR's Liver Simulated Allocation Model (LSAM, version 2014) to evaluate our proposed policy with the current Acuity Circles policy. The simulation uses historical patient and organ donor data. The results show that in comparison to the current Acuity Circles policy, an allocation policy based on our optimized heterogeneous slopes, with organ sharing up to a radius of 500 NM and full regional sharing of all organs with MELD scores ≥ 15 , reduces the variance of MMaT across DSAs (from 6.66 to 5.00) and average

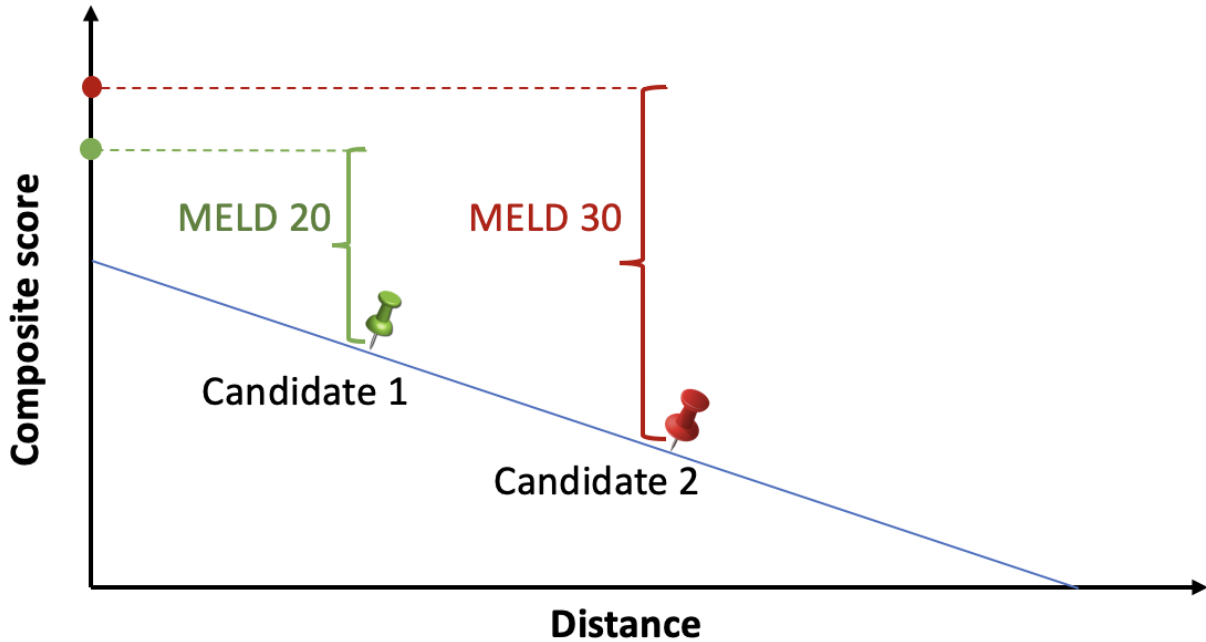


Figure 4.1: Example of continuous scoring framework. Candidate 2 has higher composite score than candidate 1, and thus gets priority.

annual deaths (from 2,513 to 2,443).

A key policy insight is that the one-size-fits-all framework (i.e., using the same slopes for the proximity score functions) approach will not adequately address the problem of reducing differences in the ratio of the donor supply to demand across the country. Rather, a customized approach that accounts for where the organ supply and demand occur and adjusts slopes of the proximity score functions more effectively addresses UNOS' stated goal of equalizing s/d ratios.

4.2 Model Formulation

Consistent with UNOS's stated principles, our approach is to design an organ distribution policy that equalizes s/d ratios across transplant centers, and thus mitigates geographical disparities. We assume that the MELD scores of candidates across geographies are independent and identically

Notation	Description
$s \in \mathcal{S} = \{1, \dots, N_{sup}\}$	Supply location or donor hospital
$t \in \mathcal{T} = \{1, \dots, N_{dem}\}$	Transplant center
y_{st}	Proximity score assigned to the candidates at t for organs from s
y_s	y-intercept of the <i>proximity score</i> function at s
Parameters:	
d_t	Number of incident waiting list additions (or demand) at t
s_s	Number of organs recovered for transplantation (or supply) at s
τ_{st}	Distance between s and t
τ	Maximum distance from a donor hospital to a transplant center for organ sharing
$\lambda_{[S-1]}^*$	Minimum s/d ratio value to be used in Stage 2 optimization
$s_{st}^{(y)}$	Apportioned share of organs from s to t when the y-intercept of the <i>proximity score</i> function at s is y
n	Maximum number of offers before the organ is discarded
Decision variables:	
x_{sy}	1 if the y-intercept at s is y , and 0 otherwise
λ	Minimum s/d ratio for an allocation
β	Maximum s/d ratio for an allocation

Table 4.1: Model Notation

distributed (i.i.d); and the distribution of organ quality are similar across donor hospitals. The proximity score is assumed to be a step function of the distance between donor hospital and transplant center, and is a decreasing one. The offers are made to the candidates whose respective transplant centers lie within a distance of τ units from the donor hospital. Each candidate accepts an offer with a probability that depends on her position in the offer queue.

4.2.1 (Expected) Supply-Demand Ratio Calculation at a Transplant Center

First, we define our s/d ratio measure. The notation is described in Table 4.1. We start by aggregating the historical supply and demand of organs by geographical location for the period of study. We allow for uncertainty in the organ acceptance behavior of a candidate, and we

model *expected* supply to a transplant center. In a continuous scoring policy, *composite score* (calculated for every candidate in consideration) plays the key role in determining the offer sequence. Therefore, it is central to s/d ratio calculation. We model the *composite score* of a candidate as the sum of their MELD score and proximity score. When an organ is recovered, the offer sequence is assumed to depend on the medical urgency of the candidates, and their distances to the donor hospital (Figure 4.1). The *proximity score* function is modeled as:

$$y_{st} = \lceil \max\{y_s(1 - \frac{\tau_{st}}{\tau}), 0\} \rceil \quad (4.1)$$

where y_{st} is the proximity score assigned to the candidates at transplant center t for organs from supply location s , y_s is the y-intercept at s , and τ_{st} is the distance between s and t . We assume y_s to be a positive integer, and using a step function (through the ceiling operator) for the proximity score ensures that the resultant distribution of *composite score* of candidates of any two transplant center is discrete. This simplifies the calculation.

We first estimate the expected share of organs from a donor hospital, s to a transplant center, t . The share will depend on the proximity score function associated with the donor location, demands at various transplant centers (that are within the specified catchment area), and offer acceptance probabilities. Now we go through the intermediate steps to calculate the probability that an organ offer will be accepted by a candidate listed at transplant center, t .

4.2.1.1 Mixture Distribution

When an organ is recovered at a supply location s , we assume that candidates at all the transplant centers that are within a distance of τ units are potential recipients. The distributions of

composite scores at the transplant centers might be different due to differences in their proximity to s (see Equation 4.1). Let $X_{t,s}$ be a discrete random variable denoting the distribution of *composite score* at transplant center, t w.r.t. s . Let X_s be a discrete random variable denoting the distribution of *composite score* at donor location s . X_s , which is a mixture of *composite scores* from of all the transplant centers within τ units of distance, can be modeled in two steps: (1) A transplant center is randomly selected; and (2) A *composite score* is drawn from the population of the selected transplant center. Formally,

$$P(X_s = x) = \sum_{t': \tau_{st'} \leq \tau} \frac{d_t}{\sum_{t': \tau_{st'} \leq \tau} d_{t'}} \times P(X_{t,s} = x)$$

4.2.1.2 Order Statistic of the Mixture Distribution

Let $n_s (\leq n)$ be the total number of candidates (from all the transplant centers) competing for an organ recovered at s . The offer sequence will follow a decreasing order of their *composite scores*, therefore, we calculate the order statistic of the mixture distribution (X_s). Let,

$$p_1 = P(X_s < x) = F_s(x) - P(X_s = x), \quad p_2 = P(X_s = x), \quad \text{and} \quad p_3 = P(X_s > x) = 1 - F_s(x)$$

The cumulative distribution function of the k^{th} order statistic (denoted by, $X_{s,(k)}$) is given by:

$$\begin{aligned}
P(X_{s,(k)} \leq x) &= P(\text{there are at least } k \text{ observations less than or equal to } x) \\
&= P(\text{there are at most } n_s - k \text{ observations greater than } x) \\
&= \sum_{j=0}^{n_s-k} \binom{n_s}{j} p_3^j (p_1 + p_2)^{n_s-j}
\end{aligned} \tag{4.2}$$

$$\begin{aligned}
P(X_{s,(k)} < x) &= P(\text{there are at least } k \text{ observations less than } x) \\
&= P(\text{there are at most } n_s - k \text{ observations greater than or equal to } x) \\
&= \sum_{j=0}^{n_s-k} \binom{n_s}{j} (p_2 + p_3)^j p_1^{n_s-j}
\end{aligned} \tag{4.3}$$

$$\begin{aligned}
P(X_{s,(k)} = x) &= P(X_{s,(k)} \leq x) - P(X_{s,(k)} < x) \\
&= \sum_{j=0}^{n_s-k} \binom{n_s}{j} \left(p_3^j (p_1 + p_2)^{n_s-j} - (p_2 + p_3)^j p_1^{n_s-j} \right)
\end{aligned} \tag{4.4}$$

For the i^{th} candidate on the offer sequence, the corresponding value of k will be $(n_s - i + 1)$. The above equation captures the distribution of *composite score* associated with a supply location s . When a candidate from transplant center t accepts an offer, there must be a sequence number associated with that offer. Next, we calculate the probability that a candidate at the i^{th} sequence belongs to transplant center t .

4.2.1.3 Probability that the i^{th} Candidate at s is From Transplant Center t and Accepts the Offer

Let the i^{th} candidate have *composite score*, x . The probability that the candidate is from transplant center t is:

$$P(i^{th} \text{ candidate is from } t | i^{th} \text{ composite score} = x) = \frac{d_t P(X_{t,s} = x)}{\sum_{t': \tau_{st'} \leq \tau} d_{t'} P(X_{st'} = x)} \quad (4.5)$$

$$\begin{aligned} P(i^{th} \text{ candidate is from } t) &= \sum_x P(i^{th} \text{ candidate is from } t \cap i^{th} \text{ composite score} = x) \\ &= \sum_x P(i^{th} \text{ composite score} = x) \times P(i^{th} \text{ candidate is from } t | i^{th} \text{ composite score} = x) \\ &= \sum_x P(X_{s,(n_s-i+1)} = x) \times \frac{d_t P(X_{t,s} = x)}{\sum_{t': \tau_{st'} \leq \tau} d_{t'} P(X_{st'} = x)} \end{aligned} \quad (4.6)$$

For the i^{th} candidate to accept an offer, the previous $(i - 1)$ candidates should have declined it.

Let p_i be the probability of accepting an offer made at the i^{th} position.

$$\begin{aligned} P(i^{th} \text{ candidate is from } t \cap \text{ accepts the offer}) &= \left[\prod_{j=2}^{i-1} (1 - p_j) \right] p_i \times P(i^{th} \text{ candidate is from } t) \\ &= \left[\prod_{j=2}^{i-1} (1 - p_j) \right] p_i \times \sum_x P(X_{s,(n_s-i+1)} = x) \times \frac{d_t P(X_{st} = x)}{\sum_{t': \tau_{st'} \leq \tau} d_{t'} P(X_{st'} = x)} \end{aligned}$$

4.2.1.4 Probability that an Organ from s is Accepted by a Candidate at Transplant

Center t

$$\begin{aligned} P(\text{an organ from } s \text{ goes to } t) &= \sum_{i=1}^{n_s} P(i^{th} \text{ candidate is from } t \cap \text{ accepts the offer}) \\ &= \sum_{i=1}^{n_s} \left[\prod_{j=2}^{i-1} (1 - p_j) \right] p_i \times \sum_x P(X_{s,(n_s-i+1)} = x) \times \frac{d_t P(X_{st} = x)}{\sum_{t': \tau_{st'} \leq \tau} d_{t'} P(X_{st'} = x)} \end{aligned} \quad (4.7)$$

Finally, the s/d ratio at a transplant center $t = \frac{1}{d_t} \sum_{s:\tau_{st} \leq \tau} s_s \times P(\text{an organ from } s \text{ is accepted at } t)$

$$= \frac{1}{d_t} \sum_{s:\tau_{st} \leq \tau} s_s \times \left(\sum_{i=1}^{n_s} [\prod_{j=2}^{i-1} (1 - p_j)] p_i \times \sum_x P(X_{s,(n_s-i+1)} = x) \times \frac{d_t P(X_{st} = x)}{\sum_{t' \in T(s)} d_{t'} P(X_{st'} = x)} \right) \quad (4.8)$$

$$= \frac{1}{d_t} \sum_{s:\tau_{st} \leq \tau} s_{st}^{(y_s)} \quad (4.9)$$

Equation 4.8 models the expected supply-to-demand ratio at a transplant center, t . It depends on the following factors: (1) The y-intercepts at the various supply locations, (2) Supply and demand volumes at s , and t , respectively, (3) Distances between the pairs of supply and demand locations (τ_{st})'s, (4) Maximum allowable sharing distance (τ), (5) The probabilities of accepting an offer as a function of position in the queue, and (6) Maximum number of offers before discarding the organ. $s_{st}^{(y_s)}$ in equation 4.9 denotes the apportioned share of organs from s to t when the y-intercept of the *proximity score* function at s is y_s . Note that only y_s is a variable.² This implies that, for a given set of y_s 's, we can calculate $s_{st}^{(y_s)}$ offline and store in a look-up table. Let $y_s \in \mathcal{Y}$, where \mathcal{Y} contains positive integers. Recall that we model the *composite score* of a candidate as the sum of their MELD score and *proximity score*. Given this functional form, it is a reasonable to postulate that the *proximity score* should have the same order of magnitude as the MELD score. The *proximity score* has the upper bound as y_s (when $\tau_{st} = 0$). We assume $\mathcal{Y} = \{1, \dots, 20\}$ in our study. A higher value of y_s places greater emphasis on distance (τ_{st}). Thus, it acts as a lever to differentiate two transplant centers in terms of their respective priorities for an organ at s .

²We assume the maximum number of offers to be a constant.

4.2.2 Heterogeneous Slopes Model

We now describe our optimization model. To design a fair allocation policy, we apply the *maximin* equity principle to maximize the performance of the worst transplant center (i.e., we maximize the value of the lowest s/d ratio across all transplant centers) in Stage 1. In Stage 2, we reduce the disparity among the different transplant centers. To do this, we minimize the disparity between the best and worst transplant centers, while ensuring the s/d ratio of the worst transplant center remains at the optimum value obtained from the Stage 1 optimization. We now present the *Set-Partitioning* formulations for the two stages.

4.2.2.1 Stage 1 Formulation

In Stage 1, we seek to maximize the s/d ratio of the worst transplant center.

$$\text{[SP-1] Maximize } \lambda \tag{4.10}$$

$$\text{subject to: } \lambda \leq \sum_{s:\tau_{st} \leq \tau} \sum_{y \in \mathcal{Y}} \frac{x_{sy} s_{st}^{(y)}}{d_t} \quad \forall t \in \mathcal{T} \tag{4.11}$$

$$\sum_{y \in \mathcal{Y}} x_{sy} = 1 \quad \forall s \in \mathcal{S} \tag{4.12}$$

$$x_{sy} \in \{0, 1\} \quad \forall s \in \mathcal{S}, \forall y \in \mathcal{Y} \tag{4.13}$$

Constraint (4.11) models λ as the lower bound of the s/d ratios across all transplant centers; and the objective is to maximize this lower bound. Constraint (4.12) allows one assignment of y to each donor hospital. x_{sy} is a binary variable that takes value 1 if the y -intercept at s is y , and 0 otherwise. The set \mathcal{Y} contains the possible values of y values.

4.2.2.2 Stage 2 Formulation:

Once the optimal solution $\lambda_{[SP-1]}^*$ to [SP-1] is obtained, we can solve [SP-2] to minimize the maximum s/d ratio while ensuring that the minimum s/d ratio remains at least $\lambda_{[SP-1]}^*$.

$$\begin{aligned} & \text{[SP-2] Minimize } \beta \\ \text{subject to: } & \beta \geq \sum_{s:\tau_{st} \leq \tau} \sum_{y \in \mathcal{Y}} \frac{x_{sy} s_{st}^{(y)}}{d_t} \quad \forall t \in \mathcal{T} \end{aligned} \quad (4.14)$$

$$\lambda \geq \lambda_{[SP-1]}^* \quad (4.15)$$

$$\text{All constraints from [SP-1]} \quad (4.16)$$

The optimal values of x_{sy} obtained by optimizing [SP-1], followed by [SP-2], are used to construct the new optimized geographical scheme. The optimization variable is the y-intercept at a donor hospital. Varying the y-intercept directly affects the slope of the *proximity score* function. Therefore, we refer our model to as *Heterogeneous Slopes Model*. The donor hospitals can have different slopes of their *proximity score* functions.

4.3 Data and Results

4.3.1 Data

This study used data from the Scientific Registry of Transplant Recipients (SRTR). The SRTR data system includes data on all donors, wait-listed candidates, and transplant recipients in the U.S., submitted by the members of the Organ Procurement and Transplantation Network (OPTN). The Health Resources and Services Administration (HRSA), U.S. Department of Health

and Human Services provides oversight to the activities of the OPTN and SRTR contractors.

In the data encompassing four years (January 2015 to December 2018), the supply or the total number of deceased-donors livers donated (and transplanted) from all donor hospitals (with at least 5 organs) in the U.S. is 26,726. The patient pool is dynamic: new patients enlist, waiting candidates die or become too sick for transplant and are removed, and the MELD scores get updated periodically. We measure demand (44,295) as the total incident adult patients whose MELD scores became at least 15 during the four years, which gives a national s/d ratio of 0.6034.³ There are two reasons for excluding low-MELD patients from the demand: (1) Patients with MELD scores <15 have no survival benefit from transplantation [40]; therefore, our demand measure is less sensitive to the number of low-MELD patients added to the waiting list, and (2) Transplant centers differ in their practices of listing low-MELD patients, across the country (which would create an artificial increase in demand for a transplant center listing low-MELD patients compared to a transplant center that does not). In practice, the fraction of transplants to low-MELD patients is relatively very low—about 1.40% (in the four years encompassing our study), supporting the decision to exclude them. We consider \mathcal{Y} set as $\{1, \dots, 20\}$, and let τ equal to 500 NM, 600 NM or 700 NM.

4.3.2 Results

We apply the set-partitioning optimization model to a setting where the supply locations are 1,193 donor hospitals and demand locations are 145 transplant centers.⁴ The distance between a donor hospital and transplant center pair is taken from the SRTR's LSAM. Consistent with

³We consider incident patients so that the model parameters are not biased due to accumulated disparity, and thus are exogenous to the geographical scheme. We exclude Hawaii and Puerto Rico from the analysis.

⁴We used R 3.5.1 and the commercial solver Gurobi 8.1.1 to solve the set-partitioning optimization models on a 3.2 GHz 6-Core Intel Core i7 iMac with 32 GB RAM.

the current policy donor hospitals in Alaska are considered to be situated at the Seattle Tacoma Airport in Washington State.

Table 4.2 compares the s/d ratios across transplant centers. The ‘No Proximity Score’ model ($\tau = 500$ NM) is the best representation of the current Acuity Circles policy (that draws a circle of 500 NM around the donor hospital for sharing organs with the transplant centers within that radius). Compared to the heterogeneous slopes policy, the current policy does a poor job in equalizing s/d ratios across transplant centers. The heterogeneous slopes policy at $\tau = 500$ NM is able to keep the ratio at transplant centers between 0.56 and 0.61 (compared to the national s/d ratio of 0.6034), while the current Acuity Circles policy has an s/d ratio variation between 0.36 and 0.87. The fixed slope policies (where all the donor hospitals have the same intercept values in their proximity score functions, and thus slopes) do not help in equalizing the s/d ratios. In other words, the ‘one-size-fits-all’ approach will not address the issue of geographic equity. As we increase τ from 500 NM to 700 NM, the range of s/d ratios decreases in most cases.

We also conducted a numerical study using a LSAM simulation model [52], replicated in Python (it is not possible to simulate the Heterogeneous Slopes model directly in LSAM, but by using a recoded version in Python there is greater flexibility to do so). We simulated our proposals and the Acuity Circles policy using the organ and patient arrival data, consisting of three years (July 2013 to June 2016). We ran the simulation 10 times (the maximum allowed by LSAM) by resampling the input files. We assume $p_1 = \dots = p_n = 0.89$ (based on the data). We allowed the maximum number of offers (for each organ), n to be 100. For optimizing the intercepts in our integer program, we used the LSAM data on supply and demand. In Table 4.3, we report a few important performance metrics. We see that as we increase τ , the benefit (compared to the Acuity Circles policy) increases in terms of the life savings and reduction in the variance of

Allocation Policy	s/d ratios (across TCs)			
	τ :	500 NM	600 NM	700 NM
No Proximity Score		0.36-0.87	0.34-0.99	0.32-0.95
Heterogeneous Slopes Model [SP-2]		0.56-0.61	0.57-0.61	0.57-0.61
Fixed Slope (Intercept = 1)		0.36-0.87	0.34-0.99	0.32-0.95
Fixed Slope (Intercept = 2)		0.36-0.85	0.37-0.92	0.38-0.92
Fixed Slope (Intercept = 3)		0.25-0.97	0.3-0.88	0.34-0.89
Fixed Slope (Intercept = 4)		0.33-0.93	0.32-0.89	0.25-0.94
Fixed Slope (Intercept = 5)		0.34-0.98	0.32-0.93	0.32-0.92
Fixed Slope (Intercept = 6)		0.33-1	0.33-0.98	0.32-0.95
Fixed Slope (Intercept = 7)		0.34-0.99	0.32-0.97	0.33-0.98
Fixed Slope (Intercept = 8)		0.34-1	0.33-0.97	0.34-0.99
Fixed Slope (Intercept = 9)		0.33-1.03	0.33-0.98	0.33-0.97
Fixed Slope (Intercept = 10)		0.35-1.03	0.33-1	0.34-0.98
Fixed Slope (Intercept = 11)		0.35-1.06	0.33-1.04	0.34-1
Fixed Slope (Intercept = 12)		0.35-1.1	0.35-1.03	0.33-1
Fixed Slope (Intercept = 13)		0.26-1.1	0.35-1.05	0.33-1.04
Fixed Slope (Intercept = 14)		0.29-1.1	0.34-1.07	0.35-1.03
Fixed Slope (Intercept = 15)		0.29-1.1	0.33-1.09	0.34-1.04
Fixed Slope (Intercept = 16)		0.28-1.13	0.27-1.1	0.35-1.07
Fixed Slope (Intercept = 17)		0.29-1.15	0.29-1.1	0.34-1.07
Fixed Slope (Intercept = 18)		0.25-1.16	0.29-1.1	0.33-1.11
Fixed Slope (Intercept = 19)		0.25-1.14	0.28-1.13	0.27-1.11
Fixed Slope (Intercept = 20)		0.25-1.17	0.28-1.15	0.3-1.1

Table 4.2: Comparison of the s/d ratios (across transplant centers) between no proximity score model, heterogeneous slopes model and fixed slopes models.

median MELD at transplant (vMMA_T) across transplant centers.

Allocation Policy	Avg. Deaths	Avg. Travel distance (in NM)	vMMA _T
Acuity Circles	7,540.8	266.3	6.66
[SP-2], $\tau = 500$ NM	7,511.9	283.6	6.54
[SP-2], $\tau = 600$ NM	7,387.5	373	6.15
[SP-2], $\tau = 700$ NM	7,329.4	472.4	5.02

Table 4.3: Comparison of various allocation policies using simulation.

4.4 Conclusions

We use the Rawlsian *maximin* principle to minimize the variability in deceased donor liver access across geographies. We develop an analytical model to calculate the s/d ratio at a transplant center in the continuous distribution framework.

We propose a heterogeneous slopes policy, where every donor hospital has a unique slope for its proximity score function. The benefit of the slopes policy is that they account for where the organ supply and demand occur, and adjust the slopes to calibrate the extent of preference to a nearby transplant center. A greater magnitude of the slope results in a greater degree of differentiation (in their proximity scores, and thus *composite scores*) between any two transplant centers. We find that reducing inherent differences in the s/d ratios at the transplant centers results in saving lives and reduced geographic disparity. Our study can guide future policy discussions in operationalizing the continuous scoring concept.

Chapter 5: Conclusions and Future Research

5.1 Conclusions

Geographic inequity in organ access is the biggest issue that transplant stakeholders (the U.S. Department of Health and Human Services, medical community, transplant hospitals, donor hospitals, waiting list patients (including their families) and general public) have been facing for more than two decades. The problem is nontrivial because of the efficiency considerations: the quality of liver deteriorates with time, and it should be transplanted within 10-12 hours of its recovery from the deceased-donor.

There are two key contributions of this thesis: (1) Developing an optimization framework to equalize the supply (deceased donors)-to-demand (waiting list patients) ratios across the geographies, and (2) Developing a framework to accurately capture the strategic response of a patient (i.e., change in their organ acceptance probability) due to a change in allocation policy. These two critical elements in the past had been missing in the literature. The three essays in this thesis illustrate that the current approach of broader sharing of organs does not solve the issue of geographic disparity. Inherent disparity in supply-to-demand ratios across the geographies is at the crux of the problem, and therefore, a policy that equalizes the supply-to-demand ratios across the geographies achieves an equitable outcome at the lowest trade-off on efficiency metrics.

The modeling and solution frameworks we propose in this thesis is general enough to be

applied to other organ settings as well. The transplantation system in the U.S. is going through a major overhaul. A new distribution framework, Continuous Scoring, will be the future for all the organ allocation policies (including liver). It is still in conceptual phase, and the exact policy parameters have not been decided yet. This study can play a vital role in reshaping the future of organ allocation policies in the U.S.

5.2 Future Research

This thesis focuses only on geographic inequity and do not consider other kinds of disparities such as race, gender, socio-economic factors, organ size, and blood type. While the latter is an extremely important concern, addressing it would necessitate developing a model to address the former (i.e., geographic inequity). In other words, a model to address other spatial inequities will be built on top of what we develop in this work. Developing a model to incorporate and mitigate these additional disparities is an interesting direction for future research.

Appendix A: Appendix to Chapter 2

A.1 Comparing Organ Quality

We use the metric, donor risk index (DRI), proposed by Feng et al. [19] to evaluate the quality of the organs in our dataset. This index measures the quality of an organ using demographic factors (age, race, height), cause and type of donor death, sharing type (local/regional/national), and cold ischemia time. A higher DRI is associated with a greater risk of graft failure. Given that we want to assess the quality of the organs at the time of recovery, we exclude cold ischemia time, which depends on the transplant locations and assumes local sharing for an adequate comparison. In Figure A.1, we compare the box plots of DRI across the regions. We see that there are no significant differences in the distributions of organ quality across the regions.

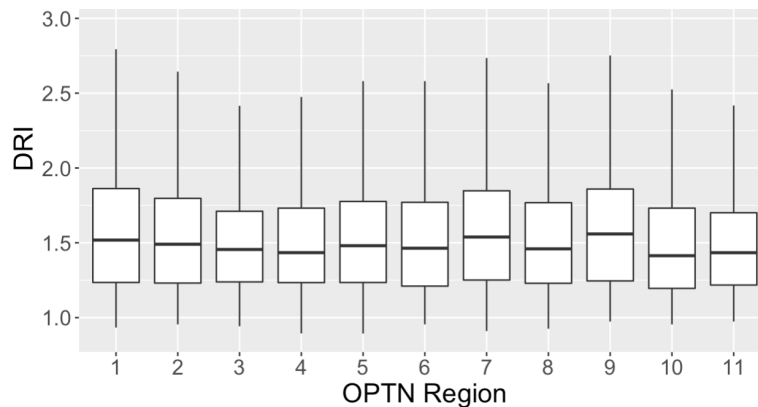


Figure A.1: Comparison of organ quality across the regions using the donor risk index (DRI).

A.2 Linearization of the s/d Ratio and Contiguity Constraints

To linearize the right-hand side of constraint (2.2) in [S-1], i.e., $\sum_{i=1}^{N_{sup}} \frac{1}{\sum_{k=1}^{N_{dem}} d_k x_{ik}} s_i x_{ij}$, we introduce auxiliary variables: $y_{ij} \geq 0$ and $t_i \geq 0$, which are defined as follows.

$$t_i = \frac{1}{\sum_{k=1}^{N_{dem}} d_k x_{ik}} \quad \forall i \in \mathcal{I} \quad (\text{A.1})$$

$$y_{ij} = t_i x_{ij} \quad \forall i \in \mathcal{I}, j \in \mathcal{J} \quad (\text{A.2})$$

Together, they imply:

$$\lambda \leq \sum_{i=1}^{N_{sup}} s_i y_{ij} \quad \forall j \in \mathcal{J} \quad (\text{A.3})$$

$$\sum_{k=1}^{N_{dem}} d_k y_{ik} = 1 \quad \forall i \in \mathcal{I} \quad (\text{A.4})$$

A set of linear constraints (A.4) model equation (A.1). We note that $t_i \leq 1$ and,

$$y_{ij} = \begin{cases} 0 & \text{if } x_{ij} = 0 \\ t_i & \text{if } x_{ij} = 1 \end{cases}. \text{ Because } y_{ij} \text{ is a product of two variables and therefore non-linear, the}$$

following linear constraints model $y_{ij} = t_i x_{ij}$:

$$y_{ij} \leq t_i \quad \forall i \in \mathcal{I}, j \in \mathcal{J} \quad (\text{A.5})$$

$$y_{ij} \leq x_{ij} \quad \forall i \in \mathcal{I}, j \in \mathcal{J} \quad (\text{A.6})$$

$$(1 - x_{ij}) + y_{ij} \geq t_i \quad \forall i \in \mathcal{I}, j \in \mathcal{J} \quad (\text{A.7})$$

$$y_{ij}, t_i \geq 0 \quad \forall i \in \mathcal{I}, j \in \mathcal{J} \quad (\text{A.8})$$

Therefore, constraint (2.2) in [S-1] can be replaced by constraints (A.3)-(A.8). Constraint (2.8) in [S-2] can be linearized identically.

Shirabe [46] describes flow-based contiguity constraints for districting problems. We adapt these constraints to model *receiving contiguity* and *sharing contiguity* in our neighborhood framework through equations (A.9)-(A.11) and (A.12)-(A.14), respectively. With receiving (sharing) contiguity, the suppliers (recipients) assigned to a recipient (supplier) form a continuous geography on the map. Let m_1 (m_2) be the maximum number of supply (demand) locations that can be assigned to a demand (supply) location. Parameter $a_{ik} = 1$, if supply locations i and k are geographically adjacent, and 0 otherwise. We use flow variables f_{ik}^j to model receiving contiguity and flow variables g_{jk}^i to model sharing contiguity. Flow variable f_{ik}^j denotes the flow from i to k (only defined when $a_{ik} = 1$) destined for demand location j , while flow variable g_{jk}^i denotes the flow from j to k (only defined when $a_{jk} = 1$) destined for supply location i . The first three constraints involving the flow variables f_{ik}^j ensure that if $x_{ij} = 1$ for a supply location i and a demand location j that are non-adjacent, then every supply location on the path from i to j also supplies demand location j . The next set of three constraints involving the flow variables g_{jk}^i ensure that if $x_{ij} = 1$ for a supply location i and a demand location j that are non-adjacent, then every demand location on the path from i to j is also supplied by i .

$$\sum_{k=1}^{N_{sup}} f_{ik}^j a_{ik} - \sum_{k=1}^{N_{sup}} f_{ki}^j a_{ki} = x_{ij} \quad \forall i \neq j, i \in \mathcal{I}, j \in \mathcal{J} \quad (\text{A.9})$$

$$\sum_{k=1}^{N_{sup}} f_{ki}^j a_{ki} \leq (m_1 - 1) x_{ij} \quad \forall i \in \mathcal{I}, j \in \mathcal{J} \quad (\text{A.10})$$

$$\sum_{k=1}^{N_{sup}} f_{jk}^j a_{jk} = 0 \quad \forall j \in \mathcal{J} \quad (\text{A.11})$$

$$\sum_{k=1}^{N_{dem}} g_{jk}^i a_{jk} - \sum_{k=1}^{N_{dem}} g_{kj}^i a_{kj} = x_{ij} \quad \forall i \neq j, i \in \mathcal{I}, j \in \mathcal{J} \quad (\text{A.12})$$

$$\sum_{k=1}^{N_{dem}} g_{kj}^i a_{kj} \leq (m_2 - 1) x_{ij} \quad \forall i \in \mathcal{I}, j \in \mathcal{J} \quad (\text{A.13})$$

$$\sum_{k=1}^{N_{dem}} g_{ik}^i a_{ik} = 0 \quad \forall i \in \mathcal{I} \quad (\text{A.14})$$

$$f_{ik}^j \geq 0 \quad \forall i, k \in \mathcal{I}, j \in \mathcal{J} \quad (\text{A.15})$$

$$g_{jk}^i \geq 0 \quad \forall i \in \mathcal{I}, k, j \in \mathcal{J} \quad (\text{A.16})$$

Together constraints (A.9)-(A.16) refer to constraint (2.6) in [S-1].

A.3 Set Partitioning Model Computational Details

Table A.1 contains the computational details of the set-partitioning model run on four-digit zip-clusters. We report the problem size, total number of cutting planes used by the solver, run time until termination, nodes explored, simplex iterations, best objective, best bound, and MIP gap. We observe that by two hours of running time, the MIP gap of [SP-1] and [SP-2] typically reaches below 0.02% and 0.12%, respectively, which corresponds to the difference in the s/d ratio at the fourth or higher decimal places between the best objective and best bound.

τ_{max} (in NM)		Size		Cutting Planes	Run time (in secs)	Nodes explored	Simplex iterations	Best obj.	Best bound	MIP gap
		Rows	Columns							
350	[SP-1]	1525	19061	2	7200	3444938	7290609	0.519	0.519	0.01%
	[SP-2]	1668	19062	22	6	1	2047	0.884	0.884	0.00%
400	[SP-1]	1527	24776	0	7200	2785686	9013065	0.537	0.537	0.01%
	[SP-2]	1670	24777	0	7200	262484	20797966	0.611	0.610	0.12%
450	[SP-1]	1528	30362	6	45	1	10922	0.543	0.543	0.01%
	[SP-2]	1671	30363	16	7200	72601	18971000	0.606	0.606	0.10%
500	[SP-1]	1528	35990	2420	7200	499437	6067640	0.551	0.551	0.02%
	[SP-2]	1671	35991	0	7200	85424	30217420	0.605	0.604	0.03%
550	[SP-1]	1528	42175	3005	7200	220154	6747918	0.554	0.554	0.01%
	[SP-2]	1671	42176	495	7200	44898	11247871	0.604	0.604	0.03%
600	[SP-1]	1528	48381	1936	7200	201431	1759417	0.555	0.555	0.01%
	[SP-2]	1671	48382	93	7200	26765	10007894	0.602	0.602	0.08%
650	[SP-1]	1528	54323	1908	7200	209106	2543837	0.554	0.554	0.01%
	[SP-2]	1671	54324	39	7200	28708	6409075	0.602	0.602	0.06%
700	[SP-1]	1528	59952	15	7200	837756	4521290	0.556	0.556	0.01%
	[SP-2]	1671	59953	20	7200	22964	5031591	0.602	0.601	0.05%

Table A.1: Computational details of the set-partitioning model run on four-digit zip-clusters.

A.4 DSA Neighborhoods

Tables A.2, A.3, and A.4, present the neighborhoods obtained by our model based on the DSA version when the maximum distance to any DSA in the neighborhood is constrained to 500 NM, 600 NM, and 700 NM, respectively. The column ‘Radius’ provides the radius (in terms of the transplant volume-weighted distance, as discussed in Section 2.4.2) of each neighborhood. The column ‘Neighbors’ contains the DSAs with which the DSA in the first column will share its organs.

DSA	Radius (in NM)	Neighbors
ALOB	336	KYDA, ALOB, NCCM, TNDS, MSOP, AROR, SCOP, TNMS, FLUF, GALL, LAOP
AROR	305	MSOP, AROR, TXSB, TNMS, MOMA, MWOB, TXGC, LAOP, OKOP
AZOB	499	AZOB, CORS, UTOP, CASD, CAOP
CADN	366	HIOP, CADN, CASD, CAOP
CAGS	318	HIOP, CADN, CAOP
CAOP	499	HIOP, AZOB, UTOP, CADN, CASD, CAOP
CASD	366	HIOP, AZOB, CADN, CASD, CAOP
CORS	316	CORS, UTOP
CTOP	203	MAOB, NYFL, CTOP, PADV, NJTO, NYRT
DCTC	339	OHOV, NCNC, MAOB, NYFL, PATF, NCCM, CTOP, DCTC, PADV, VATB, MDPC, OHLF, NJTO, OHLB, NYRT
FLFH	492	NCNC, ALOB, PRL, NCCM, TNDS, FLMP, MSOP, SCOP, FLFH, FLUF, FLWC, GALL
FLMP	472	PRL, FLMP, SCOP, FLFH, FLUF, FLWC, GALL
FLUF	422	NCNC, ALOB, PRL, NCCM, TNDS, FLMP, MSOP, SCOP, FLFH, FLUF, FLWC, GALL, LAOP
FLWC	488	NCNC, ALOB, PRL, NCCM, FLMP, MSOP, SCOP, FLFH, FLUF, FLWC, GALL
GALL	484	OHOV, NCNC, KYDA, ALOB, PATF, NCCM, DCTC, TNDS, FLMP, MSOP, AROR, SCOP, TNMS, VATB, MOMA, OHLF, FLFH, OHLB, FLUF, INOP, FLWC, GALL, LAOP
HIOP	NA	HIOP, CADN, CASD, CAOP
IAOP	210	MNOP, WIUW, IAOP, NEOR
ILIP	447	OHOV, MNOP, KYDA, PATF, TNDS, WIUW, ILIP, AROR, IAOP, TNMS, MOMA, MWOB, OHLF, WIDN, NEOR, OHLB, INOP, MIOP
INOP	224	OHOV, KYDA, ILIP, OHLF, WIDN, OHLB, INOP, MIOP
KYDA	497	OHOV, NCNC, KYDA, ALOB, NYFL, PATF, NCCM, DCTC, TNDS, PADV, WIUW, ILIP, MSOP, AROR, IAOP, SCOP, TNMS, VATB, MDPC, MOMA, MWOB, OHLF, WIDN, OHLB, FLUF, INOP, GALL, MIOP
LAOP	396	TXSA, ALOB, MSOP, AROR, TXSB, TNMS, TXGC, LAOP, OKOP
MAOB	170	MAOB, CTOP, NJTO, NYRT
MDPC	308	NCNC, MAOB, NYFL, PATF, CTOP, DCTC, PADV, VATB, MDPC, OHLF, NJTO, OHLB, NYRT
MIOP	482	OHOV, MNOP, KYDA, NYFL, PATF, NCCM, DCTC, TNDS, PADV, WIUW, ILIP, IAOP, VATB, MDPC, MOMA, OHLF, NJTO, WIDN, OHLB, INOP, NYRT, MIOP
MNOP	270	MNOP, WIUW, IAOP, NEOR
MOMA	233	ILIP, AROR, TNMS, MOMA, MWOB
MSOP	406	ALOB, TNDS, MSOP, AROR, TXSB, TNMS, MOMA, TXGC, FLUF, GALL, LAOP
MWOB	477	MNOP, KYDA, WIUW, ILIP, AROR, IAOP, TXSB, TNMS, MOMA, MWOB, WIDN, CORS, NEOR, TXGC, INOP, OKOP
NCCM	403	OHOV, NCNC, KYDA, ALOB, PATF, NCCM, DCTC, TNDS, PADV, SCOP, VATB, MDPC, OHLF, FLFH, OHLB, FLUF, INOP, GALL
NCNC	489	OHOV, NCNC, KYDA, ALOB, NYFL, PATF, NCCM, CTOP, DCTC, TNDS, PADV, SCOP, VATB, MDPC, OHLF, NJTO, FLFH, OHLB, FLUF, INOP, FLWC, NYRT, GALL, MIOP
NEOR	390	MNOP, WIUW, IAOP, MOMA, MWOB, CORS, NEOR, OKOP
NJTO	188	MAOB, NYFL, CTOP, DCTC, PADV, MDPC, NJTO, NYRT
NMOP	282	AZOB
NVLV	308	AZOB, CADN, CASD, CAOP
NYAP	182	MAOB, NYFL, CTOP, PADV, NJTO, NYRT
NYFL	458	OHOV, MAOB, NYFL, PATF, CTOP, DCTC, PADV, VATB, MDPC, OHLF, NJTO, OHLB, INOP, NYRT, MIOP
NYRT	193	MAOB, NYFL, CTOP, PADV, MDPC, NJTO, NYRT
NYWN	234	NYFL, PATF, PADV, OHLB, MIOP
OHLB	459	OHOV, NCNC, KYDA, MAOB, NYFL, PATF, NCCM, CTOP, DCTC, TNDS, PADV, WIUW, ILIP, SCOP, VATB, MDPC, MOMA, OHLF, NJTO, WIDN, OHLB, INOP, NYRT, MIOP
OHLF	329	OHOV, KYDA, PATF, DCTC, TNDS, WIUW, ILIP, OHLF, WIDN, OHLB, INOP, MIOP
OHLP	307	OHOV, KYDA, PATF, NCCM, DCTC, TNDS, ILIP, VATB, MDPC, OHLF, WIDN, OHLB, INOP, MIOP
OHOV	284	OHOV, KYDA, PATF, NCCM, TNDS, ILIP, OHLF, WIDN, OHLB, INOP, MIOP
OKOP	475	TXSA, MSOP, AROR, IAOP, TXSB, TNMS, MOMA, MWOB, CORS, NEOR, TXGC, LAOP, OKOP
ORUO	234	WALC, HIOP, ORUO
PADV	235	MAOB, NYFL, PATF, CTOP, DCTC, PADV, VATB, MDPC, NJTO, NYRT
PATF	278	OHOV, NCNC, NYFL, PATF, DCTC, PADV, VATB, MDPC, OHLF, NJTO, OHLB, NYRT, MIOP
PRL	NA	PRL, FLMP, FLWC
SCOP	326	NCNC, KYDA, ALOB, NCCM, TNDS, SCOP, VATB, FLFH, FLUF, GALL
TNDS	493	OHOV, NCNC, KYDA, ALOB, PATF, NCCM, DCTC, TNDS, ILIP, MSOP, AROR, SCOP, TNMS, VATB, MDPC, MOMA, MWOB, OHLF, WIDN, FLFH, OHLB, FLUF, INOP, GALL, MIOP, LAOP
TNMS	492	OHOV, KYDA, ALOB, NCCM, TNDS, ILIP, MSOP, AROR, IAOP, SCOP, TXSB, TNMS, MOMA, MWOB, OHLF, WIDN, TXGC, FLUF, INOP, GALL, LAOP, OKOP
TXGC	276	TXSA, TXSB, TXGC, LAOP, OKOP
TXSA	363	TXSA, TXSB, TXGC, LAOP
TXSB	218	TXSA, TXSB, TXGC, OKOP
UTOP	480	AZOB, CORS, UTOP, CADN
VATB	196	NCNC, DCTC, PADV, VATB, MDPC
WALC	234	WALC, ORUO
WIDN	284	OHOV, WIUW, ILIP, IAOP, WIDN, INOP, MIOP
WIUW	426	OHOV, MNOP, WIUW, ILIP, IAOP, MOMA, MWOB, OHLF, WIDN, NEOR, OHLB, INOP, MIOP

Table A.2: Geographical allocation policy for DSAs when the maximum permitted distance to a neighboring DSA is 500 NM

DSA	Radius (in NM)	Neighbors
ALOB	517	OHOV, NCNC, KYDA, ALOB, NCCM, TNDS, MSOP, AROR, SCOP, TNMS, VATB, MOMA, OHLP, FLFH, TXGC, FLUF, INOP, FLWC, GALL, LAOP
AROR	569	OHOV, TXSA, KYDA, ALOB, TNDS, ILIP, MSOP, AROR, IAOP, TXSB, TNMS, MOMA, MWOB, WIDN, NEOR, TXGC, FLUF, INOP, GALL, LAOP, OKOP
AZOB	546	AZOB, CORS, UTOP, CADN, CASD, CAOP
CADN	366	HIOP, CADN, CASD, CAOP
CAGS	446	HIOP, ORUO, UTOP, CADN, CASD, CAOP
CAOP	499	HIOP, AZOB, UTOP, CADN, CASD, CAOP
CASD	265	HIOP, AZOB, CASD, CAOP
CORS	316	CORS, UTOP
CTOP	244	MAOB, NYFL, CTOP, PADV, MDPC, NJTO, NYRT
DCTC	346	OHOV, NCNC, MAOB, NYFL, PATF, NCCM, CTOP, DCTC, PADV, SCOP, VATB, MDPC, OHLP, NJTO, OHLB, NYRT
FLFH	578	NCNC, ALOB, PRL, NCCM, TNDS, FLMP, MSOP, SCOP, TNMS, VATB, FLFH, FLUF, FLWC, GALL, LAOP
FLMP	573	NCNC, ALOB, PRL, NCCM, FLMP, SCOP, FLFH, FLUF, FLWC, GALL
FLUF	592	OHOV, NCNC, KYDA, ALOB, PRL, NCCM, TNDS, FLMP, MSOP, AROR, SCOP, TNMS, VATB, OHLP, FLFH, FLUF, FLWC, GALL, LAOP
FLWC	330	PRL, FLMP, FLFH, FLUF, FLWC, GALL
GALL	565	OHOV, NCNC, KYDA, ALOB, PATF, NCCM, DCTC, TNDS, PADV, FLMP, ILIP, MSOP, AROR, SCOP, TNMS, VATB, MDPC, MOMA, OHLP, FLFH, OHLB, FLUF, INOP, FLWC, GALL, MIOP, LAOP
HIOP	NA	HIOP, CADN, CASD, CAOP
IAOP	335	MNOP, WIUW, ILIP, IAOP, MOMA, MWOB, WIDN, NEOR, INOP
ILIP	365	OHOV, MNOP, KYDA, TNDS, WIUW, ILIP, IAOP, MOMA, MWOB, OHLP, WIDN, OHLB, INOP, MIOP
INOP	571	OHOV, MNOP, NCNC, KYDA, ALOB, NYFL, PATF, NCCM, DCTC, TNDS, PADV, WIUW, ILIP, MSOP, AROR, IAOP, SCOP, TNMS, VATB, MDPC, MOMA, MWOB, OHLP, NJTO, WIDN, NEOR, OHLB, INOP, NYRT, GALL, MIOP, OKOP
KYDA	497	OHOV, NCNC, KYDA, ALOB, NYFL, PATF, NCCM, DCTC, TNDS, PADV, WIUW, ILIP, MSOP, AROR, IAOP, SCOP, TNMS, VATB, MDPC, MOMA, MWOB, OHLP, WIDN, OHLB, FLUF, INOP, GALL, MIOP
LAOP	396	TXSA, ALOB, MSOP, AROR, TXSB, TNMS, TXGC, LAOP, OKOP
MAOB	170	MAOB, CTOP, NJTO, NYRT
MDPC	407	OHOV, NCNC, KYDA, MAOB, NYFL, PATF, NCCM, CTOP, DCTC, PADV, SCOP, VATB, MDPC, OHLP, NJTO, OHLB, NYRT, MIOP
MIOP	594	OHOV, MNOP, NCNC, KYDA, MAOB, NYFL, PATF, NCCM, CTOP, DCTC, TNDS, PADV, WIUW, ILIP, IAOP, SCOP, TNMS, VATB, MDPC, MOMA, MWOB, OHLP, NJTO, WIDN, NEOR, OHLB, INOP, NYRT, GALL, MIOP
MNOP	270	MNOP, WIUW, IAOP, NEOR
MOMA	600	OHOV, MNOP, NCNC, KYDA, ALOB, PATF, NCCM, TNDS, WIUW, ILIP, MSOP, AROR, IAOP, SCOP, TXSB, TNMS, MOMA, MWOB, OHLP, WIDN, NEOR, OHLB, TXGC, FLUF, INOP, GALL, MIOP, LAOP, OKOP
MSOP	482	TXSA, KYDA, ALOB, NCCM, TNDS, MSOP, AROR, SCOP, TXSB, TNMS, MOMA, MWOB, FLFH, TXGC, FLUF, FLWC, GALL, LAOP, OKOP
MWOB	590	OHOV, TXSA, MNOP, KYDA, ALOB, TNDS, WIUW, ILIP, MSOP, AROR, IAOP, TXSB, TNMS, MOMA, MWOB, WIDN, CORS, NEOR, TXGC, INOP, MIOP, LAOP, OKOP
NCCM	498	OHOV, NCNC, KYDA, ALOB, PATF, NCCM, DCTC, TNDS, PADV, ILIP, MSOP, SCOP, TNMS, VATB, MDPC, MOMA, OHLP, NJTO, FLFH, OHLB, FLUF, INOP, FLWC, NYRT, GALL, MIOP
NCNC	570	OHOV, NCNC, KYDA, ALOB, MAOB, NYFL, PATF, NCCM, CTOP, DCTC, TNDS, PADV, ILIP, MSOP, SCOP, TNMS, VATB, MDPC, OHLP, NJTO, FLFH, OHLB, FLUF, INOP, FLWC, NYRT, GALL, MIOP
NEOR	377	MNOP, IAOP, MOMA, MWOB, CORS, NEOR, OKOP
NJTO	254	MAOB, NYFL, PATF, CTOP, DCTC, PADV, VATB, MDPC, NJTO, NYRT
NMOP	282	AZOB
NVLV	308	AZOB, CADN, CASD, CAOP
NYAP	182	MAOB, NYFL, CTOP, PADV, NJTO, NYRT
NYFL	582	OHOV, NCNC, KYDA, MAOB, NYFL, PATF, NCCM, CTOP, DCTC, PADV, WIUW, ILIP, SCOP, VATB, MDPC, OHLP, NJTO, WIDN, OHLB, INOP, NYRT, MIOP
NYRT	195	MAOB, NYFL, CTOP, DCTC, PADV, MDPC, NJTO, NYRT
NYWN	326	MAOB, NYFL, PATF, CTOP, DCTC, PADV, MDPC, OHLP, NJTO, OHLB, NYRT, MIOP
OHLB	457	OHOV, NCNC, KYDA, MAOB, NYFL, PATF, NCCM, CTOP, DCTC, TNDS, PADV, WIUW, ILIP, SCOP, VATB, MDPC, OHLP, NJTO, WIDN, OHLB, INOP, NYRT, MIOP
OHLC	346	OHOV, KYDA, PATF, NCCM, DCTC, TNDS, WIUW, ILIP, MDPC, MOMA, OHLP, WIDN, OHLB, INOP, MIOP
OHLP	366	OHOV, NCNC, KYDA, NYFL, PATF, NCCM, DCTC, TNDS, PADV, ILIP, SCOP, VATB, MDPC, OHLP, WIDN, OHLB, INOP, MIOP
OHOV	599	OHOV, MNOP, NCNC, KYDA, ALOB, NYFL, PATF, NCCM, CTOP, DCTC, TNDS, PADV, WIUW, ILIP, MSOP, AROR, IAOP, SCOP, TNMS, VATB, MDPC, MOMA, MWOB, OHLP, NJTO, WIDN, NEOR, OHLB, FLUF, INOP, NYRT, GALL, MIOP
OKOP	397	TXSA, AROR, TXSB, TNMS, MOMA, MWOB, NEOR, TXGC, LAOP, OKOP
ORUO	234	WALC, HIOP, ORUO
PADV	275	MAOB, NYFL, PATF, CTOP, DCTC, PADV, VATB, MDPC, NJTO, OHLB, NYRT
PATF	406	OHOV, NCNC, KYDA, MAOB, NYFL, PATF, NCCM, CTOP, DCTC, TNDS, PADV, ILIP, SCOP, VATB, MDPC, OHLP, NJTO, WIDN, OHLB, INOP, NYRT, MIOP
PRL	NA	PRL, FLMP
SCOP	450	OHOV, NCNC, KYDA, ALOB, PATF, NCCM, DCTC, TNDS, PADV, SCOP, TNMS, VATB, MDPC, OHLP, FLFH, OHLB, FLUF, INOP, FLWC, GALL
TNDS	525	OHOV, NCNC, KYDA, ALOB, PATF, NCCM, DCTC, TNDS, PADV, ILIP, MSOP, AROR, IAOP, SCOP, TNMS, VATB, MDPC, MOMA, MWOB, OHLP, WIDN, FLFH, OHLB, FLUF, INOP, FLWC, GALL, MIOP, LAOP
TNMS	594	OHOV, TXSA, NCNC, KYDA, ALOB, PATF, NCCM, TNDS, WIUW, ILIP, MSOP, AROR, IAOP, SCOP, TXSB, TNMS, VATB, MOMA, MWOB, OHLP, WIDN, NEOR, FLFH, OHLB, TXGC, FLUF, INOP, FLWC, GALL, MIOP, LAOP, OKOP
TXGC	276	TXSA, TXSB, TXGC, LAOP, OKOP
TXSA	179	TXSA, TXSB, TXGC
TXSB	598	TXSA, ALOB, MSOP, AROR, TXSB, TNMS, MOMA, MWOB, CORS, NEOR, TXGC, LAOP, OKOP
UTOP	480	AZOB, CORS, UTOP, CADN
VATB	437	OHOV, NCNC, KYDA, MAOB, NYFL, PATF, NCCM, CTOP, DCTC, TNDS, PADV, SCOP, VATB, MDPC, OHLP, NJTO, OHLB, INOP, NYRT, GALL, MIOP
WALC	234	WALC, ORUO
WIDN	200	WIUW, ILIP, WIDN, INOP, MIOP
WIUW	248	MNOP, WIUW, ILIP, IAOP, WIDN, MIOP

Table A.3: Geographical allocation policy for DSAs when the maximum permitted distance to a neighboring DSA is 600 NM.

DSA	Radius (in NM)	Neighbors
ALOB	684	OHOV, TXSA, NCNC, KYDA, ALOB, PATF, NCCM, DCTC, TNDS, PADV, FLMP, ILIP, MSOP, AROR, IAOP, SCOP, TXSB, TNMS, VATB, MDPC, MOMA, MWOB, OHLF, WIDN, FLFH, OHLB, TXGC, FLUF, INOP, FLWC, GALL, MIOP, LAOP, OKOP
AROR	297	MSOP, AROR, TXSB, TNMS, MOMA, MWOB, LAOP, OKOP
AZOB	546	AZOB, CORS, UTOP, CADN, CASD, CAOP
CADN	655	WALC, HIOP, AZOB, ORUO, UTOP, CADN, CASD, CAOP
CAGS	318	HIOP, CADN, CAOP
CAOP	316	HIOP, AZOB, CADN, CASD, CAOP
CASD	537	HIOP, AZOB, UTOP, CADN, CASD, CAOP
CORS	316	CORS, UTOP
CTOP	343	MAOB, NYFL, PATF, CTOP, DCTC, PADV, MDPC, NJTO, NYRT
DCTC	421	OHOV, NCNC, KYDA, MAOB, NYFL, PATF, NCCM, CTOP, DCTC, PADV, SCOP, VATB, MDPC, OHLF, NJTO, OHLB, INOP, NYRT, MIOP
FLFH	687	OHOV, NCNC, KYDA, ALOB, PRLL, NCCM, DCTC, TNDS, FLMP, MSOP, SCOP, TNMS, VATB, MDPC, OHLF, FLFH, FLUF, FLWC, GALL, LAOP
FLMP	287	PRLL, FLMP, FLFH, FLUF, FLWC
FLUF	674	OHOV, NCNC, KYDA, ALOB, PATF, PRLL, NCCM, DCTC, TNDS, FLMP, MSOP, AROR, SCOP, TNMS, VATB, MDPC, MOMA, OHLF, FLFH, OHLB, FLUF, INOP, FLWC, GALL, LAOP
FLWC	488	NCNC, ALOB, PRLL, NCCM, FLMP, MSOP, SCOP, FLFH, FLUF, FLWC, GALL
GALL	671	OHOV, NCNC, KYDA, ALOB, NYFL, PATF, NCCM, DCTC, TNDS, PADV, FLMP, ILIP, MSOP, AROR, SCOP, TNMS, VATB, MDPC, MOMA, MWOB, OHLF, NJTO, WIDN, FLFH, OHLB, TXGC, FLUF, INOP, FLWC, NYRT, GALL, MIOP, LAOP, OKOP
HIOP	NA	HIOP, CASD
IAOP	235	MNOP, WIUW, ILIP, IAOP, MWOB, WIDN, NEOR
ILIP	447	OHOV, MNOP, KYDA, PATF, TNDS, WIUW, ILIP, AROR, IAOP, TNMS, MOMA, MWOB, OHLF, WIDN, NEOR, OHLB, INOP, MIOP
INOP	510	OHOV, MNOP, NCNC, KYDA, ALOB, NYFL, PATF, NCCM, DCTC, TNDS, PADV, WIUW, ILIP, MSOP, AROR, IAOP, SCOP, TNMS, VATB, MDPC, MOMA, MWOB, OHLF, WIDN, NEOR, OHLB, INOP, GALL, MIOP
KYDA	696	OHOV, MNOP, NCNC, KYDA, ALOB, MAOB, NYFL, PATF, NCCM, CTOP, DCTC, TNDS, PADV, WIUW, ILIP, MSOP, AROR, IAOP, SCOP, TNMS, VATB, MDPC, MOMA, MWOB, OHLF, NJTO, WIDN, NEOR, FLFH, OHLB, TXGC, FLUF, INOP, FLWC, NYRT, GALL, MIOP, LAOP, OKOP
LAOP	396	TXSA, ALOB, MSOP, AROR, TXSB, TNMS, TXGC, LAOP, OKOP
MAOB	170	MAOB, CTOP, NJTO, NYRT
MDPC	645	OHOV, NCNC, KYDA, ALOB, MAOB, NYFL, PATF, NCCM, CTOP, DCTC, TNDS, PADV, WIUW, ILIP, SCOP, VATB, MDPC, OHLF, NJTO, WIDN, OHLB, FLUF, INOP, NYRT, GALL, MIOP
MIOP	216	OHOV, ILIP, OHLF, WIDN, OHLB, INOP, MIOP
MNOP	270	MNOP, WIUW, IAOP, NEOR
MOMA	694	OHOV, TXSA, MNOP, NCNC, KYDA, ALOB, PATF, NCCM, DCTC, TNDS, WIUW, ILIP, MSOP, AROR, IAOP, SCOP, TXSB, TNMS, VATB, MDPC, MOMA, MWOB, OHLF, WIDN, CORS, NEOR, OHLB, TXGC, FLUF, INOP, GALL, MIOP, LAOP, OKOP
MSOP	418	KYDA, ALOB, TNDS, MSOP, AROR, TXSB, TNMS, MOMA, TXGC, FLUF, INOP, FLWC, NYRT, GALL, LAOP, OKOP
MWOB	590	OHOV, TXSA, MNOP, KYDA, ALOB, TNDS, WIUW, ILIP, MSOP, AROR, IAOP, TXSB, TNMS, MOMA, MWOB, WIDN, CORS, NEOR, TXGC, INOP, MIOP, LAOP, OKOP
NCCM	238	NCNC, KYDA, NCCM, TNDS, SCOP, VATB, GALL
NCNC	320	NCNC, KYDA, PATF, NCCM, DCTC, TNDS, PADV, SCOP, VATB, MDPC, OHLF, GALL
NEOR	377	MNOP, IAOP, MOMA, MWOB, CORS, NEOR, OKOP
NJTO	254	MAOB, NYFL, PATF, CTOP, DCTC, PADV, MDPC, NJTO, NYRT
NMOP	282	AZOB
NVLV	311	AZOB, UTOP, CADN, CASD, CAOP
NYAP	182	MAOB, NYFL, CTOP, PADV, NJTO, NYRT
NYFL	186	NYFL, PADV
NYRT	195	MAOB, NYFL, CTOP, DCTC, PADV, MDPC, NJTO, NYRT
NYWN	153	NYFL, OHLB
OHLB	484	OHOV, NCNC, KYDA, MAOB, NYFL, PATF, NCCM, CTOP, DCTC, TNDS, PADV, WIUW, ILIP, SCOP, VATB, MDPC, MOMA, OHLF, NJTO, WIDN, OHLB, INOP, NYRT, GALL, MIOP
OHLF	678	OHOV, MNOP, NCNC, KYDA, ALOB, MAOB, NYFL, PATF, NCCM, CTOP, DCTC, TNDS, PADV, WIUW, ILIP, MSOP, AROR, IAOP, SCOP, TNMS, VATB, MDPC, MOMA, MWOB, OHLF, NJTO, WIDN, NEOR, OHLB, FLUF, INOP, NYRT, GALL, MIOP, OKOP
OHLP	624	OHOV, MNOP, NCNC, KYDA, ALOB, MAOB, NYFL, PATF, NCCM, CTOP, DCTC, TNDS, PADV, WIUW, ILIP, MSOP, AROR, IAOP, SCOP, TNMS, VATB, MDPC, MOMA, MWOB, OHLF, NJTO, WIDN, OHLB, FLUF, INOP, NYRT, GALL, MIOP
OHOV	410	OHOV, NCNC, KYDA, ALOB, PATF, NCCM, DCTC, TNDS, PADV, WIUW, ILIP, SCOP, TNMS, VATB, MDPC, MOMA, OHLF, WIDN, OHLB, INOP, GALL, MIOP
OKOP	418	TXSA, MSOP, AROR, TXSB, TNMS, MOMA, MWOB, NEOR, TXGC, LAOP, OKOP
ORUO	662	WALC, HIOP, ORUO, UTOP, CADN, CAOP
PADV	235	MAOB, NYFL, PATF, CTOP, DCTC, PADV, VATB, MDPC, NJTO, NYRT
PATF	544	OHOV, NCNC, KYDA, ALOB, MAOB, NYFL, PATF, NCCM, CTOP, DCTC, TNDS, PADV, WIUW, ILIP, SCOP, VATB, MDPC, MOMA, OHLF, NJTO, WIDN, OHLB, INOP, NYRT, GALL, MIOP
PRLL	NA	PRLL, FLMP, FLFH, FLWC
SCOP	263	NCNC, NCCM, TNDS, SCOP, VATB, FLUF, GALL
TNDS	694	OHOV, NCNC, KYDA, ALOB, NYFL, PATF, NCCM, CTOP, DCTC, TNDS, PADV, WIUW, FLMP, ILIP, MSOP, AROR, IAOP, SCOP, TXSB, TNMS, VATB, MDPC, MOMA, MWOB, OHLF, NJTO, WIDN, NEOR, FLFH, OHLB, TXGC, FLUF, INOP, FLWC, NYRT, GALL, MIOP, LAOP, OKOP
TNMS	561	OHOV, TXSA, NCNC, KYDA, ALOB, NCCM, TNDS, WIUW, ILIP, MSOP, AROR, IAOP, SCOP, TXSB, TNMS, MOMA, MWOB, OHLF, WIDN, NEOR, OHLB, TXGC, FLUF, INOP, GALL, MIOP, LAOP, OKOP
TXGC	276	TXSA, TXSB, TXGC, LAOP, OKOP
TXSA	179	TXSA, TXSB, TXGC
TXSB	598	TXSA, ALOB, MSOP, AROR, TXSB, TNMS, MOMA, MWOB, CORS, NEOR, TXGC, LAOP, OKOP
UTOP	537	AZOB, ORUO, CORS, UTOP, CADN, CASD, CAOP
VATB	517	OHOV, NCNC, KYDA, ALOB, MAOB, NYFL, PATF, NCCM, CTOP, DCTC, TNDS, PADV, SCOP, VATB, MDPC, OHLF, NJTO, OHLB, FLUF, INOP, NYRT, GALL, MIOP
WALC	234	WALC, ORUO
WIDN	423	OHOV, MNOP, KYDA, PATF, WIUW, ILIP, IAOP, MOMA, MWOB, OHLF, WIDN, OHLB, INOP, MIOP
WIUW	248	MNOP, WIUW, ILIP, IAOP, WIDN, MIOP

Table A.4: Geographical allocation policy for DSAs when the maximum permitted distance to a neighboring DSA is 700 NM.

Appendix B: Appendix to Chapter 3

B.1 Summary Statistics

Table [B.1](#) reports the summary statistics of various patients, donors, and transplant attributes used in the model. We see that the new patients' age, MELD at listing, and life support status remain almost the same in the Pre-Share 35 and Share 35 policy eras. There is a slight difference in the distribution of the medical condition between the two periods. The donors' age, race distribution, and donation after circulatory death (DCD) status do not change much. However, there is a difference in the cause of death distribution between the two periods. Thus, it is important to control for the donor characteristics in the model. After the Share 35 implementation, on average, offers were accepted later in the queue. Comparing the transplant sharing types, the Share 35 policy resulted in a greater (lower) proportion of regional (local) sharing. Interestingly, the cold ischemia time (CIT), time between organ recovery and transplantation decreased on average (although the coefficient of variation is more than 40%). One might expect the CIT to increase with broader sharing. However, CIT does not follow a linear relationship with distance (due to switching the mode of transport, e.g., from driving to flying for a longer distance). In addition, non-transport factors play a significant role in determining CIT. See Gentry et al. [\[24\]](#) for a detailed discussion on modeling CIT.

In Figure [B.1](#), for every MELD class, we plot the mean position at which the candidates

in that MELD class received offers. We see a clear dip in offer positions under Share 35 to MELD ≥ 35 candidates, suggesting that patients with a higher MELD were at the top of the offer list. This observation is consistent with what one would expect with the Share 35 policy; organ access increased (decreased) for candidates with a MELD ≥ 35 (MELD < 35) in general.

We plot the year-wise trend of new patients joining the waiting list (demand) and deceased donors (supply) in Figure B.2. The gap between supply and demand has been persisting. The supply has been increasing; for example, it increased 30% from 2010 to 2018, while the demand does not show a clear trend. To study the impact of the Share 35 policy, it is important to delineate the effect of increased supply and demand changes from the Pre-Share 35 to Share 35 policy eras.

Of all the offers, 93.3% were made to the patient-donor pairs of identical blood types, and only 2.4% and 4.3% were made to compatible and incompatible pairs, respectively. Therefore, to keep our model simple and tractable, we do not consider blood type compatibility. Since 94% of offers were made to patient-donor pairs of identical blood types and only 3% each were made to compatible and incompatible pairs, therefore, to keep our model simpler, we ignore blood type compatibility.

In Table B.2, we report the candidate's offer acceptance probabilities in the Share 35 policy era, and compare them with the Pre-Share 35 policy era in parentheses. We used a straightforward metric to calculate the acceptance probability (ratio of the number of offers accepted and the number of offers received). We see cases of both an increase and decrease in their acceptance probabilities (e.g., MELD 6-14 in Region 10 saw a 6% increase, whereas MELD 33-34 in Region 6 saw a 26% decrease).

Characteristic	Pre-Share 35 (January 2010-June 2013)	Share 35 (July 2013-December 2018)
<u>Patients</u>		
Age (in years): Mean/SD	54.9/10.3	55.8/11.0
MELD (at listing): Mean/SD	19.3/9.2	19.7/9.8
Life support status:		
Yes	4%	5%
No	96%	95%
Medical condition:		
Intensive care unit (ICU)	8%	3%
Hospitalized	12%	4%
Not hospitalized	80%	93%
<u>Donors</u>		
Age (in years): Mean/SD	44.3/15.2	43.6/14.9
Race:		
White	80%	80%
Black	17%	16%
Others	3%	4%
Cause of death:		
Anoxia	26%	38%
Cerebrovascular accident (CVA)	40%	31%
Others	34%	30%
Donation after circulatory death:		
Yes	13%	17%
No	87%	83%
Fraction of discards	0.252	0.250
<u>Match</u>		
Position at acceptance: Mean/SD	10.6/38.0	15.2/42.5
Cold Ischemia Time (of accepted offers): Mean/SD	6.3/3.0	6.0/2.5
Sharing type (of accepted offers):		
Local	78%	65%
Regional	20%	31%
National	3%	4%

Table B.1: Summary statistics of patient, donor, and transplant characteristics.

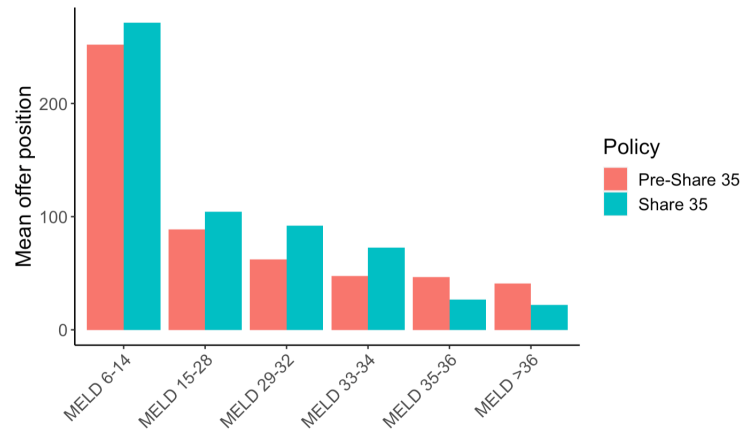


Figure B.1: Comparison of positions at which offers were made to patients at different MELD scores between policies (Status 1A is assigned a MELD score of 41).

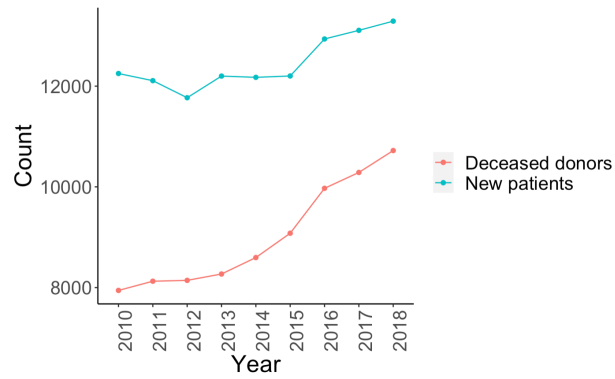


Figure B.2: Supply and demand trends over time.

B.2 Comparing the Organ Quality of Declined Offers

We use the metric, the donor risk index (DRI), proposed by Feng et al. [19] to evaluate the quality of declined offers. This index measures the quality of an organ using demographic factors (age, race, height), cause and type of donor death, sharing type (local/regional/national), and CIT. A higher DRI is associated with a greater risk of graft failure. Because CIT is observed only for accepted offers, we use the median value (=6.9 hours) in our calculation. In Figure B.3, we compare the box plots of the DRI between the Pre-Share 35 and Share 35 policy eras. We see that there are no significant differences in the distributions of organ quality.

B.3 Details on Logit Inclusive Value

In a dynamic model, agents (patients, in our case) have perceptions over future states. They need to know the evolution of every element in the state space. If the number of elements is large, it can make the model very complex. To make the problem tractable, a simplifying assumption is often made: the evolution of the space space is approximated using a lower dimensional

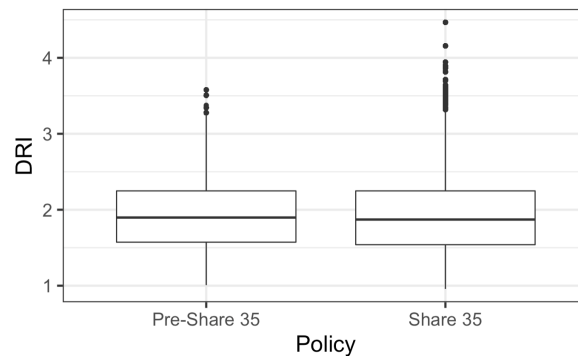


Figure B.3: Comparison of the organ quality of declined offers between the Pre-Share 35 and Share 35 policy eras using the donor risk index (DRI).

	MELD 6-14	MELD 15-28	MELD 29-32	MELD 33-34	MELD 35-36	MELD >36
Region 1	4.8% (1.5%)	4.5% (-2.8%)	6.1% (-7.6%)	13.9% (-10.4%)	26% (1.5%)	29.5% (-2.3%)
Region 2	1% (0.9%)	2.8% (-1.5%)	8% (-6.1%)	9.1% (-7.8%)	17% (-3%)	22.3% (-3.6%)
Region 3	3.4% (1%)	12.1% (-0.1%)	23.6% (-11.1%)	26.4% (-15%)	37.6% (1.9%)	36.9% (-8.6%)
Region 4	0.7% (0.4%)	2.5% (-4.3%)	9.2% (-18%)	16.8% (-21.3%)	25% (-11.7%)	32% (-4.9%)
Region 5	1.2% (0.9%)	2.1% (-0.8%)	3.4% (-7.3%)	5.1% (-10.9%)	10.9% (-13.4%)	23.7% (-9%)
Region 6	0% (0%)	6.1% (-6.3%)	14.9% (-17.7%)	20.4% (-25.9%)	27.2% (-24.8%)	28.6% (-17.1%)
Region 7	1% (-0.3%)	3.4% (-6.4%)	9.7% (-9.9%)	14.5% (-14%)	22.4% (-10.5%)	27.8% (-8.9%)
Region 8	0.5% (0.2%)	7.5% (-2.1%)	16.8% (-19.6%)	20.8% (-19.3%)	34.5% (4.2%)	38.3% (-3.4%)
Region 9	0.9% (0.8%)	1.4% (-0.3%)	2.6% (-5.1%)	6.4% (-9.6%)	14.1% (-6.9%)	25.6% (-11%)
Region 10	8.3% (6.2%)	10.7% (-5.2%)	20.6% (-12.9%)	20.3% (-10.6%)	34.6% (-8.5%)	40.3% (0.6%)
Region 11	1.5% (1.3%)	8.7% (-5.2%)	21.4% (-18%)	24.6% (-15.9%)	42.4% (-6.2%)	45% (0.8%)

Table B.2: Offer acceptance probabilities (in the Share 35 policy era) as a function of the MELD category. Parentheses report the change, compared to the Pre-Share 35 policy era. Values are calculated using summary statistics.

Markov process [29]. In other words, agents are considered boundedly rational, and they use fewer elements to form predictions about the future.

In our context, the graft survival probability is calculated using the SRTR Risk Adjustment Model,¹ which is based on a total of 41 predictors (Z_{it}) that include the candidate’s and donor’s medical attributes, and CIT. Including all the 41 predictors in the state space will result in a curse of dimensionality. Following the extant literature [29] on the *logit inclusive value*, we simplify the evolution of those 41 medical attributes using the evolution of one-dimensional GS_{it} .

We model GS_{it} as a function of the MELD category ($MELD_{it}$), age group (Rec_age_{it}), life support status ($Rec_life_support_{it}$), medical condition ($Rec_med_cond_{it}$), and organ type (Q_{it}). For every combination of the (values taken by the) above variables, we first filter the offers. For this subset of offers, we observe the values of all the 41 predictors,² and we calculate the

¹<https://www.srtr.org/reports-tools/posttransplant-outcomes/> accessed on July 12, 2020.

²We use a constant value of CIT (=6.9 hours) in our model. We do not consider GS_{it} to depend on $Sharing_type_{it}$.

graft survival probability (using the SRTR Risk Adjustment Model) for each offer. The average of the graft survival probabilities is the value of GS_{it} . In other words, we group the offers by $(MELD_{it}, Rec_age_{it}, Rec_life_support_{it}, Rec_med_cond_{it}, Q_{it})$, and GS_{it} is the average of the graft survival probabilities for these offers. Thus, GS_{it} is always ≤ 1 . In this way, we approximate the evolution of 41-dimensional Z_{it} with the evolution of GS_{it} , which is one-dimensional. As a sanity check, we regress GS_{it} with the MELD category, age group, life support status, medical condition, and organ type in Table B.4. We find that the signs and the relative ordering of the regression estimates are reasonable.

B.4 State Transition Probability

A patient's health condition evolves stochastically and is a major determinant of her priority in a queue in the organ allocation policies studied. The state transition probability is written as:

$$\begin{aligned} \mathcal{P}(S_{i,t+1}|S_{it}, d_{it} = 0) = & \mathcal{P}(MELD_{i,t+1}, Rec_age_{i,t+1}, Rec_life_support_{i,t+1}, Rec_med_cond_{i,t+1}, \\ & Q_{i,t+1}, Z_{i,t+1}, Sharing_type_{i,t+1} | MELD_{it}, Rec_age_{it}, Rec_life_support_{it}, \\ & Rec_med_cond_{it}, Q_{it}, Z_{it}, Sharing_type_{it}, d_{it} = 0) \end{aligned} \quad (B.1)$$

Because the priority of a candidate on the offer list does not depend on past offers, by dropping the history of the previous period's offer, the transition probability can be rewritten as:

$$\begin{aligned} \mathcal{P}(S_{i,t+1}|S_{it}, d_{it} = 0) = & \mathcal{P}(MELD_{i,t+1}, Rec_age_{i,t+1}, Rec_life_support_{i,t+1}, Rec_med_cond_{i,t+1}, \\ & Q_{i,t+1}, Z_{i,t+1}, Sharing_type_{i,t+1} | MELD_{it}, Rec_age_{it}, Rec_life_support_{it}, \\ & Rec_med_cond_{it}, Z_{it}, d_{it} = 0) \end{aligned} \quad (B.2)$$

We assume that the MELD state transition is the same for all age groups, life support statuses, and medical conditions (the pooling of various patient types enables the estimation of the MELD state transition matrix with greater confidence than estimating multiple (18 in our case, see Section 3.6.2) matrices for different patient types). *Death* is an absorbing state. Next, when an organ arrives, the allocation policy does not depend on the candidate's age, life support status, or medical condition. Thus, only MELD plays a role in determining the organ offer probabilities, $\mathcal{P}(Q)$, in a policy. These allow us to simplify the transition probability as:

$$\begin{aligned} \mathcal{P}(S_{i,t+1}|S_{it}, d_{it} = 0) &= \mathcal{P}(MELD_{i,t+1}|MELD_{it}, d_{it} = 0) \times \mathcal{P}(Q_{i,t+1}|MELD_{i,t+1}, d_{it} = 0) \times \\ &\mathcal{P}(Rec_age_{i,t+1}, Rec_life_support_{i,t+1}, Rec_med_cond_{i,t+1}, Z_{i,t+1}, Sharing_type_{i,t+1} | \\ &MELD_{i,t+1}, Q_{i,t+1}, MELD_{it}, Rec_age_{it}, Rec_life_support_{it}, Rec_med_cond_{it}, Z_{it}, d_{it} = 0) \end{aligned} \quad (\text{B.3})$$

We estimate $\mathcal{P}(MELD_{i,t+1}|MELD_{it}, d_{it} = 0)$ from the data (January 2003 to February 2019) on MELD transitions (Table B.3). To estimate $\mathcal{P}(Q_{i,t+1}|MELD_{i,t+1}, d_{it} = 0)$, we adopt an approach identical to [6]:

$$\mathcal{P}(Q_{i,t+1}|MELD_{i,t+1}, d_{it} = 0) = \frac{\sum_i \# \text{ of offers of type } Q_{i,t+1} \text{ candidate } i \text{ received at } MELD_{i,t+1}}{\sum_i \# \text{ of days candidate } i \text{ waited at } MELD_{i,t+1}} \quad (\text{B.4})$$

It is possible that a candidate does not receive an offer on a given day. We add *no_offer* to Q_{it} (calculated as per equation B.4) and $Sharing_type_{it}$ (if $Q_{it} = no_offer$, $Sharing_type_{it} = no_offer$, and vice versa).

Now, we are left with modeling the evolution of $Sharing_type_{it}$, Z_{it} , Rec_age_{it} , $Rec_life_support_{it}$, and $Rec_med_cond_{it}$. The $Sharing_type$ depends on the candidate's MELD and organ characteristics. Low-quality organs are usually declined more often and are likely

	MELD class						Death
	MELD 6-14	MELD 15-28	MELD 29-32	MELD 33-34	MELD 35-36	MELD >36	
MELD 6-14	0.9958	0.0036	0.0002	0.0001	0.0000	0.0000	0.0003
MELD 15-28	0.0049	0.9922	0.0016	0.0002	0.0001	0.0002	0.0008
MELD 29-32	0.0041	0.0120	0.9693	0.0082	0.0022	0.0020	0.0021
MELD 33-34	0.0042	0.0070	0.0092	0.9508	0.0166	0.0086	0.0036
MELD 35-36	0.0062	0.0112	0.0114	0.0114	0.8809	0.0688	0.0102
MELD >36	0.0098	0.0123	0.0051	0.0036	0.0059	0.9335	0.0299
Death	0	0	0	0	0	0	1

Table B.3: MELD transition matrix.

to be shared nationally. Sicker patients get higher priority; therefore, they are likely to receive local/regional offers more often. Thus, we model the transition of $Sharing_type_{it}$ as in equation B.6. Next, Z_{it} consists of 41 predictors, each of which takes a set of values. Including them in the structural model will cause a state space explosion and impede the transition probability matrix estimation. We use the *logit inclusive value* technique to simplify the evolution of 41 predictors using the transition of one-dimensional GS_{it} (see Section B.3). We replace Z_{it} with GS_{it} in the state transition probability expression (equation B.5). A patient predicts the value of $GS_{i,t+1}$ using $(MELD_{i,t+1}, Rec_age_{i,t+1}, Rec_life_support_{i,t+1}, Rec_med_cond_{i,t+1}, Q_{i,t+1})$. Next, the data do not include the patient's transition of life support or medical condition. Only the MELD of the patient evolves over time. Patients differing in age group, life support status, and medical condition can be thought of as different patient types. These assumptions allow us to simplify the transition probability to:

$$\begin{aligned}
\mathcal{P}(S_{i,t+1}|S_{it}, d_{it} = 0) &= \mathcal{P}(MELD_{i,t+1}|MELD_{it}, d_{it} = 0) \times \mathcal{P}(Q_{i,t+1}|MELD_{i,t+1}, d_{it} = 0) \times \\
\mathcal{P}(GS_{i,t+1}|MELD_{i,t+1}, Rec_age_{i,t+1}, Rec_life_support_{i,t+1}, Rec_med_cond_{i,t+1}, Q_{i,t+1}, d_{it} = 0) &\times \\
\mathcal{P}(Sharing_type_{i,t+1}|MELD_{i,t+1}, Q_{i,t+1}, d_{it} = 0) &\times \\
\mathbb{1}_{\{Rec_age_{i,t+1}=Rec_age_{it}, Rec_life_support_{i,t+1}=Rec_life_support_{it}, Rec_med_cond_{i,t+1}=Rec_med_cond_{it}\}}, & \quad (B.5)
\end{aligned}$$

where $\mathcal{P}(Sharing_type_{i,t+1}|MELD_{i,t+1}, Q_{i,t+1}, d_{it} = 0)$ is estimated as:

$$\frac{\sum_i \# \text{ of offers of type } Q_{i,t+1} \text{ received at } MELD_{i,t+1} \text{ that have } Sharing_type_{i,t+1}}{\sum_i \# \text{ of offers of type } Q_{i,t+1} \text{ received at } MELD_{i,t+1}} \quad (B.6)$$

The MELD transition matrix and GS_{it} are estimated based on the data of the entire U.S. However, the estimation of $\mathcal{P}(Q_{i,t+1}|MELD_{i,t+1}, d_{it} = 0)$ and $\mathcal{P}(Sharing_type_{i,t+1}|MELD_{i,t+1}, Q_{i,t+1}, d_{it} = 0)$ are done for every DSA-policy era pair separately (while evaluating a policy that uses TC instead of DSA, we estimate the quantities for every TC). This is because the organ offer and sharing-type probabilities might differ across the DSAs and, in the Pre-Share 35 and Share 35 policy eras.

B.5 Log-Likelihood Function

When an offer is made, the probability of accepting an offer, equation (3.6), can be rewritten as:

$$P(d_{it} = 1|S_{it}) = \frac{e^{EU(S_{it})}}{e^{EU(S_{it})} + e^{-EW(S_{it}) + \delta EV(S_{it})}}, \quad (B.7)$$

Taking the log of both sides,

$$\ln (P(d_{it} = 1|S_{it})) = \ln [e^{EU(S_{it})}] - \ln [e^{EU(S_{it})} + e^{-EW(S_{it})+\delta EV(S_{it})}] \quad (\text{B.8})$$

Also,
$$\ln (P(d_{it} = 0|S_{it})) = \ln [e^{-EW(S_{it})+\delta EV(S_{it})}] - \ln [e^{EU(S_{it})} + e^{-EW(S_{it})+\delta EV(S_{it})}] \quad (\text{B.9})$$

The log-likelihood of a candidate's observed decision is:

$$\{\ln (P(d_{it} = 1|S_{it}))\}^{d_{it}} \times \{\ln (P(d_{it} = 0|S_{it}))\}^{(1-d_{it})} \quad (\text{B.10})$$

Grouping over all patients' decisions, the log-likelihood function is:

$$\begin{aligned} & \sum_{i,t} (\mathbb{1}_{\{d_{it}=1\}} \ln (P (d_{it} = 1|S_{it})) + \mathbb{1}_{\{d_{it}=0\}} \ln (P (d_{it} = 0|S_{it}))) \\ &= \sum_{S_{it}} (n_{accept}^{S_{it}} \ln (P (d_{it} = 1|S_{it})) + n_{decline}^{S_{it}} \ln (P (d_{it} = 0|S_{it}))) \\ &= \sum_{S_{it}} n_{accept}^{S_{it}} (EU(S_{it}) - \ln[e^{EU(S_{it})} + e^{-EW(S_{it})+\delta EV(S_{it})}]) + \\ & n_{decline}^{S_{it}} (-EW(S_{it}) + \delta EV(S_{it}) - \ln[e^{EU(S_{it})} + e^{-EW(S_{it})+\delta EV(S_{it})}]) \\ &= \sum_{S_{it}} n_{accept}^{S_{it}} EU(S_{it}) + n_{decline}^{S_{it}} (-EW(S_{it}) + \delta EV(S_{it})) - \\ & (n_{accept}^{S_{it}} + n_{decline}^{S_{it}}) \times (\ln[e^{EU(S_{it})} + e^{-EW(S_{it})+\delta EV(S_{it})}]) \quad (\text{B.11}) \end{aligned}$$

Every candidate i has an associated state S_{it} at time t ; therefore, we can sum over the elements in the state space, accounting for the number of candidates in those states (instead of summing over the candidates and time periods when they made the decisions). The first equality follows from this fact, where $n_{accept}^{S_{it}}$ and $n_{decline}^{S_{it}}$ denote the number of candidates who accepted

Independent variable	Estimate
Intercept	0.9582***
MELD 15-28	0.0028
MELD 29-32	-0.0058*
MELD 33-34	-0.008**
MELD 35-36	-0.0127***
MELD >36	-0.0203***
Candidate age group: R2 (45-65 years)	-0.0211***
Candidate age group: R3 (≥ 65 years)	-0.0268***
Candidate life support: Yes	-0.0492***
Candidate medical condition: H	-0.0182***
Candidate medical condition: ICU	-0.0649***
Donor controls: Yes	
No. of parameters: 58	
(Adjusted) R-squared = (0.5438) 0.5518	
No. of observations = 3,264	

*** $p < 0.001$; ** $p < 0.01$; * $p < 0.05$

Table B.4: Estimation results of regressing GS .

and declined the offers in state S_{it} , respectively.

B.6 Details on Identification of β_{GS}

We want to check whether the variables (on which we rely to identify GS_{it} , and whose variation we observe in the data) are correlated with GS_{it} or not. In Table B.4, we regress GS_{it} with the MELD category, age group, life support status, medical condition, and organ type. We find that most of the regression estimates are statistically significant, and 55% of the variability in GS_{it} is explained by the independent variables used in the regression. Thus, we can identify GS_{it} in the structural model through the variation of these independent variables in the observed data.

B.7 Relaxing the Assumption of a Fixed Value of CIT

In our main model, we assumed a fixed value of CIT and endogenized *sharing_type* (which captured the effect of CIT) with the allocation policy. As a robustness check, we relax the assumption and build a CIT prediction model (a linear regression model). We need a prediction model because CIT is only observed for accepted offers, and not for declined offers. We then used the predicted CIT values (instead of a fixed value of 6.9 hours) in calculating the one-year graft survival probability. In Table B.5, we compare the structural model estimates (when we use fixed CIT versus the predicted CIT). We find that there's only a slight change in the estimates of the utility and waiting cost functions parameters. The estimates of the parameters associated with regional and national sharing are closer to zero in the predicted CIT model than the fixed CIT model. This is because some of the disutilities (associated with regional/national sharing) are captured by the higher CIT in the predicted CIT model. Although the log-likelihood value is slightly better in the latter case, we prefer to use the fixed CIT model in our main analysis due to the following reasons: (1) Nonavailability of the key variables (mode of organ transport) for predicting CIT; (2) In counterfactual studies, we would need to predict CIT. Because we are less confident in the CIT prediction model, the prediction inaccuracies will make the policy evaluation less reliable; and (3) The measurement error in CIT (due to using a predicted value) will be passed over to the structural model.

Variable	Parameter	Fixed CIT	Predicted CIT
		Estimate (SE)	Estimate (SE)
<u>Utility Function:</u>			
Intercept	β_0	-21.7803 (0.3145)	-22.5536 (0.3257)
Sharing type: Regional	$\beta_{Sharing}$	-1.0348 (0.0113)	-0.9655 (0.0114)
Sharing type: National		-2.3328 (0.0243)	-2.0680 (0.0247)
Graft survival probability (GS)	β_{GS}	19.5200 (0.3353)	20.3111 (0.3468)
<u>Waiting Cost Function:</u>			
Death	ω_d	0.1160 (0.0007)	0.1153 (0.0007)
Candidate age group: R2 (45-65 years)	ω_{Age}	0.0057 (0.0002)	0.0058 (0.0002)
Candidate age group: R3 (≥ 65 years)		0.0061 (0.0003)	0.0063 (0.0003)
Candidate life support: Yes	ω_{LS}	0.0134 (0.0008)	0.0130 (0.0008)
Candidate medical condition: H	ω_{MC}	0.0114 (0.0004)	0.0115 (0.0004)
Candidate medical condition: ICU		0.0229 (0.0008)	0.0232 (0.0008)
No. of observations		890,402	890,402
Log-likelihood		-173,630.9	-173,579.2

Table B.5: Comparison of the estimation results of the structural models (when CIT is fixed versus predicted).

B.8 Iterative Method for Estimating the Equilibrium

We simulate different organ allocation policies. The common inputs across the policies are the sampled organ and candidate arrivals, the MELD transition matrix, and the estimates from the structural model. We randomly sample 5,000 patients and 3,600 donors from the 11 regions, which arrive at different points in time ($t = 1, \dots, 730$). Every organ is offered to a maximum of 500 candidates (which is close to the 99th percentile in the actual dataset) before being discarded. We let 34% of the patients be on the waiting list at $t = 1$, and the initial MELD distribution of the patients is chosen so that they represent the actual data. We consider two patient groups ($\{(Rec_age < 45 \text{ years}, Rec_life_support = \text{'No'}, Rec_med_cond = \text{'NH'})$ and $(Rec_age: (45 - 65) \text{ years}, Rec_life_support = \text{'No'}, Rec_med_cond = \text{'NH'})$ }, which constitutes 83% of the patient pop-

ulation in the UNOS data) and 48 organ types in the simulation study. Various patient groups may have different probabilities of acceptance for the same organ due to differences in the expected utilities (derived from the transplant) and waiting costs. The equilibrium behavior of each group will depend on the presence of the others; further, by considering two groups in our study, we capture their interactions in the equilibrium offer acceptance probabilities. The steps (followed by the pseudo algorithm) to estimate the steady-state equilibrium (for each allocation policy) using the iterative method are given below:

1. Start with the organ offer and sharing-type probabilities: $\mathcal{P}^{(k)}(Q_{it}|MELD_{it})$ and $\mathcal{P}^{(k)}(Sharing_type_{it}|MELD_{it}, Q_{it})$. This enables us to calculate the state transition matrix, $\Pi^{(k)}$. Using the ‘inner’ algorithm of the nested fixed point algorithm, estimate $EV^{(k)}(\cdot)$. When $k = 0$, we start with arbitrary values of the above quantities. Skip the next step if $k = 0$.
2. If $\|EV^{(k)}(\cdot) - EV^{(k-1)}(\cdot)\|_{\infty} < \varepsilon_1$, stop, or else go to the next step. We use $\varepsilon_1 = 10^{-5}$.
3. Calculate the probability of acceptance: $P^{(k)}(d_{it} = 1|S_{it}) = \frac{e^{EU(S_{it})}}{e^{EU(S_{it})} + e^{-EW(S_{it}) + \delta EV^{(k)}(S_{it})}}$.
4. Policy simulation: For an allocation policy, we analytically calculate the expected number of offers, expected number of transplants, and expected waiting period by any time t . Using analytical expressions avoids the randomness introduced due to candidates’ accept/decline decisions and their MELD transitions, which helps achieve faster convergence with tighter tolerance limits. First, we create a table of states for every geography (DSA or TC) and tabulate the patient counts in those states. Each state has its own probability of acceptance. A patient’s state might transition to other states (the patient’s geography does not change).

At different points in time, new patients join the waiting list, and donors arrive; some patients receive offers, get a transplant, and leave the system. To analytically calculate the expected number of offers received and transplants (to patients in various MELD classes and geographies) due to an organ arriving at time t , we sum the finite geometric series sequentially in the order (determined by the allocation policy) in which the offers are made to the various patient groups. The patients who received transplants are removed from the waiting list. Using the MELD transition matrix, we calculate the expected number of patients transitioning to different MELD categories at time $t + 1$ and update the waiting list. New patients who join the waiting list at time $t + 1$ are added. If no donor arrives at time $t + 1$, only the MELD transitions occur. We can track the expected number of patients on the waiting list, number of offers received, and number of transplants at different instances of t . This enables us to calculate the quantities of interest to us, which are the organ offer and sharing-type probabilities: $\mathcal{P}^{(k)}(Q_{it}|MELD_{it})$ and $\mathcal{P}^{(k)}(Sharing_type_{it}|MELD_{it}, Q_{it})$ in the k^{th} step of the iterative method.

5. Update k to $k + 1$. Go to Step 1.

Each iteration took approximately 25 hours for policies using the TC as the geographic unit (and approximately nine hours for DSA-based policies), and we were able to achieve convergence within 10 iterations for every policy. For the Acuity Circles policy, we define ‘local’ sharing if the distance between the donor hospital and the TC is <66 NM (average of the distance between the donor hospital and TC pairs in the same DSA), ‘regional’ sharing if the distance is ≥ 66 NM and <262 NM (average of the distance between the donor hospital and TC pairs in the same region), and ‘national’ otherwise.

Algorithm 1 Steady State Equilibrium

Input: Candidate and organ characteristics, allocation policy, structural parameters ($\beta_0, \beta_{GS}, \beta_{Sharing}, \omega_d, \omega_{Age}, \omega_{LS}, \omega_{MC}$), MELD transition matrix. Let t be the arrival time of an organ.

Output: $EV^*(S_{it}), \mathcal{P}^*(Q_{it}|MELD_{it}), \mathcal{P}^*(Sharing_type_{it}|MELD_{it}, Q_{it})$.

1 Initialize $k=0$ and beliefs $EV^k(S_{it}), \mathcal{P}^k(Q_{it}|MELD_{it})$, and $\mathcal{P}^k(Sharing_type_{it}|MELD_{it}, Q_{it})$ for all possible values of $S_{it}, Q_{it}, MELD_{it}$ and $Sharing_type_{it}$.

repeat

2 $\Pi^k \leftarrow$ Compute state transition matrix (see equation B.5)

Initialize $m = 0$ and $EV^m(\cdot)$

repeat

3 $EV^m(\cdot) \leftarrow \Pi^k \times \ln [e^{EU(\cdot)} + e^{-EW(\cdot)+\delta EV^m(\cdot)}]$

$m \leftarrow m + 1$

4 **until** $m \geq 1, \|\mathcal{P}^m(\cdot) - \mathcal{P}^{m-1}(\cdot)\|_\infty < 10^{-9}$;

5 $EV^k(\cdot) \leftarrow EV^m(\cdot)$

$p_{acpt}^k(S_{it}) := P^k(d_{it} = 1|S_{it}) \leftarrow$ Compute offer acceptance probabilities $\forall S_{it}$ (see equation B.7)

$\mathcal{P}^k(Q_{it}|MELD_{it}), \mathcal{P}^k(Sharing_type_{it}|MELD_{it}, Q_{it}) \leftarrow$ Policy Simulation ($p_{acpt}^k(\cdot)$)

$k \leftarrow k + 1$

6 **until** $k > 1, \|\mathcal{P}^k(\cdot) - \mathcal{P}^{k-1}(\cdot)\|_\infty < 10^{-5}$;

7 $EV^*(S_{it}) \leftarrow EV^k(S_{it}), \mathcal{P}^*(Q_{it}|MELD_{it}) \leftarrow \mathcal{P}^k(Q_{it}|MELD_{it}),$

$\mathcal{P}^*(Sharing_type_{it}|MELD_{it}, Q_{it}) \leftarrow \mathcal{P}^k(Sharing_type_{it}|MELD_{it}, Q_{it})$

B.9 Numerical Study to Derive Insights from the Structural Model

The allocation policies essentially differ in the utility of waiting or the future prospects of being offered an organ (through the expected future value, $EV(S_{it})$). The objective of this exercise is to generate insights about how a patient would react to the possibility of a transplant based on her health status and her future prospect of being offered an organ. This, in turn, depends on the organ offer probability, which depends on the supply and demand at the various DSAs and the allocation policy in place. For this reason, we study the effect of a change in supply and demand on a patient's organ acceptance behavior.

Setup

We simulate the organ and candidate arrivals for a two-year time period ($t = 1, \dots, 730$). We use a

stylized setup of two regions and three DSAs (Region A: DSA 1 and DSA 2; Region B: DSA 3), each with a single TC, in our numerical study. We let 34% of the patients be on the waiting list at $t = 1$, and the initial MELD distribution of the patients is chosen so that they represent the actual data. We only consider a single patient type (Rec_age : (45 – 65) years, $Rec_life_support$ ='No', Rec_med_cond ='NH'), and a single organ type (Don_age : (18 – 39) years, Don_race = 'White', Don_cod = 'Others', Don_dcd = 'No'). They represent the most frequent patient and organ types.

We study a total of five settings of demand and supply across the DSAs (Set 1,..., Set 5; see Table 3.5). The organ and the candidate's arrival times are random; we run 20 iterations for each setting. The steady state equilibrium organ acceptance probabilities are estimated using Algorithm 1 in Section B.8. We consider two organ allocation policies: Share 35 and the Acuity Circles. The insights, as we will see, remain the same.

Discussion of Insights

In Table 3.5, we report the probability of offer acceptance (95% confidence interval) as a function of a patient's MELD category and DSA. We select Set 1 as the baseline scenario: a similar supply and demand volume (in aggregate) is there at Region A and Region B, and at DSA 1 and DSA 2. We then change either the demand or s/d ratio, one at a time. We conduct an intra-set analysis (discuss the results of each set on its own), and an inter-set analysis (compare a set with the baseline setting, Set 1). Before we proceed, it is useful to do a quick sanity check. The two DSAs in Region A have similar characteristics in Set 1, Set 3 and Set 5. Therefore, the probability of offer acceptance should also be the same for a patient in DSA 1 and DSA 2 (for a given MELD category and a given set). Our results are consistent with our expectation, i.e., the confidence intervals overlap. We note that there are more observations for lower-MELD categories; therefore, the confidence interval is smaller for lower-MELD categories.

Set 1 (baseline setting): The aggregate s/d ratio is the same for Regions A and B. One may expect that the probability of offer acceptance should also be the same. However, sharing within Region B is all local, whereas sharing within Region A will be a mix of local and regional. Therefore, the behavior of Region B patients might be different from their counterparts in Region A.

We find that DSA 3 patients are more selective than DSA 1 and 2 patients. This selective nature is more prominent in middle-MELD categories (such as MELD 29-34). For a lower-MELD patient to receive an organ offer, it has to be declined by the higher-MELD patients of both the regions. Thus, we do not see a significant difference between the organ acceptance probabilities between the two regions in lower-MELD patients. Higher-MELD (MELD \geq 35) patients do not have significant difference in organ access, in this stylized model, due to broader sharing under both the Share 35 and Acuity Circles policies.

Set 2 (and its comparison with Set 1): In Set 2, we decrease the supply at DSA 2 such that the new s/d ratio in DSA 2 becomes 0.5 (from 0.7). The DSA 2 patients have a higher probability of offer acceptance than DSA 1 patients due to lesser organ access. This aggressive behavior is especially at lower MELD scores (the impact of difference in the s/d ratio is attenuated at higher MELD scores due to the prioritization of higher-MELD patients through broader sharing).

Upon comparing with Set 1, we see that DSA 2 patients react by increasing their probability of offer acceptance (especially at MELD 6-32). We also observe that a decrease in supply at DSA 2 affects other DSAs as well. DSA 1 patients became aggressive (than Set 1), especially at MELD 6-28. DSA 3 patients were less impacted than DSA 1 patients, and we did not see a significant change in their probability of offer acceptance (compared to Set 1).

Set 3 (and its comparison with Set 1): In Set 3, we decrease the supply at DSA 3 such that

the new s/d ratio in DSA 3 becomes 0.5 (from 0.7). The DSA 3 patients have a higher probability of offer acceptance than DSA 1 and 2 patients in lower-MELD categories (MELD 6-28).

Upon comparing with Set 1, we see that DSA 3 patients react by increasing their probability of offer acceptance (especially at MELD 6-32). DSA 1 and 2 patients also felt the effect, and they became more aggressive (than Set 1), especially at MELD 6-32.

Set 4 (and its comparison with Set 1): In Set 4, we increase the supply and demand volume at DSA 2 by 40%. The DSA 2 patients became more selective than DSA 1 patients at MELD 15-28 (and MELD 29-32 in the Share 35 policy but not in the Acuity Circles policy) due to an enlarged supply from where the patients could receive an offer.

Upon comparing with Set 1, we see that DSA 2 patients react by becoming more selective, especially at MELD 15-36 (except that MELD 33-34 did not see a significant effect in the Acuity Circles policy). DSA 1 and DSA 3 patients also became more selective (than Set 1), especially at MELD 29-36 and MELD 29-34, respectively. The selectiveness in the patient's behavior (compared to Set 1) is driven by the enlarged supply (even though demand also proportionally increased) from where the patients could receive an offer.

Set 5 (and its comparison with Set 1): In Set 5, we increase the supply and demand volume at DSA 3 by 40%. The DSA 3 patients are more selective than DSA 1 and 2 patients at MELD 15-34.

Upon comparing with Set 1, we see that DSA 3 patients react by becoming more selective, especially at MELD 15-36. DSA 1 and 2 patients also became more selective (than Set 1), especially at MELD 29-36. Again, the selectiveness in the patient's behavior (compared to Set 1) is driven by the enlarged supply (even though demand also proportionally increased) from where the patients could receive an offer.

To summarise, the main insights are: (1) When the s/d ratio differs between two DSAs, its impact (in terms of the probability of offer acceptance) is felt more in lower-MELD patients. The impact becomes attenuated at higher MELD scores due to the prioritization of higher-MELD patients through broader sharing (Share 35 and the Acuity Circles policy). If the s/d ratio decreases at a DSA, their patients react by becoming aggressive in organ acceptance behavior. (2) Increasing the supply and demand volume (keeping the s/d ratio the same) in a DSA leads to an enlarged supply from where the patients can receive an offer, which induces selective behavior. This behavioral change is not just limited to the DSA at which a change is made; it also has a spillover effect on other DSAs.

B.10 Models for Benchmarking

In Table B.6, we report the coefficients corresponding to various logistic regression models (RM1, RM2, and RM3) that we used for benchmarking. The dependent variable in all the models is the accept/decline decision.

In Figure B.4(a), we plot the average probability of offer acceptance (calculated as a fraction of offers that were accepted) by MELD category, which we use as a reference. In Figure B.4(b), (c), and (d), we plot the reduced-form models' predicted probabilities of offer acceptance. RM1 and RM2 do not capture the trend of the offer acceptance probability (with the MELD category), and the regime shift (from the Pre-Share 35 to Share 35 policy). RM3, which has more variables, is relatively better.

Independent variable	Reduced-form Models		
	RM1	RM2	RM3
Intercept	-20.659***	-16***	-5.714***
Graft survival probability (GS)	19.322***	15.136***	-
MELD 15-28	-	-	3.287***
MELD 29-32	-	-	3.987***
MELD 33-34	-	-	4.419***
MELD 35-36	-	-	4.899***
MELD >36	-	-	5.2***
P(death MELD)	80.745***	-	-
Wait time (in years)	-	-0.423***	-
Sharing type: Regional	-1.228***	-1.224***	-1.089***
Sharing type: National	-2.105***	-1.969***	-2.38***
Candidate age group: R2 (45-65 years)	0.433***	0.278***	0.182***
Candidate age group: R3 (≥ 65 years)	0.546***	0.356***	0.085**
Candidate life support: Yes	0.962***	1.165***	-0.058
Candidate medical condition: H	1.079***	1.278***	0.549***
Candidate medical condition: ICU	1.735***	2.398***	0.625***
Log-likelihood	-57,861.72	-58,629.47	-53,815.62
No. of observations = 277,367			

*** $p < 0.001$; ** $p < 0.01$; * $p < 0.05$

Table B.6: Regression estimates of the reduced-form models used for benchmarking.

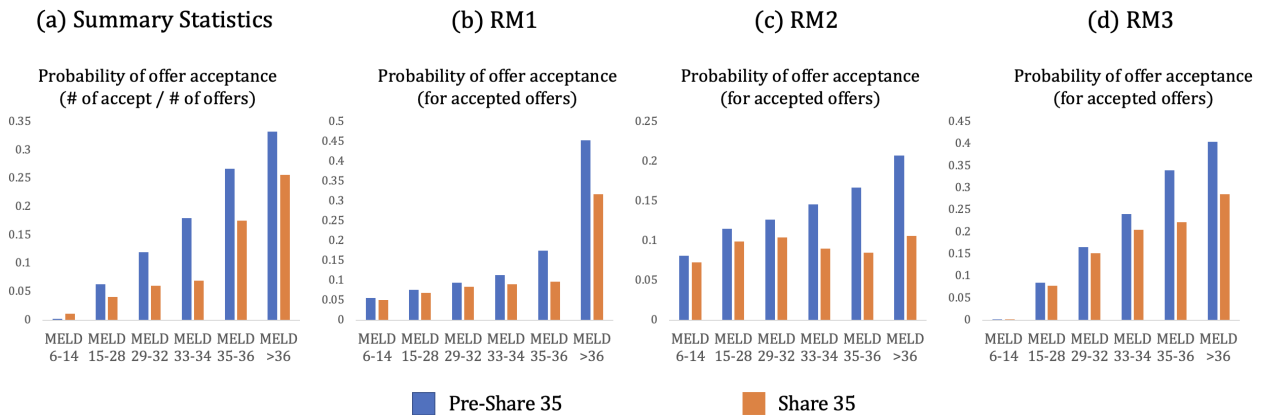


Figure B.4: Out-of-sample comparison of reduced-form models.

B.11 Comparison of the Pre-Share 35 and Share 35 Policies on Geographic Equity Using Simulation

We use the simulation setup described in Section B.8 to compare the Pre-Share 35 and Share 35 policies on a few geographic equity metrics. Referring to Figure 3.3, we see that not all regions benefit from introducing the Share 35 policy (compared to the Pre-Share 35 policy). For example, Region 11 becomes adversely impacted: the number of deaths and the amount of waiting time increased, and the number of transplants decreased. To gain more insights, we performed a simple correlation study (at the regional level) between the reduction in the number of deaths (normalized by the waiting-list volume) and the s/d ratios (deceased donors in a region constitute the supply, and the total number of patients joining the waiting list in that region constitute the demand). We observed a strong negative correlation coefficient ($r = -0.91$; $P < 0.001$), suggesting that the benefit in terms of life savings due to the Share 35 policy is higher for regions with lower s/d ratios. This is reflective of the change brought due to the Share 35 policy that prioritized MELD ≥ 15 national patients before MELD < 15 local or regional patients (see Table 1.1). A similar correlation study between the increase in the number of transplants (from the Pre-Share 35 to Share 35 policy) and the s/d ratios revealed a strong negative correlation coefficient ($r = -0.89$; $P < 0.001$). The reduction in the expected waiting period was also negatively correlated ($r = -0.93$; $P < 0.001$) with the s/d ratios. Along these same lines, the increase in the expected offers was negatively correlated ($r = -0.68$; $P = 0.021$) with the s/d ratios.

Covariate	Graft survival	Patient survival without transplant
	Hazard ratio	Hazard ratio
MELD 6-14	1.13*	0.45***
MELD 29-32	0.91*	3.63***
MELD 33-34	0.75***	4.49***
MELD 35-36	0.92	5.97***
MELD >36	1.04	11.24***
Candidate age group: R1 (<45 years)	1.51***	0.63***
Candidate age group: R3 (≥65 years)	0.65***	1.28***
Candidate life support: Yes	1.09	2.67***
Candidate medical condition: H	1.18***	1.65***
Candidate medical condition: ICU	1.09	2.07***
Donor age group: (40 to 49 years)	1.35***	-
Donor age group: (50 to 59 years)	1.58***	-
Donor age group: (≥60 years)	1.78***	-
Donor race: Other	1.08**	-
Donor cause of death: Anoxia	0.84***	-
Donor cause of death: CVA	1.10**	-
Donor DCD: Yes	1.56***	-
Sharing type: Regional	1.00	-
Sharing type: National	1.34***	-

*** $p < 0.001$; ** $p < 0.01$; * $p < 0.05$

Table B.7: Survival model estimates.

B.12 Survival Benefit due to a Transplant

We estimate the survival benefit due to a transplant as the difference between the probability of graft survival and the probability of a patient’s survival without a transplant, both calculated at the end of one year. The baseline survival functions are estimated using the Kaplan-Meier curves. The estimated graft survival probability (at $t=1$ year) of the baseline is 0.98 (standard error = 0.05), and the patient’s survival probability without a transplant of the baseline is 0.875 (standard error = 0.04). We use the Cox-proportional hazards model [16] to estimate the hazard ratios (HR) associated with the organ and patient characteristics used in our simulation study. The estimates of the HRs are reported in Table B.7.

B.13 s/d Match Policy (Maximum Radius = 600 NM)

When we allow the maximum radius around the donor hospital to be 600 NM, the s/d ratio (at the TC level) ranges from 0.62 to 0.73. In Table B.8, we compare the geographic equity metrics between the two s/d Match policies (maximum radius equals 500 NM versus 600 NM) using the simulation setup described in Section B.8. Although we do not observe improvement in all the metrics, the expected number of deaths decreases from 459.9 (maximum radius = 500 NM) to 455.4 (maximum radius = 600 NM), and the expected number of transplants increases from 3,570.8 to 3,578.5.

In Figure B.5, we compare the efficiency metrics such as the position at offer acceptance, fractional change in the utility from the transplant (with respect to the Pre-Share 35 policy), and cost of fairness (with respect to the Outcome-based policy) between the two s/d Match policies. We see that the bigger radius policy results in greater efficiency. The average increase in a patient's survival probability due to a transplant is also slightly higher (0.185 versus 0.183) in the bigger radius s/d Match policy. Table B.9 compares the distance traveled by the organ between the two s/d Match policies. While the mean distance is lower in the bigger radius policy, the other measures are marginally higher. In conclusion, if broader sharing is done right by matching supply and demand, it results in greater equity with minimal impact on the efficiency metrics!

Geographic equity metrics (normalized)	Standard deviation across the regions	
	s/d Match (500 NM)	s/d Match (600 NM)
Deaths	0.013	0.013
Transplants	0.028	0.034
Waiting (in months)	0.801	0.793
Offers	1.553	1.994

Table B.8: Comparison of the standard deviation of various geographic equity measures between s/d Match policies.

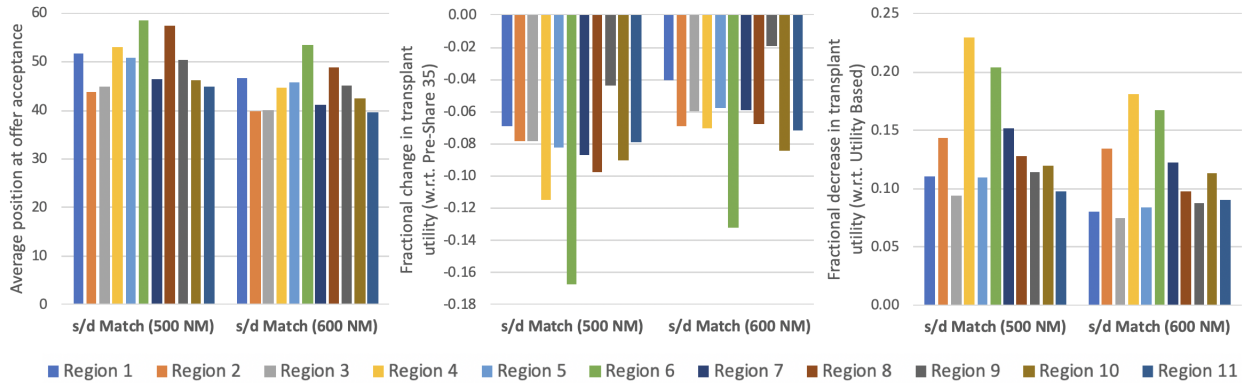


Figure B.5: Comparison of the position at offer acceptance, fractional change in utility from the transplant (with respect to Pre-Share 35), and cost of fairness (with respect to Outcome-based) between the two s/d Match policies.

	s/d Match (500 NM)	s/d Match (600 NM)
Mean	360	337
1st quartile	52	60
Median	180	206
3rd quartile	417	427

Table B.9: Comparison of travel distance (in NM) between the two s/d Match policies.

Bibliography

- [1] Nikhil Agarwal, Itai Ashlagi, Michael Rees, Paulo Somaini, and Daniel Waldinger. Equilibrium allocations under alternative waitlist designs: Evidence from deceased donor kidneys. *Econometrica*, 89(1):37–76, 2021.
- [2] Shubham Akshat, Sommer E. Gentry, and S. Raghavan. Heterogeneous donor circles for fair liver transplant allocation. *Health Care Management Science*, Forthcoming, 2022.
- [3] Oguzhan Alagoz, Lisa M. Maillart, Andrew J. Schaefer, and Mark S. Roberts. The optimal timing of living-donor liver transplantation. *Management Science*, 50(10):1420–1430, 2004.
- [4] Oguzhan Alagoz, Lisa M. Maillart, Andrew J. Schaefer, and Mark S. Roberts. The optimal timing of living-donor liver transplantation. *Management Science*, 50(10):1420–1430, 2004.
- [5] Oguzhan Alagoz, Lisa M. Maillart, Andrew J. Schaefer, and Mark S. Roberts. Choosing among living-donor and cadaveric livers. *Management Science*, 53(11):1702–1715, 2007.
- [6] Oguzhan Alagoz, Lisa M. Maillart, Andrew J. Schaefer, and Mark S. Roberts. Determining the acceptance of cadaveric livers using an implicit model of the waiting list. *Operations Research*, 55(1):24–36, 2007.
- [7] Mazhar Arikan, Baris Ata, J. Friedewald, John, and P. Parker, Rodney. Enhancing kidney supply through geographic sharing in the United States. *Production and Operations Management*, 27(12):2103–2121, 2018.
- [8] Baris Ata, Yichuan Ding, and Stefanos Zenios. An achievable-region-based approach for kidney allocation policy design with endogenous patient choice. *Manufacturing & Service Operations Management*, 23(1):36–54, 2021.
- [9] Baris Ata, John Friedewald, and A. Cem Randa. Structural estimation of kidney transplant candidates’ quality of life scores: Improving national kidney allocation policy under endogenous patient choice and geographical sharing. Working Paper, University of Chicago, 2022.

- [10] Baris Ata, Anton Skaro, and Sridhar Tayur. Organjet: Overcoming geographical disparities in access to deceased donor kidneys in the United States. *Management Science*, 63(9):2776–2794, 2017.
- [11] Anthony B. Atkinson. On the measurement of inequality. *Journal of Economic Theory*, 2(3):244–263, 1970.
- [12] Dimitris Bertsimas, Vivek F. Farias, and Nikolaos Trichakis. On the efficiency-fairness trade-off. *Management Science*, 58(12):2234–2250, 2012.
- [13] Dimitris Bertsimas, Vivek F. Farias, and Nikolaos Trichakis. Fairness, efficiency, and flexibility in organ allocation for kidney transplantation. *Operations Research*, 61(1):73–87, 2013.
- [14] Dimitris Bertsimas, Theodore Papalexopoulos, Nikolaos Trichakis, Yuchen Wang, Ryutaro Hirose, and Parsia A. Vagefi. Balancing efficiency and fairness in liver transplant access: Tradeoff curves for the assessment of organ distribution policies. *Transplantation*, 104(5):981–987, 2020.
- [15] F Caro, T Shirable, M Guignard, and A Weintraub. School redistricting: Embedding GIS tools with integer programming. *Journal of the Operational Research Society*, 55(8):836–849, 2004.
- [16] D. R. Cox. Regression models and life-tables. *Journal of the Royal Statistical Society. Series B (Methodological)*, 34(2):187–220, 1972.
- [17] Mehmet C. Demirci, A. J Schaefer, H. Edwin Romeijn, and M. S Roberts. An exact method for balancing efficiency and equity in the liver allocation hierarchy. *INFORMS Journal on Computing*, 24(2):260–275, 2012.
- [18] Haluk Ergin, Tayfun Sönmez, and M. Utku Ünver. Efficient and incentive-compatible liver exchange. *Econometrica*, 88(3):965–1005, 2020.
- [19] S Feng, N. P. Goodrich, J. L. Bragg-Gresham, D. M. Dykstra, J. D. Punch, M. A. DeBroy, S. M. Greenstein, and R. M. Merion. Characteristics associated with liver graft failure: The concept of a donor risk index. *American Journal of Transplantation*, 6:783–790, 2006.
- [20] Richard B. Freeman, Russell H. Wiesner, Ann Harper, Sue V. McDiarmid, J Lake, E Edwards, R Merion, R Wolfe, J Turcotte, and L Teperman. The new liver allocation system: Moving toward evidence based transplantation policy. *Liver Transplantation*, 8(9):851–858, 2002.
- [21] R S. Garfinkel and G L. Nemhauser. Optimal political districting by implicit enumeration techniques. *Management Science*, 16(8):B495–B508, 1970.
- [22] J M. Garonzik-Wang, N T. James, K J. Van Arendonk, N. Gupta, B J. Orandi, E C. Hall, A B. Massie, R A. Montgomery, N N. Dagher, A L. Singer, A M. Cameron, and D L. Segev. The aggressive phenotype revisited: Utilization of higher-risk liver allografts. *American Journal of Transplantation*, 13(4):936–942, 2013.

- [23] Sommer E. Gentry, Eric K. Chow, Allan B. Massie, and Dorry L. Segev. Gerrymandering for justice: Redistricting U.S. liver allocation. *Interfaces*, 45(5):462–480, 2015.
- [24] Sommer. E Gentry, Eric K. Chow, Corey E. Wickliffe, Allan B. Massie, Tabitha Leighton, and Dorry L. Segev. Impact of broader sharing on transport time for deceased donor livers. *Liver Transplantation*, 20(10):1237–1243, 2014.
- [25] Alexandra K. Glazier. The lung lawsuit: A case study in organ allocation policy and administrative law. *Journal of Health & Biomedical Law*, XIV:139–148, 2018.
- [26] Aparna Goel, W. Ray Kim, Joshua Pyke, David P. Schladt, Bertram L. Kasiske, Jon J. Snyder, John R. Lake, and Ajay K. Israni. Liver simulated allocation modeling: Were the predictions accurate for Share 35? *Transplantation*, 102(5):769–774, 2018.
- [27] David S. Goldberg, Matthew Levine, Seth Karp, Richard Gilroy, and Peter L. Abt. Share 35 changes center level liver acceptance practices. *Liver Transplantation*, 23(5):604–613, 2017.
- [28] Ram Gopalan, Steven O. Kimbrough, Frederic H. Murphy, and Nicholas Quintus. The Philadelphia districting contest: Designing territories for city council based upon the 2010 census. *Interfaces*, 43(5):477–489, 2013.
- [29] Gautam Gowrisankaran and Marc Rysman. Dynamics of consumer demand for new durable goods. *Journal of Political Economy*, 120(6):1173–1219, 2012.
- [30] Jeffrey B. Halldorson, Harry J. Paarsch, Jennifer L. Dodge, Alberto M. Segre, Jennifer Lai, and John Paul Roberts. Center competition and outcomes following liver transplantation. *Liver Transplantation*, 19(1):96–104, 2013.
- [31] Christine E. Haugen, Tanveen Ishaque, Abel Sapirstein, Alexander Cauneac, Dorry L. Segev, and Sommer E. Gentry. Geographic disparities in liver supply/demand ratio within fixed–distance and fixed–population circles. *American Journal of Transplantation*, 19(7):2044–2052, 2019.
- [32] S W. Hess, J B. Weaver, J N. Whelan, and P A. Zitlau. Nonpartisan political redistricting by computer. *Operations Research*, 13(6):998–1006, 1965.
- [33] HHS. Organ procurement and transplantation network; (42 CFR Part 121). *Federal Register*, 63(63):16296–16338, 1998.
- [34] Christopher B. Hughes. The history of trying to fix liver allocation: Why a consensus approach will never work. *Clinical Transplant*, 29(6):477– 483, 2015.
- [35] V Kilambi and S Mehrotra. Improving liver allocation using optimized neighborhoods. *Transplantation*, 101(2):350–359, 2017.
- [36] Myung Kim and Ningchuan Xiao. Contiguity-based optimization models for political redistricting problems. *International Journal of Applied Geospatial Research*, 8(4):1–18, 2017.

- [37] W. R. Kim, J R. Lake, J M. Smith, D P. Schladt, M A. Skeans, A M. Harper, J L. Wainright, J J. Snyder, A K. Israni, and B L. Kasiske. OPTN/SRTR 2016 Annual data report: Liver. *American Journal of Transplantation*, 18, Suppl 1:172–253, 2018.
- [38] Nan Kong, Andrew J. Schaefer, Brady Hunsaker, and Marks S. Roberts. Maximizing the efficiency of the U.S. liver allocation system through region design. *Management Science*, 56(12):2111–2122, 2010.
- [39] Charles Y. Lee and Martin J. Mangino. Preservation methods for kidney and liver. *Organogenesis*, 5(3):105–112, 2009.
- [40] Robert M. Merion, Douglas E. Schaubel, Dawn M. Dykstra, Richard B. Freeman, Friedrich K. Port, and Robert A. Wolfe. The survival benefit of liver transplantation. *American Journal of Transplantation*, 5:307–313, 2005.
- [41] Martha Pavlakis. Continuous distribution in organ allocation: Stepping back from the edge. *Transplantation*, 105(12):2517–2519, 2021.
- [42] J Rawls. *A Theory of Justice*. Harvard University Press, Cambridge, MA, 1971.
- [43] Federica Ricca, Andrea Scozzari, and Bruno Simeone. Political districting: From classical models to recent approaches. *Annals of Operations Research*, 204(1):271–299, 2013.
- [44] John Rust. Optimal replacement of GMC bus engines: An empirical model of Harold Zurcher. *Econometrica*, 55(5):999–1033, 1987.
- [45] D E. Schaubel, M K. Guidinger, S W. Biggins, J D. Kalbfleisch, E A. Pomfret, P. Sharma, and R M. Merion. Survival benefit-based deceased-donor liver allocation. *American Journal of Transplantation*, 9:970–981, 2009.
- [46] Takeshi Shirabe. Districting modeling with exact contiguity constraints. *Environment and Planning B: Planning and Design*, 36(6):1053–1066, 2009.
- [47] J M. Smith, S W. Biggins, D G. Haselby, W R. Kim, J. Wedd, K. Lamb, B. Thompson, D L. Segev, S. Gustafson, R. Kandaswamy, P G. Stock, A J. Matas, C J. Samana, Sleeman E F., D. Stewart, A. Harper, E. Edwards, J J. Snyder, B L. Kasiske, and A K. Israni. Kidney, pancreas and liver allocation and distribution in the United States. *American Journal of Transplantation*, 12:3191–3212, 2012.
- [48] Jon J. Snyder, Nicholas Salkowski, Andrew Wey, Joshua Pyke, Ajay K. Israni, and Bertram L. Kasiske. Organ distribution without geographic boundaries: A possible framework for organ allocation. *American Journal of Transplantation*, 18(11):2635–2640, 2018.
- [49] James E. Stahl, Nan Kong, S M. Shechter, Andrew J. Schaefer, and Mark S. Roberts. A methodological framework for optimally reorganizing liver transplant regions. *Medical Decision Making*, 25(1):35–46, 2005.

- [50] Xuanming Su and Stefanos A. Zenios. Patient choice in kidney allocation: A sequential stochastic assignment model. *Operations Research*, 53(3):443–455, 2005.
- [51] Xuanming Su and Stefanos A. Zenios. Recipient choice can address the efficiency-equity trade-off in kidney transplantation: A mechanism design model. *Management Science*, 52(11):1647–1660, 2006.
- [52] David Thompson, Larry Waisanen, Robert Wolfe, Robert M. Merion, Keith Mccullough, and Ann Rodgers. Simulating the allocation of organs for transplantation. *Health Care Management Science*, 7(4):331–338, 2004.
- [53] Hamidreza Validi, Austin Buchanan, and Eugene Lykhovyd. Imposing contiguity constraints in political districting models. *Operations Research*, 70(2):867–892, 2022.
- [54] Kenneth Washburn, Ann Harper, Baker Timothy, and Erick Edwards. Changes in liver acceptance patterns after implementation of Share 35. *Liver Transplantation*, 22:171–177, 2016.
- [55] Andrew Wey, Joshua Pyke, David P. Schladt, Sommer E. Gentry, Tim Weaver, Nicholas Salkowski, Bertram L. Kasiske, Ajay K. Israni, and Jon J. Snyder. Offer acceptance practices and geographic variability in allocation model for end-stage liver disease at transplant. *Liver Transplantation*, 24(4):478–487, 2018.
- [56] H Yeh, E Smoot, D. A. Schoenfeld, and J. F. Markmann. Geographic inequity in access to livers for transplantation. *Transplantation*, 91(4):479–486, 2011.
- [57] Stefanos A. Zenios, Glenn M. Chertow, and Lawrence M. Wein. Dynamic allocation of kidneys to candidates on the transplant waiting list. *Operations Research*, 48(4):549–569, 2000.
- [58] Juanjuan Zhang. The sound of silence: Observational learning in the U.S. kidney market. *Marketing Science*, 29(2):315–335, 2010.
- [59] Andris A. Zoltners and Prabhakant Sinha. Sales territory alignment: A review and model. *Management Science*, 29(11):1237–1256, 1983.